Harnessing Evolutionary Fitness in Plasmodium falciparum for Drug Discovery and Suppressing Resistance

HARNESSING EVOLUTIONARY FITNESS IN *PLASMODIUM FALCIPARUM* FOR DRUG DISCOVERY AND SUPPRESSING RESISTANCE

A DISSERTATION PRESENTED

BY

LEILA SAXBY ROSS

TO

THE DIVISION OF MEDICAL SCIENCES

IN PARTIAL FULFILLMENT OF THE REQUIREMENTS

FOR THE DEGREE OF

DOCTOR OF PHILOSOPHY

IN THE SUBJECT OF

BIOLOGICAL CHEMISTRY AND MOLECULAR PHARMACOLOGY

HARVARD UNIVERSITY

CAMBRIDGE, MASSACHUSETTS

AUGUST 2013

Dissertation Advisor: Dyann F. Wirth Leila Saxby Ross

HARNESSING EVOLUTIONARY FITNESS IN *PLASMODIUM FALCIPARUM* FOR DRUG DISCOVERY AND SUPPRESSING RESISTANCE

Abstract

Malaria is a preventable and treatable disease caused by infection with *Plasmodium* parasites. Complex socioeconomic and political factors limit access to vector control and antimalarial drugs, and an estimated 600,000 people die from malaria every year. Rising drug resistance threatens to make malaria untreatable. As for all new traits, resistance is limited by fitness, and a small number of pathways are heavily favored by evolution. These pathways are targets for drug discovery. Pairing compounds active against the wild-type and the small emerging resistant population, a strategy we termed “targeting resistance,” could block the rise of competitively viable resistance.

We characterized resistance pathways to dihydroorotate dehydrogenase (PfDHODH) inhibitors. PfDHODH is a novel target with several compounds in development for clinical use. *In vitro* resistance selections led to a variety of point mutations in the gene *pfdhodh*, which all lined the tunnel for electron transfer between cofactors: L172F, E182D, F188I/L, F227I, I263F, L527I, and L531F. We chose to focus on E182D, as it arose in response to two structurally unrelated inhibitors. Screening

identified an E182D-selective inhibitor (IDI-6273). Selection of the E182D mutant parasites with IDI-6273 led to a novel mutation in *pfdhodh,* which resulted in a reversion to the wild-type protein sequence. Simultaneous rather than sequential selection of wild-type parasites with a wild-type and mutant-type inhibitor failed to give resistance in 80 days.

The *in vitro* selection work was corroborated with biochemical assays of protein activity, which also allowed us to determine that the E182D mutation led to a reduced catalytic efficiency. In keeping with this, competitive growth assays showed that the E182D mutant and D182E revertant were less fit than the wild-type parent. Crystallography revealed that changes in aromatic stacking and helix packing were the likely mechanisms of resistance.

We believe that evolutionary fitness constraints allow few pathways to resistance, and these pathways can be anticipated and preemptively blocked. The combination of well-chosen antimalarial agents active against sensitive and resistant parasites effectively kills parasites in the short-term, and in the long-term, can help shape parasite evolution away from the development of drug resistance.

Contents

Listing of Figures

Listing of Tables

Acknowledgements

I am immensely grateful for my experience working in the malaria community at Harvard. I was fortunate to have been surrounded by people passionate about their work who offered insightful critiques as well as friendly support as needed – and I did need it.

Dyann Wirth was a fabulous mentor, and once we set practical milestone goals, I had enormous freedom in choosing the tone of my research. This let me take this project in directions outside of the traditional areas of the lab and initiate what will hopefully be long-term collaborations. Dyann's knack for narrative – building scientific stories accessible and appealing to scientists and the general public alike – is a skill that I hope to develop further in my own career. Roger Wiegand introduced me to the business side of science, and working on grant applications with him was invaluable experience. Much of the initial work described in this thesis was completed by Amanda Lukens, and her advice and dry humor were vital to this project. Other members of the Wirth lab gave useful feedback on experiments and writing in addition to being pleasant co-workers with sometimes questionable musical tastes.

I must thank the structural support of the Biological and Biomedical Sciences (BBS) program: I was constantly amazed that Kate Hodgins, Maria Bollinger, Danny Gonzalez, and Steve Obuchowski in the BBS office ever got anything done with all of the students constantly stopping by. Whenever I had a problem, personal or professional, they encouraged me to come by and talk it out. Whenever they thought I could help someone, they did not hesitate to put the two of us in contact. This approach helped me build a supportive network with fellow students that I would likely have never otherwise met.

My dissertation advisory committee – Michael Wolfe, Matthias Marti, Steve Harrison, and Nathaniel Gray – was also a very positive force in my life. In particular, Michael Wolfe, my committee chair, was above-and-beyond supportive when I ended up switching labs. He held regular meetings with me to check on my progress and also just to see if I was happy and handling everything the way I wanted to.

Not all of graduate school life is working in the lab, and my friends and classmates made sure that I at least occasionally left work for worthy causes like potlucks and costume parties. We enjoyed good food and good company, made up new dances, and excelled at Rock Band and karaoke. We built remote-controlled shark balloons, duct tape sharks, paper sharks, and generally had an aquatic theme to life. I thank them for their love and silliness, for putting up with my sometimes-strange work hours, and for listening to me talk about “the DNA and the protein and stuff.”

Chapter One:

Introduction

1.1 MALARIA

Malaria is an infectious disease transmitted by female *Anopheles* mosquitoes. Disease symptoms typically include severe fever and headache, but there are many possible manifestations including respiratory distress, coma, and death. Malaria is caused by infection with protozoan parasites of the genus *Plasmodium*. *Plasmodium* parasites are highly host-specific, and five out of several hundred species are known to infect humans: *falciparum, vivax, malariae, ovale,* and *knowlesi*. *Plasmodium falciparum* infection is the most deadly. Malaria is widespread in tropical and subtropical regions, including parts of the Americas, Asia, and Africa. Nearly half the world's population is at risk of infection, and an estimated 200 million people are infected each year, resulting in approximately 600,000 malaria-related deaths in 2012 [1]. The majority of malaria-related deaths occur in children under the age of five in Sub-Saharan Africa. Morbidity and mortality from malaria costs the African continent an estimated US$12 billion and 1.3% GDP growth per year [1], and as such, is a global public health and economic concern.

1.2 PARASITE BIOLOGY

The phylum *Apicomplexa* contains several unicellular protist parasites of medical and veterinary significance, including *Plasmodium, Toxoplasma, Babesia, Eimeria,* and *Cryptosporidium.* Apicomplexans are characterized by a three-membrane outer pellicle and an apical set of structures – often including rhoptries, micronemes, and dense granules – which are specialized for invasion of the host. Most, but not all, also contain a unique double-endosymbiotic organelle dubbed the apicoplast.

The genus *Plasmodium* contains hundreds of species, each with a narrow range of hosts and vectors. Hosts include specific mammals, birds, and reptiles. Vectors are

typically specific mosquito species. Infection with a *Plasmodium* parasite leads to the disease malaria. *Plasmodium* has a complex life cycle (Figure 1.2.1), and human-infecting parasites must cycle between an *Anopheles* mosquito vector and a human host. When an infected mosquito takes a blood meal from a human, 10-20 parasite sporozoites in the mosquito salivary glands enter the human bloodstream. Sporozoites migrate to the liver, where they pass through several hepatocytes before settling in a final host cell. In this final hepatocyte, the sporozoite replicates to 30-40 thousand cells over a period of days to weeks, depending on the species [2]. Kinship sensing leads to manipulation of the host hormone hepcidin to reduce the risk of superinfection (and thus competition) with other lineages of malaria parasites [3]. The infected liver cells burst, releasing tens of thousands of merozoites into the bloodstream. Merozoites rapidly invade red blood cells, establishing infection in this MHC class II-negative, immunologically sheltered, nutritionally-replete cell within 30-120 seconds [4]. Rapid invasion limits exposure to the immune system, and parasites also directly and indirectly suppress the immune response through methods like antigenic variation, adherence of infected red blood cells to the vascular endothelium, tandem repeats in antigens that provide a smokescreen for formation of antibodies against “true” functional moieties, and induction of suppressive cytokines such as IL-10 and TGF-β [5]. This intricate interplay with the human immune system reflects our long co-evolutionary history.

All symptoms come from the blood stages. Typical symptoms include anemia, cycles of severe chills and fever, and headache. These symptoms are rather non-specific and better diagnostics to distinguish among bacterial, viral, and malaria infections would simplify treatment. More severe symptoms include respiratory distress, metabolic acidosis, coma, seizure, organ failure (lung, liver, and spleen being the most common), splenomegaly, and death. Cerebral malaria results when parasites overwhelm the

vasculature in the brain, and patients rapidly deteriorate into coma and seizures. The mortality rate of cerebral malaria is much higher than so-called “uncomplicated” malaria, and survivors often suffer from neurological sequelae [6].

In the blood stages, merozoites mature into ring stages, which rapidly build a plasma membrane parasitophorous vacuole and remodel the host cell. Ring stages mature into trophozoites, which are more metabolically active and begin DNA synthesis. Trophozoites mature into schizonts, which form daughter merozoites from the mass of free nuclei and burst out of the host cell to begin the cycle anew. Trophozoites and schizonts – so-called “late stages” – adhere to the vascular endothelium, and ring stages circulate freely in the bloodstream. In *P. falciparum*, 16-32 daughter nuclei are formed in a 48-hour life cycle.

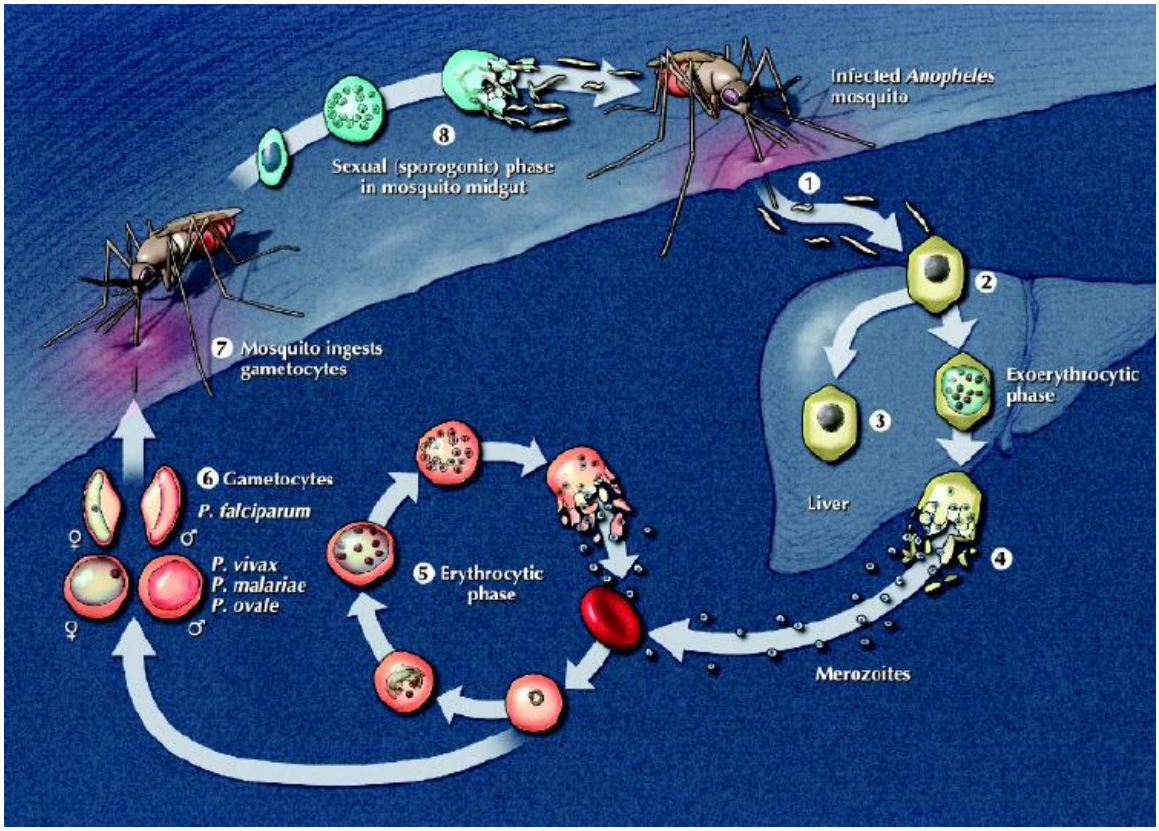

Figure 1.2.1: *Plasmodium spp.* life cycle (Suh et al 2004) [7]

A small fraction of the blood stage cells will follow a different path, and commit to sexual development [8]. This process produces male and female gametocytes. Forming gametocytes sequester in the bone marrow, and are released into the bloodstream when mature. Mature gametocytes can thus be taken up by a mosquito blood meal. Once in the mosquito, male and female gametocytes must rapidly find each other and fuse in the mosquito midgut to form the diploid ookinete. The ookinete burrows through the mosquito midgut and forms the oocyst. After development, the oocyst ruptures and free sporozoites migrate to the salivary glands. These sporozoites can then infect a person when the mosquito takes a blood meal.

1.3 CONTROL AND ERADICATION

Infectious disease control relies on a combination of reducing transmission and treating cases on an individual and population-wide level. Transmission is traditionally interrupted by eliminating the vector and/or population-wide vaccination or drug administration. Treating infected patients requires that the patients be identifiable and that there are effective and available treatments for those patients.

The sexual forms of malaria (gametocytes) are transmitted by the bite of female *Anopheles* mosquitoes. Mosquitoes breed in standing water and tend to feed at dusk, but changing patterns of behavior are complicating efforts to deploy localized insecticides, bed nets, and larval control methods like draining standing water and the use of larvivorous fish. In addition, rising levels of resistance or “behavioral resilience” to a variety of insecticides greatly limits our ability to control mosquito populations [9].

There is no effective vaccine for malaria, despite valiant and long-running efforts [10, 11]. The vast majority of exposed people develop at most partial and short-lasting immunity

to malaria, and this requires several years of exposure to locally circulating parasite strains. This is part of the reason why young children are so susceptible to malaria – their immune systems are still developing, and they do not yet have partial immune protection from surviving repeated bouts of malaria. Malaria parasites also have sophisticated strategies for immune evasion, including residing in MHC class II-negative erythrocytes, general immune suppression of the host, and antigenic variation [5].

Given the difficulties with vector control and vaccination, it is clear that antimalarial treatments will be key in controlling and eradicating malaria [12]. Antimalarial agents tend to come from ethnobotany or war-time development efforts [13]. The first widely-used antimalarial, quinine, came from the bark of the cinchona tree in the Peruvian Amazon [14]. Quinine and its later derivative, chloroquine, are still effective antimalarials in the Americas, but are largely obsolete in Africa and Asia due to at least four chloroquine resistance founder events and strong directional selective sweeps [15].

Malaria is an ancient foe, and descriptions of intermittent fevers and proposed treatments can be found in Chinese physician Ge Hong's *Si Ku Quan Shu* (*Emergency Prescriptions Kept Up One's Sleeve*), which was first published in 340 A.D. [16]. One proposed treatment, *qing hao* (*Artemisia annua*) steeped in cold water, eventually led to what we now know as artemisinin [17, 18] - although it should be noted that the active natural product was not isolated until 1971 and Cold War politics prevented the widespread adoption of artemisinin for years afterward [13]. Artemisinin-based therapies are the core of most modern antimalarial therapies, and reports of delayed patient clearance and potential resistance to artemisinin have raised serious alarms over the future of malaria control [19].

In 1955, The World Health Organization (WHO) spearheaded the Global Malaria

Eradication Programme (GMEP). Culturally, the “golden age of antibiotics” led to a sense of invincibility against microbes, DDT (dichloro-diphenyl-trichloroethane) had been used with great success as an insecticide in World War II, and the antimalarial chloroquine was effective, easily available, and cheap. There was considerable optimism, but also considerable naivety regarding implementation and how quickly drug resistance could develop and spread. Fourteen years later, the GMEP was ended and worldwide malaria eradication was declared unachievable with the existing tools and resources. Despite this outcome, malaria was eradicated from many locales with mild to moderate transmission, including the United States of America (Figure 1.3.1). The WHO learned the hard way that applying a single strategy worldwide would not work, and that merely reducing transmission and case loads was not sufficient – total elimination with vigilant and long-term agile surveillance was required to prevent malaria resurgence [20].

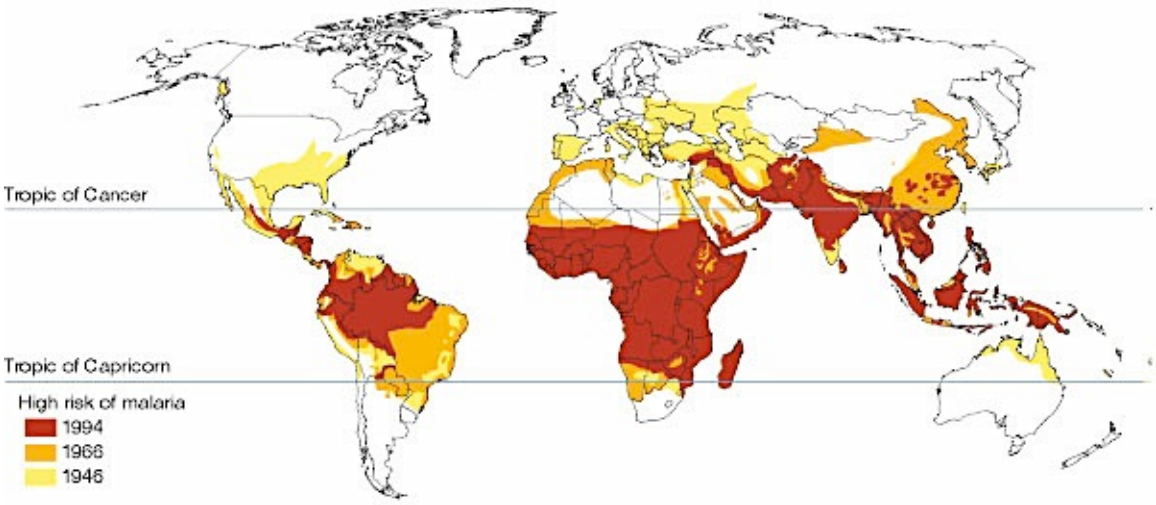

Figure 1.3.1: The risk of malaria infection over time (Sachs et al 2002) [21]

The last decade has seen a renewed commitment toward malaria control and eradication, and malaria deaths have fallen by 26% worldwide [1]. Research into the biology of the malaria parasite and mosquito vector have led to improved methods and

programs, such as intermittent preventative treatment for pregnant women and indoor residual spraying, as well as a larger arsenal of antimalarial drugs. However, the progress achieved is fragile and complacency as transmission and perceived risk decrease is a major concern. Complex societal issues such as poor health infrastructure, war and forced displacement, counterfeit or substandard drugs, loss of political will, and loss of financial support threaten to erode or even reverse recent gains. Rising drug resistance in the mosquito vector and the malaria parasite are also grave threats. Sustained commitment to key interventions (such as proper use of insecticide-treated bednets and access to effective, affordable antimalarial drugs) will be crucial.

1.4 DRUG RESISTANCE

Resistance has emerged to nearly all antimalarial drugs. *Plasmodium* parasites have a remarkably agile stress response, and drug pressure is no exception (Figure 1.4.1).

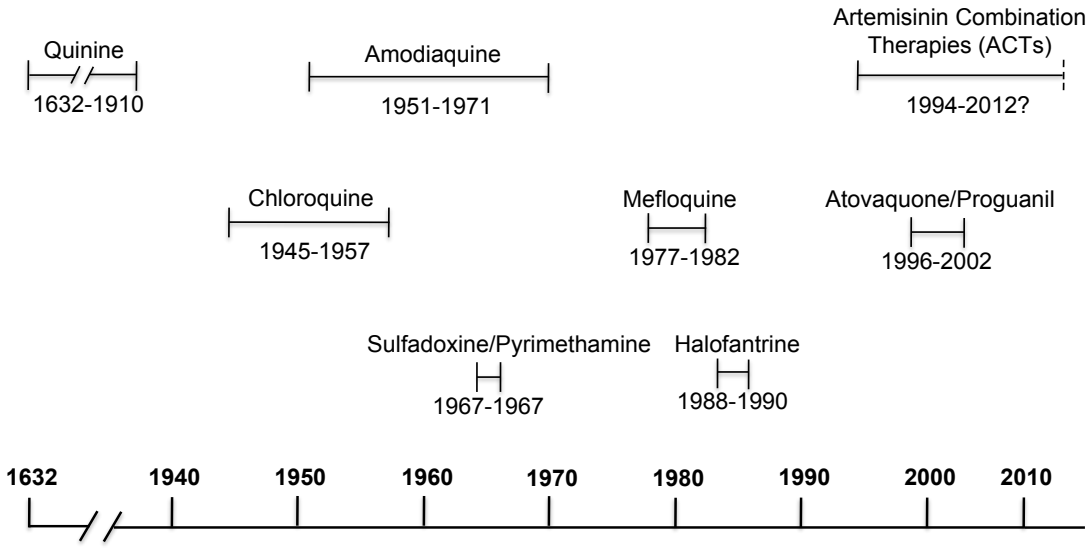

Data from Ekland, E. H. et al. (2008). *International Journal for Parasitology, 38(7), 743–747.*

Figure 1.4.1: Useful lifetimes of antimalarial therapies [22]

While some antimalarials, such as quinine, have had long effective lifetimes, other drugs have not – e.g., significant atovaquone resistance occurred during clinical trials, and 30% of treated patients recrudesced (meaning that the infection was not eliminated and subsequently bounced back, in this case with resistant parasites) [23]. No drugs with novel mechanisms of action will be ready for clinical use for at least five years [13], so research to protect new and old antimalarials from drug resistance will be critical. *In vitro* resistance selections can mirror *in vivo* patient isolate results, but are rarely identical. For example, chloroquine and mefloquine resistance are negatively correlated *in vitro* and *in vivo* [24]. Chloroquine resistance in the field is largely due to the K76T mutation in *pfcrt*, and *in vitro* chloroquine selections gave K76I or K76N mutations in *pfcrt* [25].

1.5 EVOLUTION, FITNESS, AND STRESS RESISTANCE

Malaria has co-evolved with humans, and each has shaped the other's genome (Figure 1.5.1). Human alleles that afford protection from malaria infection or severe disease largely match the distribution of malaria, even though several are highly deleterious when homozygous - e.g., heterozygous hemoglobin S protects from severe malaria, but homozygous hemoglobin S results in the disease sickle cell anemia (Figure 1.5.1 A). Conversely, alleles that allow parasites to escape selective pressures like the human immune system or antimalarial drugs (Figure 1.5.1 B) have emerged and spread [26].

Drug resistance is limited by trade-offs among growth, transmissibility, and resistance: fitness costs limit the diversity of escape pathways. For the *P. falciparum* dihydrofolate reductase inhibitor pyrimethamine, there is a single dominant resistance-fitness maximum accessible by a small number of mutational paths, and these paths are not equally accessible [27, 28]. Resistance can leave organisms vulnerable to other stresses. For example, M184V/I mutations in HIV-1 reverse transcriptase confer resistance to

nucleoside reverse transcriptase inhibitors such as lamivudine. However, these mutants are hypersensitive to zidovudine, stavudine, and tenofovir-DF, and have a compromised ability to incorporate natural nucleotide substrates [29]. Point mutations in the BCR-ABL kinase that drives chronic myeloid leukemia can give resistance to imatinib [30], but these mutated kinases differ in their transforming ability and second-generation inhibitors like nilotinib and dasatinib target many of the imatinib-resistant kinases [31]. We propose that the universal balance between fitness costs and the development of new traits can be exploited to prevent the development and spread of drug resistance.

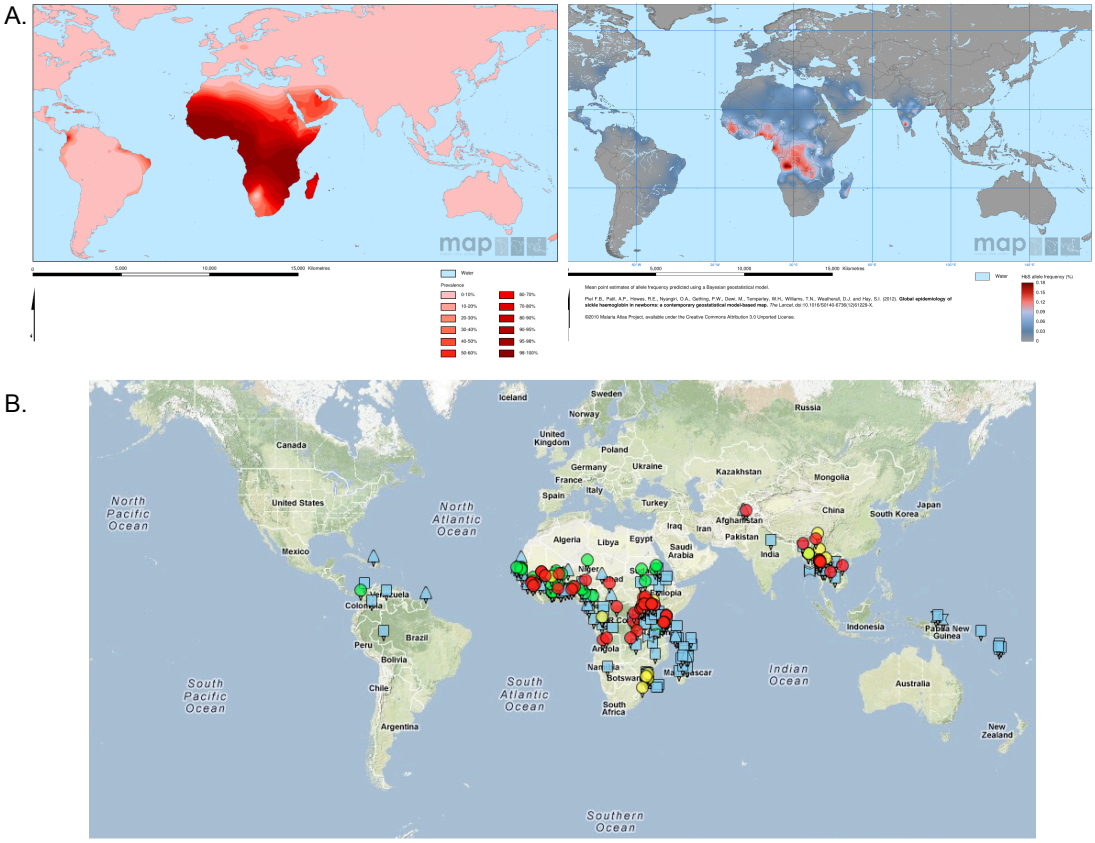

Figure 1.5.1: Co-evolution has shaped the human and *Plasmodium* genomes
(A). Malaria has shaped human evolution: the geographic distribution of alleles that give partial protection from malaria infection coincides with the distribution of malaria. Duffy negative erythrocytes, left, and hemoglobin S, right <http://www.map.ox.ac.uk/>
(B). Humans have shaped malaria evolution: the use of antimalarial chemotherapy has led to selective sweeps for *Plasmodium* spp. Observed antimalarial drug resistance (1975-2013). <http://www.wwarn.org/>

Evolutionary fitness impacts both the emergence of resistance in a single patient and its spread in a population. Conceptually, the strength of selective pressure will determine the relative fitness of wild-type (WT) and mutant-type (MT) parasites (Figure 1.5.2). A drug-resistant mutant is typically less fit than the WT at low concentrations of drug, and more fit at higher concentrations. The mutant selection window (MSW) defines the range of drug concentrations where a MT will outcompete the WT as long as it is reproducing above replacement levels (fitness = 1). The wild type growth window (WGW) is the range of drug concentrations where the WT will outcompete the MT – in this low drug range, treatment failures can occur without drug resistance. Treatment failure without resistance is often seen for protease inhibitor-based HIV-1 therapies, particularly with non-compliant patients [32]. Treatment failure with or without resistance can occur in the WGW-MSW overlapping area. Drug concentrations above the MSW theoretically kill everything, but such concentrations may not be physically possible due to toxicity or drug stability.

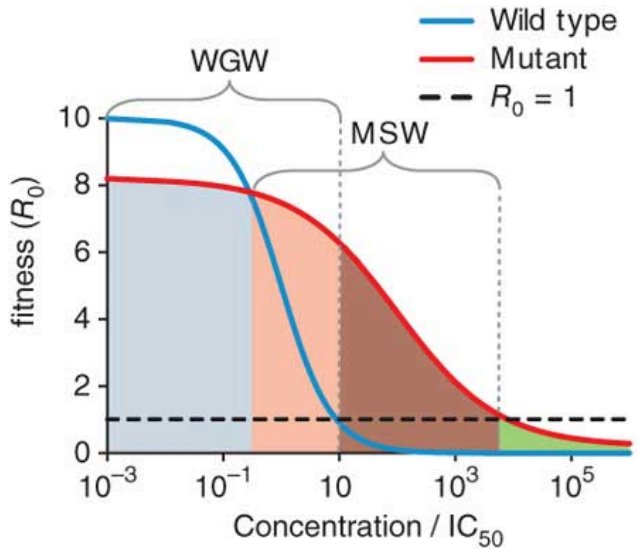

Figure 1.5.2: Selection windows that drive drug resistance and treatment failure (modified from Rosenbloom et al 2012) [32]

1.6 METHODS TO SUPPRESS DRUG RESISTANCE

The classic strategy for suppressing drug resistance is combination therapy, with the central idea being that it is difficult to become resistant to multiple compounds at the same time. Combination therapies may inhibit targets in different pathways, distinct nodes in the same pathway, or the same target in different ways [33]. They may also be synergistic, additive, or antagonistic (Figure 1.6.1).

In a synergistic combination, the effect of two compounds is greater than the additive sum of their individual effects. Synergistic combinations can be highly potent, but also provide strong selective pressure towards the development of resistance. In strongly antagonistic combinations, dubbed “suppressive” combinations, the effect of two compounds is less than the additive sum and even less than the individual effects – e.g., the compounds in some way mask the effect of each other.

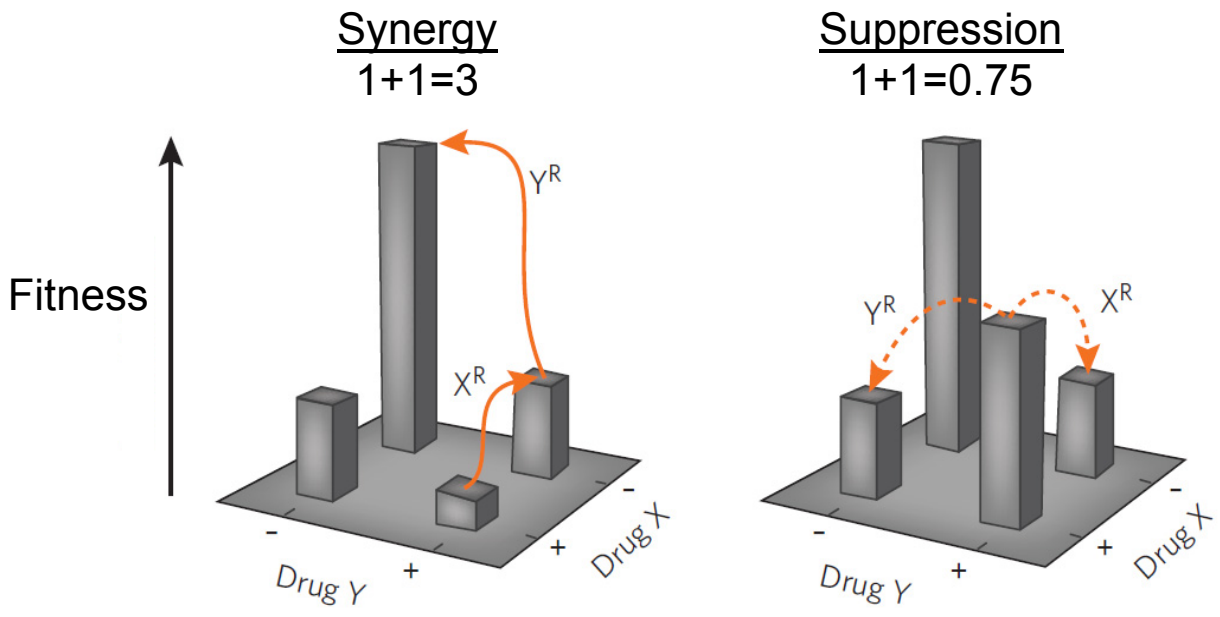

Figure 1.6.1: Fitness and resistance to combination therapies: synergy versus strong antagonism (“suppression”) (modified from Chait et al 2012 [34])

In a suppressive combination, an organism is more fit if it remains sensitive to both compounds than if it gains resistance to one. Thus, resistant organisms are at a fitness disadvantage compared to the parental sensitive type, and will be outcompeted. Gaining stepwise resistance to both compounds is less likely in a suppressive combination than in a synergistic combination [35, 36, 37].

We propose an alternative strategy for combination therapy which we call “targeting resistance” (Figure 1.6.2): simultaneously inhibiting the wild-type and the most fit mutant forms can suppress the emergence of competitively viable resistance. If an organism becomes resistant to the wild-type inhibitor, it will very likely be through one of few resistance pathways that maintain a competitive level of fitness. These pathways can be anticipated and pre-emptively blocked. Resistance to the wild-type compound would result in increased sensitivity to the mutant-type compound. With appropriate combinations, the risk of resistance is reduced as resistance to one compound decreases fitness more than remaining sensitive to both.

We explore here the possibility of blocking the emergence of resistance with a population biology trap: by identifying situations where resistance to one compound confers hypersensitivity to another, we can design combination therapies that not only kill the parasite, but also guide its evolution away from resistance. This concept trades short-term potency for long-term protection from resistance. We tested the idea of “targeting resistance” with antimalarial agents not yet in clinical use in an effort to protect their efficacy once deployed. The antimalarial agents discussed block pyrimidine biosynthesis by inhibiting the enzyme dihydroorotate dehydrogenase (DHODH).

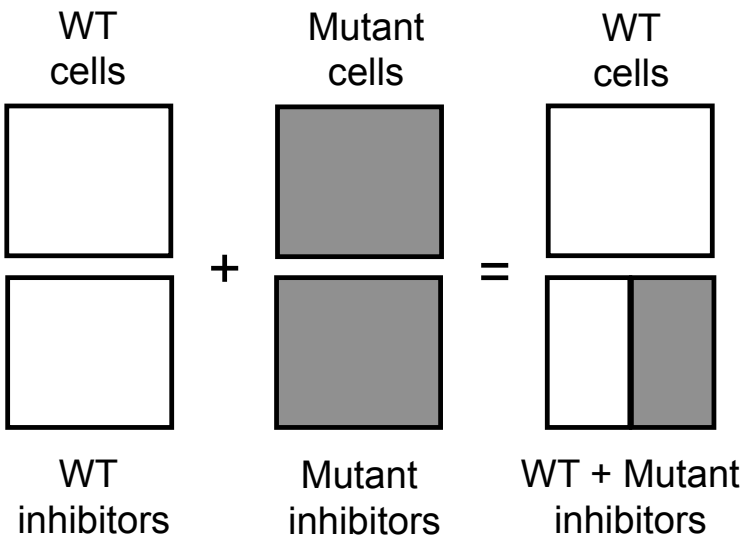

Figure 1.6.2: Targeting resistance: combining wild-type and mutant-type drugs suppresses resistance

In "targeting resistance," WT parasites are inhibited by WT inhibitors. The small population of emerging resistant mutants is inhibited by mutant inhibitors. Combining WT and mutant inhibitors should prevent the emergence of highly fit, and thus viable, resistant mutants.

1.7 PYRIMIDINE BIOSYNTHESIS

Pyrimidines - including thiamine (vitamin B1) and the nucleobases thymine, cytosine, and uracil - are ubiquitous and essential in cells. There are two ways to obtain pyrimidines: *de novo* synthesis and salvage. Humans can do both, and salvage is sufficient for nearly all cell types. Exceptions include rapidly-proliferating lymphocytes, which was exploited for the treatment of rheumatoid arthritis with the HsDHODH inhibitor Leflunomide [38], and the fetal neural crest. Partial disruption of HsDHODH function during fetal development results in abnormal neural crest-derived tissues, resulting in postaxial acrofacial dysostosis (Miller syndrome) [39]. Unlike humans, malaria parasites lack pyrimidine salvage pathways, and are completely reliant upon *de novo* synthesis [40]. The enzyme dihydroorotate dehydrogenase (DHODH) is the rate-limiting step in pyrimidine biosynthesis.

DHODH enzymes are broadly categorized in two classes (Table 1.7.1), which differ in their final electron acceptor, subcellular localization, oligomerization state, and catalytic residue. Humans and *Plasmodium* parasites both have class II DHODH enzymes.

Table 1.7.1: Classes of dihydroorotate dehydrogenase (DHODH) enzymes

Class	Electron acceptor	Location	Example	Oligomerization	Catalytic base
IA	Fumarate	Cytosol	*Saccharomyces cerevisiae*	Homodimer	Cysteine
IB	NAD^+	Cytosol	*Bacillus subtilis*	Heterotetramer	Cysteine
IS	NAD^+	Cytosol	*Sulfolobus solfataricus*	Heterotetramer	Serine
II	Ubiquinone	Membrane	*Plasmodium spp., Homo sapiens*	Monomer	Serine

Crystal structures showed significant structural differences in the human and *P. falciparum* DHODH enzymes, which suggested the possibility of selective inhibitors [41, 42]. PfDHODH is anchored in the inner mitochondrial membrane, where it couples the reduction of L-dihydroorotate to orotate with the oxidation of respiratory chain ubiquinone to dihydro-ubiquinone (Figure 1.7.1). The ping-pong redox reaction catalyzed by PfDHODH is the rate-limiting step in pyrimidine biosynthesis. Several groups have developed inhibitors specific for the human or malarial enzymes (Figure 1.7.2) [43, 44], and PfDHODH is seen as a promising antimalarial drug target [45, 46].

Parallel efforts at the University of Texas at Southwestern [47], GlaxoSmithKline [48], and Harvard [49] led to the development of several structural classes of PfDHODH inhibitors. Several of these compounds are active in rodent models of disease and are progressing in the drug development pipeline [44, 50].

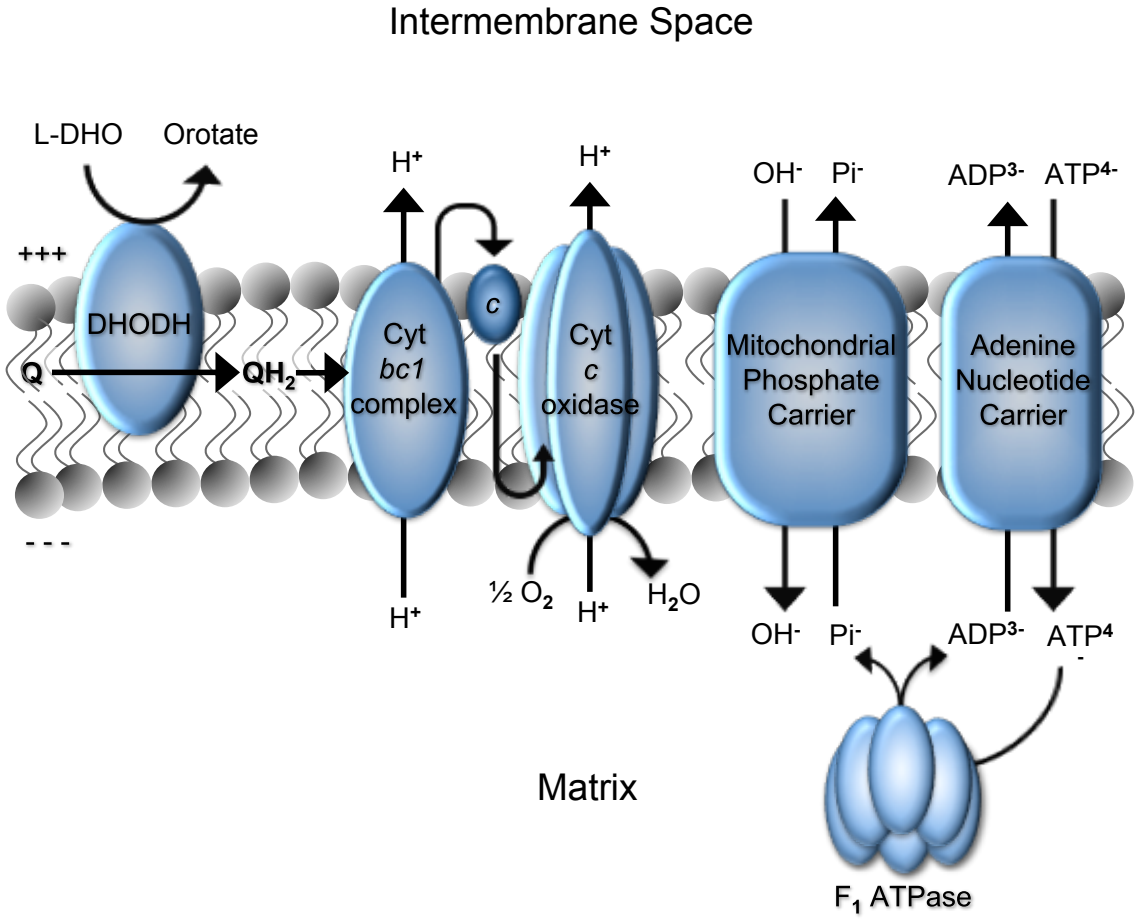

Figure 1.7.1: The *Plasmodium* mitochondrial electron transport chain

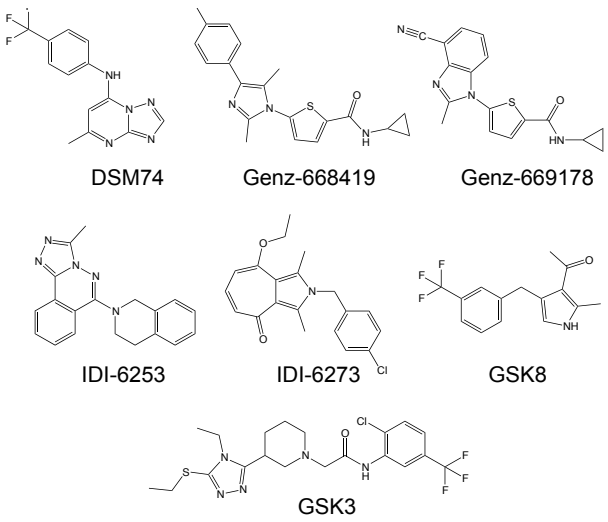

Compound	SMILES
DSM74	FC(F)(F)C1=CC=C(NC2=CC(C)=NC3=NC=NN32)C=C1
Genz-668419	O=C(NC1CC1)C2=CC=C(N3C(C)=C(C4=CC=C(F)C=C4)N=C3C)S2
Genz-669178	O=C(NC1CC1)C2=CC=C(N3C(C=CC=C4C#N)=C4N=C3C)S2
IDI-6253	CC1=NN=C2C3=C(C=CC=C3)C(N4CCC5=C(C=CC=C5)C4)=NN21
IDI-6273	ClC1=CC=C(CN2C(C)=C3C(C=CC=C(OCC)C3=C2C)=O)C=C1
GSK3	CCSC1=NN=C(N1CC)C2CCCN(C2)CC(NC3=C(Cl)C=CC(C(F)(F)F)=C3)=O
GSK8	CC(C1=C(NC=C1CC2=CC=CC(C(F)(F)F)=C2)C)=O

Figure 1.7.2: PfDHODH inhibitors

1.8 STRUCTURE OF THE THESIS

In this work, we sought to better understand drug resistance in *Plasmodium falciparum*, the causative agent of the most severe form of human malaria, and to design strategies to help suppress the emergence of resistance. We used *in vitro* drug resistance selections to identify optimal resistance pathways to PfDHODH inhibitors. Protein activity assays recapitulated the changes in drug sensitivity seen in selected parasite lines, suggesting that point mutations in the target gene *pfdhodh* explain the observed changes. We then used the concepts of evolutionary fitness and competitive advantage to set a trap: by pairing antimalarial drugs targeting the sensitive and resistant alleles of a target gene, we can prevent the spread of those resistant alleles. This strategy, coined "targeting resistance," would maintain a sensitive population and thereby extend the useful lifetime for antimalarial drugs.

Chapter Two:

Evolutionary Oscillations for a Highly Fit PfDHODH Mutant

2.1 ATTRIBUTIONS

Leila S. Ross[1], Amanda K. Lukens[2], Amar bir Singh Sidhu[1], Richard Heidebrecht[1,2], Francisco-Javier Gamo[3], Maria Jose Lafuente-Monasterio[3], Michael L. Booker[4], Roger C. Wiegand[2], Dyann F. Wirth[1,2]

1. Department of Immunology and Infectious Diseases, Harvard School of Public Health, Boston, MA
2. Infectious Disease Initiative, Broad Institute, Cambridge, MA
3. Tres Cantos Medicine Development Campus, GlaxoSmithKline, Tres Cantos, Spain
4. Genzyme Corporation, Waltham, MA

Chemical synthesis was carried out by R.H., F-J.G, M.J.L-M. and M.L.B. M.L.B performed a PfDHODH screen which led to the Genz-666136 series of compounds. F-J.G. and M. J.L-M performed a PfDHODH screen which led to the GSK3 and GSK8 compounds. A.B-S.S performed the selection that resulted in the PfDHODH E182D, PfDHODH F227I, and PfDHODH L531F mutants. A.K.L. performed initial characterization of A.B-S.S's selected parasite lines. L.S.R. performed all parasite proliferation assays shown. L.S.R. performed the selection that resulted in the PfDHODH E182D: D182E parasite line. Cloning, purification, and biochemical assays with recombinant PfDHODH protein were performed by L.S.R. Competitive growth assays and allelic discrimination analysis were performed by L.S.R.

Funding for this work was provided by grants from the Medicines for Malaria Venture, the Bill and Melinda Gates Foundation, the Broad Institute SPARC program, the Genzyme Humanitarian Assistance for Neglected Disease Program, and NIH grant R01 AI093716-01A1.

2.2 INTRODUCTION

The evolution of new traits requires diversity and selection. In *Plasmodium* parasites, population diversity is generated through sexual recombination in the mosquito, errors in DNA replication and repair, and random sampling of genomic amplifications [51]. Selection occurs through parasite-host interactions such as immune responses as well as more modern forces such as antimalarial drugs.

Malaria is currently preventable and treatable. This is threatened by rising levels of resistance of the mosquito vector to insecticides and of the parasite to antimalarial drugs. Drug resistance can develop quickly in malaria: in the case of atovaquone, resistance emerged during clinical trials and 30% of treated patients recrudesced with resistant parasites [23]. The antimalarial pipeline contains few compounds with novel mechanisms of action [52], so cross-resistance with existing therapies is a major concern.

The control and eradication of malaria requires a steady supply of cheap, stable, and effective antimalarial drugs that are safe for entire populations, including pregnant women and infants. Drug resistance complicates this already-lofty goal. Given that an infected person may on the order of 10^{10} - 10^{13} parasites in their bodies, and that there are an estimated 350-500 million cases of malaria per year, the potential for resistance is enormous [53]. New therapies must take potential resistance into account, or we will forever be in a Red Queen's race where each new drug only buys a short amount of time before becoming obsolete.

Methods to limit resistance have largely relied on combination therapy, where the driving concept is that it is more difficult to become resistant to two compounds than one. This is logical, but the truth is more complicated. Synergistic combinations, often chosen

because of their greater-than-additive potency, actually accelerate the evolution of drug resistance when compared to single drugs or antagonistic combinations [54]. This is thought to be because a mutant resistant to one of the two drugs has a selective advantage over the sensitive parent. Conversely, strongly antagonistic combinations, referred to as “suppressive” combinations, select away from resistance [36]. Thus, it would be wise to trade in short-term potency for long-term resistance suppression.

Evolutionary fitness constraints limit the diversity of resistance pathways in a population. In *Plasmodium falciparum*, pyrimethamine resistance is best accomplished with a quadruple mutant in dihydrofolate reductase (DHFR). Although there are twenty-four (i.e., 4!) possible orders of mutations to get these four residues, three pathways account for 90% of observed resistance, and all veer to the same outcome of four specific mutated residues. Similarly, a limited number of paths to resistance were followed with high probability for bacterial beta-lactamase inhibitors, indicating that this is a widespread phenomenon that applies to both prokaryotes and eukaryotes [27].

Over time, compensatory mutations can restore fitness [55] – this expands the number of possible resistance pathways. Thus, acting early to prevent the initial emergence of resistance may restrict parasite options to those few heavily favored, highly fit pathways. These pathways can be predicted through *in vitro* selection experiments [22], and pre-emptively blocked through the development of mutant-selective inhibitors. As a caveat, *in vitro* experiments do not replicate a key factor of human infection: the immune response.

Identifying and combining antimalarial compounds that selectively target the bulk wild-type (WT) population and the small, emerging resistant population (mutant type, MT) is

a novel approach to antimalarial combination therapy. We tested this idea, coined "targeting resistance," with antimalarial agents targeting pyrimidine biosynthesis.

We performed resistance selections with PfDHODH inhibitors against wild-type parasites (3D7 and Dd2). Characterization of the resulting resistant lines showed point mutations in the PfDHODH target: E182D, F227I, and L531F. Testing of a small set of PfDHODH inhibitors revealed an interesting pattern: while cross-resistance was observed, as expected, for structurally related compounds, different structural classes of inhibitors were often unaffected or even more potent against the mutant parasites than the parental wild-type. We performed further resistance selections with these mutant-selective inhibitors. Selection of the 3D7 E182D parasite line with IDI-6273, a mutant-selective inhibitor, led to a novel mutation in *pfdhodh* that resulted in a reversion to the wild-type protein sequence. Simultaneous selection of a Dd2 wild-type parasite with a combination of Genz-669178 (a wild-type inhibitor) and IDI-6273 (a mutant-selective inhibitor) did not yield resistance in 80 days. Activity assays with purified protein recapitulated the results seen in whole cells, and suggest that the PfDHODH E182D mutant has a lower catalytic efficiency than the wild-type protein.

2.3 MATERIALS AND METHODS

PARASITE CULTURE:

The erythrocytic stages of *P. falciparum* were grown at 37°C in solutions of 4% O+ hematocrit in RPMI 1640 medium supplemented with 28 mM $NaHCO_3$, 25 mM HEPES, 5% albumax II (w/v), and 20 µm gentamicin sulfate. Human blood was supplied from Research Blood Components or Interstate Blood Bank. Cultures were grown in a gas mixture of 5% O_2, 5% CO_2, and 90% N_2. Cultures were maintained with media changes every other day and were sub-cultured to maintain parasitemia below 4%. At least 25% of the hematocrit was replaced weekly. Parasite growth was synchronized by treatment with sorbitol [56]. Frozen stocks were prepared using a sterile solution composed of 28% glycerol, 3% sorbitol, and 0.65% sodium chloride. The Dd2 parasite used was MR4 strain MRA-156.

RESISTANCE SELECTION:

Approximately 1 x 10^9 ring stage Dd2 or 3D7 parasites were treated with ten times the EC_{50} of a compound for 6-8 days in four independent flasks to eliminate all viable parasites visible by microscopy. Compound pressure was then removed and the cultures were fed on alternate days with compound-free complete RPMI media. Once healthy parasites reappeared in the culture flasks, compound exposure was repeated. These steps were executed for 30-60 days. Selected parasites were cloned by limiting dilution in a 96-well plate with an inoculum of 0.5 infected red blood cells per well. Parasite clones were detected after 2.5 weeks of growth by microscopy.

GENOMIC DNA ANALYSIS:

Genomic DNA was extracted from parasites using the QIAamp blood kit (Qiagen) for sequence analysis of the *pfdhodh* gene (PlasmoDB ID: Pf3D7_0603300). A 2.2 kb

fragment encompassing the complete *pfdhodh* ORF was PCR amplified from drug-resistant clones and parental lines (primer sequences below). PCR-amplified fragments were fully sequenced using *pfdhodh*-specific primers. The *pfmdr1* and *pfcrt* genetic determinants of Genz-666136-resistant clones were analyzed using previously published protocols, and comparison was performed with the parental lines [57].

PfDHODH Forward 5'- GATCCCTAGGATGATCTCTAAATTGAAACCTCAATTTATG -3'
PfDHODH Reverse 5'- GATACTCGAGTTAACTTTTGCTATGCTTTCGGCCAATG -3'
PfDHODH internal 5'- CATTATTTGGATTATATGGTTTTTTTGAATCTTATAATCCTG -3'

The *pfdhodh* gene was amplified with Pfu Ultra II Fusion DNA polymerase (Agilent) with the following conditions: 95°C 120 seconds, 55°C 20 seconds, 60°C 100 seconds, go to step two and repeat 30 times. PCR amplicons were purified with a PCR clean-up kit (Qiagen) and sequenced via Genewiz.

WHOLE GENOME SEQUENCING AND ANALYSIS:

Genomic DNA was sheared and made into a 200 bp fragment Illumina sequencing library, and sequenced with paired-end reads on an Illumina GAIIx machine at the Broad Institute. The sequenced reads were aligned against the *P. falciparum* 3D7 reference from PlasmoDB (version 7.1*) [58] using BWA version 0.5.7 [59]. Duplicate reads were marked using the Picard MarkDuplicates tool <http://picard.sourceforge.net/>. The consensus bases were called using the Genome Analysis Toolkit's (GATK) Unified Genotyper (version 1.0.5974) [60] and the SAMtools (version 0.1.16)[61] mpileup command. Only bases that were called as homozygous for the reference or the alternate allele with a genotype quality of at least 30 were considered. The GATK Unified Genotyper called 3685 SNPs in the Genz-66136-resistant strain relative to stock (2108 intergenic, 248 intronic, 423 synonymous coding and 906 nonsynonymous coding). By contrast, only 47 SNPs passed all the quality filters when using the SAMtools genotyper (25 intergenic, 2 intronic, 3 synonymous, 17 nonsynonymous). Of these, only eight overlapped with the

GATK set (2 intergenic and 6 nonsynonymous). The nonsynonymous mutations fell in four genes: 1) F227I in PFF0160c (the *dhodh* gene), 2) I352T and E355D in PF07_0111, a highly polymorphic gene of unknown function, 3) adjacent mutations in the PfEMP PF08_0106, and 4) I1548M in PFI1280c, a putative protein kinase that is also highly polymorphic. Whole genome sequencing was also performed for the 3D7 E172D: D182E parasite line with similar procedures and results.

IN VITRO DRUG SENSITIVITY AND EC_{50} DETERMINATIONS:

Drug susceptibility was measured using the SYBR Green method [62]. Twelve point curves based on 2-fold dilutions of the test compound were carried out in triplicate and replicated on three different days. EC_{50} values were calculated using the log(inhibitor) vs. response – Variable slope equation in GraphPad Prism version 5.0d (described below):

$$Y = Bottom + \frac{(Top - Bottom)}{1 + 10^{\,Log(IC50 - X) \times Hill\ Slope}}$$

Where X = concentration of compound, and Y = normalized percent viability.

Note that the fold-change values are the EC_{50} of the described parasite line divided by that of the parent for a single, paired assay – so the fold changes may not exactly match the EC_{50} values given if different cultures were assayed on different days (and are thus normalized to different parental values than what is shown). The trends are very similar even if the exact numbers do not match.

SYNTHESIS OF DSM74:

The compound DSM74 was prepared following the literature procedure [63] and was recrystallized from ethanol. ^{1}H NMR spectra matched reported results [43] and HPLC analysis indicated > 95% purity.

SYNTHESIS OF GSK8:

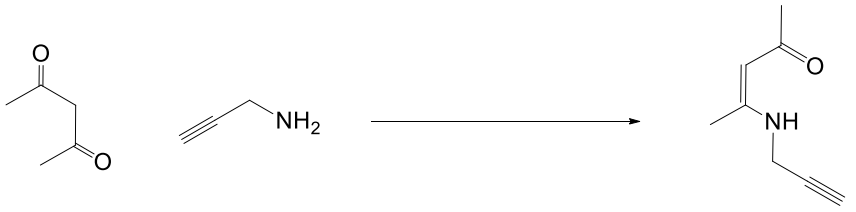

Pentane-2,4-dione (0.206 mL, 2.00 mmol) was added to a solution of 2-propyn-1-amine (0.274 mL, 4.00 mmol) in water (5 mL) and the resulting mixture was stirred at room temperature for 16 hr. The reaction was extracted with dichloromethane and the organic layer was dried over anhydrous Na_2SO_4, filtered, and concentrated under reduced pressure to give 275 mg of (Z)-4-(prop-2-yn-1-ylamino)pent-3-en-2-one (275 mg, 2.005 mmol, 100 % yield) as a yellow oil: ^{1}H-NMR ($CDCl_3$, 400 MHz) *d* 2.02 (s, 3H), 2.28 (t, *J* = 2.4 Hz, 1H), 3.99 (dd, *J* = 6.2, 2.4 Hz, 2H), 5.06 (s, 1H), 10.76 (br. s, 1H). MS: m/e 138 ($M+H^+$). Purity was determined as >95 % by HPLC (308 nm), Rt: 0.95 (Acquity UPLC BEH C18 1.7u 3x50mm, $CH_3CO_2NH_4$ 25mM + 10%ACN at pH 6.6 / ACN).

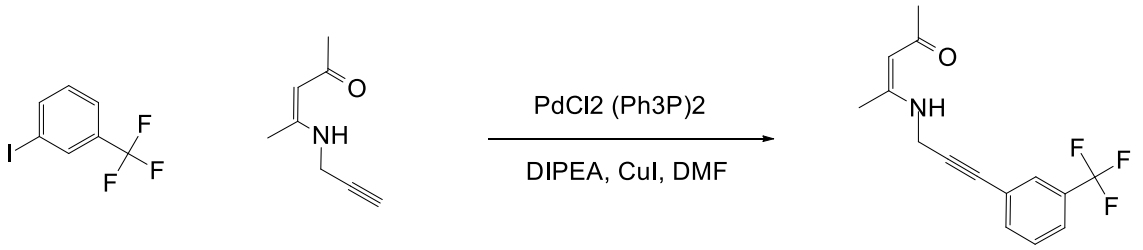

To a solution of (Z)-4-(prop-2-yn-1-ylamino)pent-3-en-2-one (260 mg, 1.895 mmol), CuI (7.22 mg, 0.038 mmol), $PdCl_2(Ph_3P)_2$ (26.6 mg, 0.038 mmol) and DIPEA (3.89 mL, 22.74 mmol) in *N,N*-Dimethylformamide (DMF) (1 mL) under argon atmosphere, 3-iodobenzotrifluoride (0.410 mL, 2.84 mmol) was added and the resultant mixture was stirred at room temperature for 1 h 45 min, the reaction was partitioned between water and EtOAc. The layers were separated and the aqueous was extracted with EtOAc. The combination of the organic layers was washed with aq. 0.5 N HCl and brine. After drying

over anhydrous Na_2SO_4, the organic layer was filtered and concentrated under reduced pressure. The resulting crude was purified by column chromatography (10g, Merck, CyHex:EtOAc gradients from 100:0 to 90:10 to 50:50) to give 365 mg of (Z)-4-((3-(3-(trifluoromethyl)phenyl)prop-2-yn-1-yl)amino)pent-3-en-2-one (365 mg, 1.298 mmol, 68.5 % yield) as a yellow solid: ^{1}H-NMR ($CDCl_3$, 400 MHz) *d* 2.04 (s, 3H), 2.07 (s, 3H), 4.23 (d, *J* = 6.1 Hz, 2H), 5.09 (s, 1H), 7.43 (t, *J* = 7.7 Hz, 1H), 7.58 (m, 2H), 7.67 (s, 1H), 10.87 (br. s, 1H). MS: m/e 282 ($M+H^+$). Purity was determined as > 95 % by HPLC (309 nm), Rt: 1.28 (Acquity UPLC BEH C18 1.7u 3x50mm, $CH_3CO_2NH_4$ 25mM + 10% ACN at pH 6.6 / ACN).

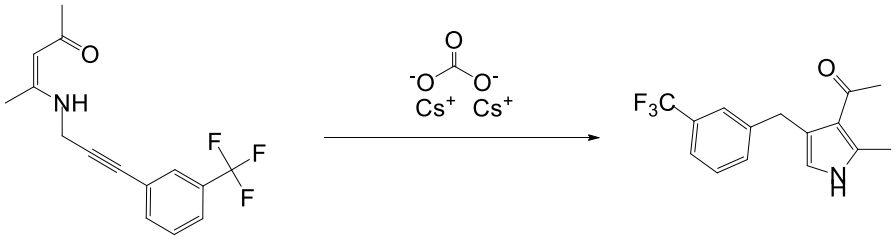

To a solution of 3-iodobenzotrifluoride (100 mg, 0.368 mmol) in anhydrous Dimethyl Sulfoxide (DMSO) (5 mL) under argon atmosphere, cesium carbonate (240 mg, 0.735 mmol) was added and the resultant mixture was stirred at room temperature for 1 h. The reaction was then diluted with EtOAc and 0.5 N aq. HCl. The layers were separated and the aqueous was extracted with EtOAc. The combination of the organic layers was washed with water, then brine, and then dried over anhydrous Na_2SO_4, filtered, and concentrated under reduced pressure. The resulting crude was purified by column chromatography (dry head, 2g, Isolute, CyHex:EtOAc gradients from 100:0 to 80:20 to 0:100) to give 83 mg of 1-(2-methyl-4-(3-(trifluoromethyl)benzyl)-1H-pyrrol-3-yl)ethanone as a pale brown solid: ^{1}H-NMR (DMSO-D_6, 400 MHz) *d* 2.24 (s, 3H), 2.42 (s, 3H), 4.03 (s, 2H), 6.36, (d, *J* = 3 Hz, 1H), 7.46 (m, 4H), 11.05 (s, 1H). ^{13}C-NMR (DMSO-D_6, 100

MHz) d 15.4, 31.2, 32.9, 120.1, 122.7 (t, *J* = 3.7 Hz), 123.3, 125.0 (q, *J* = 272 Hz), 125.3 (q, J = 3.7 Hz), 129.2 (q, *J* = 31.5 Hz), 129.5,133,2, 135.9, 144.2, 193.9. ^{19}F-NMR (DMSO-D6, 376 MHz) *d* -60.8 (s, 3F). MS: m/e 282 ($M+H^+$). Purity was > 95 % by HPLC (249 nm), Rt: 1.20 (Acquity UPLC BEH C18 1.7u 3x50 mm, $CH_3CO_2NH_4$ 25mM + 10% ACN at pH 6.6 / ACN).

PFDHODH PLASMID CONSTRUCTION AND MUTAGENESIS:

A synthetic codon-optimized gene encoding residues 159-565 of PfDHODH [41] (Genbank accession No. AY685129) was cloned into a pET28b plasmid with an amino-terminal 6xHistidine tag followed by an rTEV cleavage site as described by Deng et al [64], resulting in pET28b-6xHistidine-rTEV-PfDHODH (codon optimized) del 1-158. The PfDHODH E182D mutation was created with the following primers, then cloned into the tagged pET28b construct described above:

E182D Forward	5'-GTACATCGATGGTGACATTTGCCATGACCTG-3'
E182D Reverse	5'-CAGGTCATGGCAAATGTCACCATCGATGTAC-3'

PFDHODH PROTEIN EXPRESSION AND PURIFICATION:

BL21(DE3)Star *Escherichia coli* (Invitrogen) were transformed with WT and E182D PfDHODH expression constructs. Transformed cells were grown in Terrific Broth with 100 µg/mL kanamycin at 37°C and 180 rpm, then dropped to 20°C and induced with 200 µm isopropyl-D-thiogalactoside. Cultures were grown 12-16 hours post-induction, then pelleted by centrifµation at 10,000*x g* and frozen at -80°C for later use. For purification, conical tubes of frozen cell pellets were thawed in 25°C water. Thawed pellets were then resuspended in buffer A (100 mM HEPES pH 8.0, 150 mM NaCl, 10% glycerol, 0.05% Thesit). The cells were lysed by sonication on ice (Branson digital sonifer 450, 5 minutes at 40% amplitude with a pattern of 5 seconds on and 10 seconds off). The cell lysate was clarified by centrifugation at 40,000 *x g* for 45 minutes at 4°C, then filtered through a

0.45 µm filter. The clarified and filtered lysate was applied to a HisPrep FF 16/10 column (GE Healthcare) pre-equilibrated with buffer A on an AKTA Purifier FPLC. The column was washed with 30 cV of buffer A, then eluted with stepwise increments of buffer B (100 mM HEPES pH 8.0, 150 mM NaCl, 10 glycerol, 0.05% Thesit, 400 mM imidazole). The eluted protein was concentrated by centrifugation in concentrator spin columns (Pierce), then injected into a HiLoad 16/60 Superdex 200 size exclusion column pre-equilibrated with running buffer (10 mM HEPES pH 7.8, 100 mM NaCl, 5% glycerol, 1 mM *N,N*-dimethyldodecylamine *N*-oxide, 10 mM DTT). Fractions containing PfDHODH were pooled and concentrated. Protein concentration was assessed by Bradford assay (Pierce). Catalytically active protein concentration was assessed by boiling 50 µLof protein, clarifying by centrifugation for 10 minutes at 13,200*x g*, and then measuring absorbance of the cleared supernatant at 445 nm to determine the flavin mononucleotide concentration (ε_{445} = 12.5 mM^{-1} cm^{-1}). Aliquots of protein were flash-frozen in liquid nitrogen, then stored at -80°C.

PfDHODH BIOCHEMICAL ASSAYS:

Substrate-dependent inhibition of recombinant PfDHODH protein was assessed in an *in vitro* assay in 60 µLvolumes in 384-well clear plates (Corning 3702). A 16-point dilution series of inhibitor concentrations were assayed against 2-10 nM protein with 500 µm µm L-dihydroorotate substrate (L-DHO, excess), 18 mM dodecylubiquinone electron acceptor (CoQ_D, ~ Km), and 100 µm 2,6-dichloro-indophenol indicator dye in DHODH assay buffer (100 mM HEPES pH 8.0, 150 mM NaCl, 5% glycerol, 0.5% Triton X-100). Assays were incubated at 25°C for twenty minutes, then assessed by measuring the absorbance at 600 nM in a SpectraMax M5 plate reader. Molecular oxygen, which can act as an electron acceptor in this reaction, was depleted through the addition of 0.1 mg/mL of glucose oxidase, 0.02 mg/mL of catalase, and 50 mM glucose, followed by

incubation at 25° for five minutes prior to assay assembly. Data were normalized to 1% DMSO and excess inhibitor (500 nM Genz-669178 unless another compound was appropriate). Steady-state kinetic parameters were determined by directly assessing the production of orotic acid (ε_{296} = 4.3 mM^{-1} cm^{-1}) in UV-transparent 384-well plates (Corning 3672). For enzyme oxidase activity, 100 nM of enzyme was assayed against a range of L-DHO concentrations (5-500 uM). For oxidant affinity, 5-50 nM of enzyme was assayed against a range of CoQd (1-150 uM) or dissolved molecular oxygen (~300 uM) with excess substrate (500 μm L-DHO). Unless otherwise specified, oxygen was depleted from the reactions using the glucose oxidase-catalase system described above. Data were fitted to the Michaelis-Menten equation in GraphPad Prism 5 to determine the steady-state parameters (kcat and Km).

$$Y = \frac{(Et \times X)}{(Km + X)}$$

Y = enzyme velocity, Et = total enzyme concentration, and X = substrate concentration.

COMPARATIVE FITNESS ASSAYS:

Parasite lines to be used were synchronized with sorbitol [56] for two consecutive life cycles. 2 mL cultures were seeded in triplicate with a mixture of two synchronized parasite lines. Initial parasitemia was 1% total in 4% hematocrit. Cultures were grown at 37°C in complete RPMI with 40 rpm gentle shaking. 80-90% of the cultures were taken every other day (one life cycle) to isolate genomic DNA. This DNA was then analyzed by allelic discrimination qPCR to determine the relative ratios of the two parasite lines in question (primers and reporters listed on page 31, polymorphism site bolded and underlined). Note that at this parasitemia and hematocrit, there is no competition for red blood cells, so this assay measures comparative growth and not competitive growth.

Parasite lines	Forward primer	Reverse primer	Reporter 1 (VIC), Wild-type	Reporter 2 (FAM), Mutant
3D7 versus 3D7: E182D	TGGTTTTT TTGAATCT TATAATCC TGAATTTT TTT	CTATCATT ACTAGTAT CATATGGT AATATATT ATATTTTC	ATTGATGGTG A**A**ATATGTC	ATTGATGGTG A**T**ATATGTC
3D7 versus 3D7: D182E	TGGTTTTT TTGAATCT TATAATCC TGAATTTT TTT	CTATCATT ACTAGTAT CATATGGT AATATATT ATATTTTC	ATTGATGGTG A**A**ATATGT	TTGATGGTGA **G**ATATGT

Competitive growth assays were carried out for six generations. Allelic discrimination assays were performed with TaqMan Universal PCR Master Mix with no AmpErase UNG (Applied Biosystems) on a 7900 HT real-time PCR machine (Applied Biosystems). Cycling conditions were 95°C for 10 minutes, followed by 45 cycles of 95°C for 15 seconds and 56°C for 1 minute.

STATISTICAL ANALYSES:

EC_{50} data are shown as mean ± standard deviation and were analyzed by one-way ANOVA with Dunnett's multiple comparison *post hoc* test (for three or more groups) or a two-tailed t-test (for two groups) via Graph Pad Prism 5.0d Software. Differences were considered significant for $P < 0.05$.

2.4 RESULTS

PRIMARY PFDHODH INHIBITOR SELECTIONS: WILD-TYPE PARASITES

Two classes of PfDHODH inhibitors are the alkylthiophenes [44] and the triazolopyrimidines [43] (Figure 2.4.1).

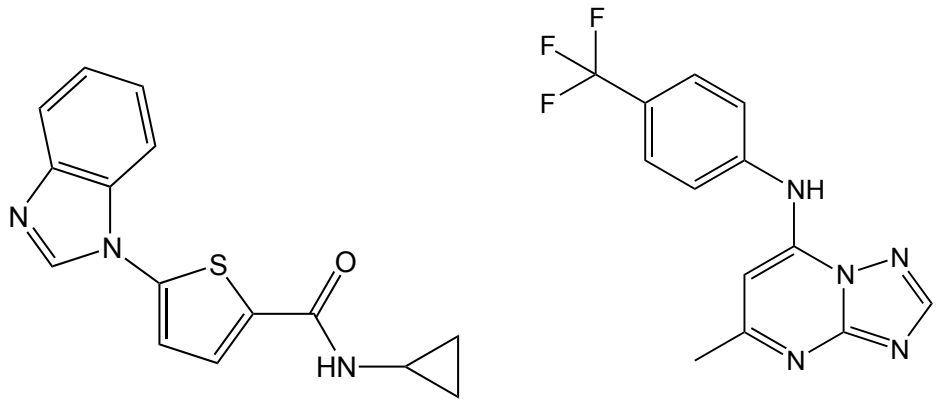

Genz-666136 DSM74

Figure 2.4.1: Two classes of PfDHODH inhibitors
Alkylthiophenes (left) and triazolopyrimidines (right)

We did *in vitro* resistance selections on a lead candidate from each inhibitor class: Genz-666136 and DSM74. Genz-66136 is closely related to the derivatives Genz-668419 and Genz-669178, both of which are discussed later. We carried out selections with these two compounds against two well-characterized parasite lines, 3D7 and Dd2 (Table 2.4.1).

Table 2.4.1: Initial PfDHODH inhibitor resistance selections

Selection Information			PfDHODH allele		
Parasite Line	**Drug**	**Resistance**	**Residue**	**Nucleotide**	**Copy #**
Dd2	Genz-666136	Y	F227I	T687A	1
	DSM74	Y	L531F	G1593T	1
3D7	Genz-666136	Y	E182D	A516T	1
	DSM74	Y	E182D	A516T	1

These selections resulted in three point mutations in *pfdhodh*: E182D, F227I, and L531F. Note that E182D appeared for both compounds, even though they are from different structural classes. This suggests that E182D is a common route to resistance for PfDHODH inhibitors, and may thus be a fitness maximum for resistance. Whole-genome sequencing was performed on the F227I mutant to identify other potential resistance mechanisms, but no known or logical polymorphisms were detected. This does not rule out resistance by copy number variation, which whole genome sequencing is notoriously ineffective at detecting, or non-genetic changes such as epigenetic changes, signal transduction, and generalized stress responses. The known efflux pumps PfMDR1 and PfCRT1 were not amplified. PfDHODH was not amplified (see Chapter 3).

We then screened these three resistant lines against a small panel of structurally diverse PfDHODH inhibitors, and made an interesting observation: while cross-resistance was observed for some PfDHODH inhibitors, other inhibitors were much more potent against the mutant lines than the wild-type (WT) (Figure 2.4.2 and Table 2.4.2). We termed these potentiated agents “PfDHODH mutant-type (MT) inhibitors.” For example, when compared to the parental 3D7 parasite line, the 3D7: E182D line was 8.7-fold less sensitive to Genz-669178, a “WT inhibitor,” but 12.5-fold more sensitive to IDI-6273, which was deemed a “MT inhibitor.” IDI-6273 is a relatively poor inhibitor of WT parasites, with whole cell EC_{50} values of 181.4 nM. The IDI-6273 EC_{50} improves to 13.5 nM in the 3D7: E182D mutant line. This induced hypersensitivity implied that the resistant form of the target can be a target itself.

Given that resistance emerges in an ecological context where fitness costs limit the diversity of escape pathways, we proposed that we could anticipate resistance pathways and preemptively block them with mutant-specific inhibitors. In theory, this idea of “targeting resistance” would prevent the emergence of competitively viable resistance.

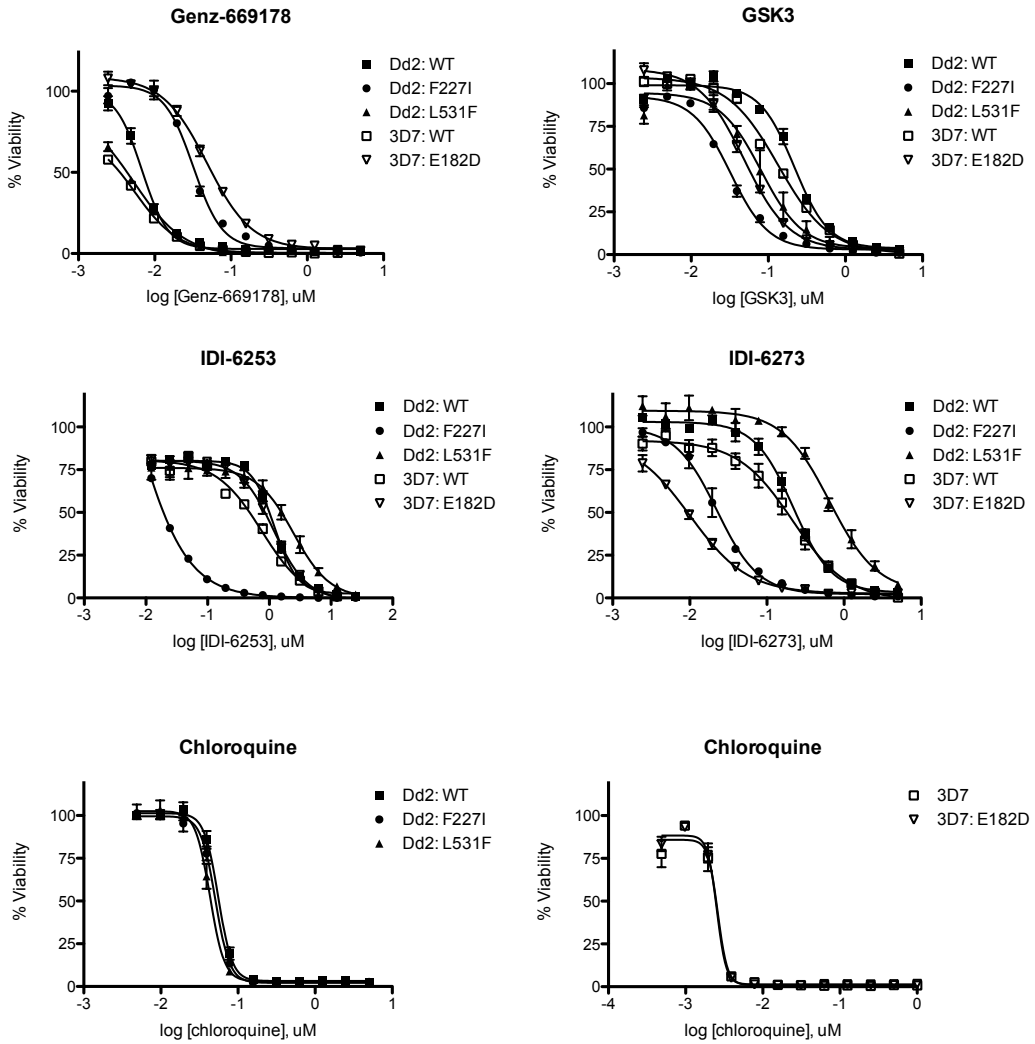

Figure 2.4.2: Resistance and induced sensitivity

(A). Parasite lines resistant to WT PfDHODH inhibitors show cross-resistance to some PfDHODH inhibitors, but are hypersensitive to others, which were deemed “mutant PfDHODH inhibitors.”
(B). The unrelated antimalarial chloroquine shows no difference in the parasite lines tested. Note that 3D7-based lines are much more sensitive to chloroquine than Dd2. EC_{50} values were calculated using a whole-cell SYBR Green assay. Error bars indicate the standard deviation of triplicate measurements.

“Targeting resistance” could be accomplished with a combination therapy where one compound targeted WT parasites (the bulk population), and a partner drug targeted the emerging resistant population (a much smaller population, and much less likely to have the diversity necessary to develop resistance). This paired treatment could occur

concurrently or sequentially. To minimize selective pressure towards resistance to the partner drug, the partner would ideally have negligible activity against the WT, and only become an active drug with a target(s) after resistance to the primary drug arose. As the compounds tested here were initially identified as WT PfDHODH inhibitors, we have no completely specific compounds. Identifying or designing mutant-specific inhibitors would be an interesting area of future work.

Table 2.4.2: PfDHODH inhibitor resistant line data

A.

		EC_{50} fold shift over parent ± s.d.			
		Parent	E182D	F227I	L531F
PfDHODH allele		WT	E182D	F227I	L531F
PfDHODH WT Inhibitors	Genz-669178	1	8.73 ± 5.03	4.06 ± 0.95	0.31 ± 0.07
	Genz-668419	1	6.65 ± 4.36	9.19 ± 3.75	0.36 ± 0.04
PfDHODH Mutant Inhibitors	IDI-6253	1	1.64 ± 0.13	0.02 ± 0.01	1.52 ± 0.71
	IDI-6273	1	0.08 ± 0.03	0.12 ± 0.01	2.23 ± 1.05
	GSK-3	1	15.14 ± 10.15	0.26 ± 0.12	0.41 ± 0.06
Standard Antimalarials	Chloroquine	1	1.20 ± 0.56	0.82 ± 0.10	0.76 ± 0.04

B.

		EC_{50} (nM) ± s.d.				
		Dd2	Dd2: F227I	Dd2: L531F	3D7	3D7: E182D
PfDHODH allele		WT	F227I	L531F	WT	E182D
PfDHODH WT Inhibitors	Genz-669178	6.88 ± 0.14	25.02 ± 6.51	3.87 ± 1.65	5.66 ± 3.30	38.4 ± 8.75
	Genz-668419	5.71 ± 3.62	44.4 ± 14.68	5.98 ± 0.93	6.8 ± 3.78	35.68 ± 19.88
PfDHODH Mutant Inhibitors	IDI-6253	1049.33 ± 267.1	62.8 ± 87.64	3750 ± 494.97	778.93 ± 159.96	1295 ± 373.73
	IDI-6273	209.17 ± 72.76	24.82 ± 10.41	1170 ± 177.48	181.4 ± 53.25	13.48 ± 5.25
	GSK3	182.43 ± 71.7	49.27 ± 36.26	249.35 ± 11.46	145 ± 49.76	1872.17 ± 1063.0
Standard Antimalarials	Chloroquine	58.03 ± 10.35	66 ± 34.58	284.6 ± 6.51	6.95 ± 4.74	6.74 ± 4.0

(A). EC_{50} fold shifts relative to the parental parasite line demonstrate both increased and decreased sensitivity to different classes of PfDHODH inhibitors.
(B). EC_{50} values demonstrate both increased and decreased sensitivity to different classes of PfDHODH inhibitors.
EC_{50} values were calculated using a whole-cell SYBR Green assay. The s.d. is the standard deviation of three biological replicates, each with triplicate measurements.

Although these resistance selections gave three point mutations in PfDHODH, we chose to focus on the E182D mutation as it appeared in response to both an alkylthiophene

inhibitor (Genz-666136) and a triazolopyrimidine inhibitor (DSM74), and may therefore be an evolutionarily favored pathway to resistance.

Analysis of a crystal structure of PfDHODH (Figure 2.4.3) showed that E182 forms a strong salt bridge with R262, and that this bond is one of surprisingly few interactions holding the membrane-adjacent α1-α2 helix lid in place. This two-helix lid defines the "species-selective inhibitor site" [65], and is the presumed tunnel for electron transfer between respiratory chain ubiquinone and the flavin mononucleotide (FMN) cofactor.

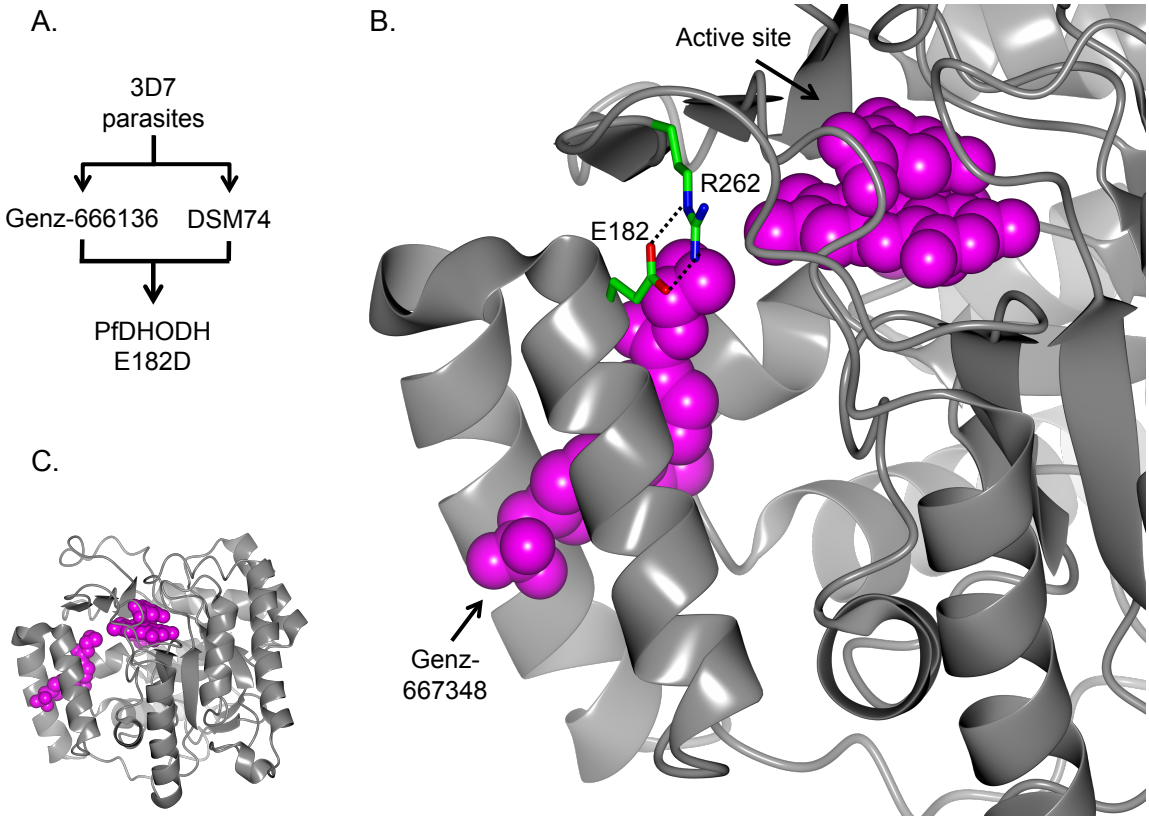

Figure 2.4.3: PfDHODH E182D mutation

(A). Selection of 3D7 parasites with either of the structurally unrelated PfDHODH inhibitors Genz-666136 and DSM74 led to the same resistance mutation, E182D. This implies that E182D is a fitness maximum for resistance.
(B). Close-up structure of PfDHODH showing the position of residue E182. Note the hydrogen bonding to R262 and location near the drug-binding site.
(C). Overall structure of PfDHODH for orientation.
All images shown are of PDB ID: 3o8a and were created with CCP4mg [66].

A glutamate to aspartate (E to D) mutation is quite conservative, with only one carbon in a chain removed, but this may weaken the hydrogen bond to R262, which could then weaken the overall interactions holding the lid in place. The triazolopyrimidine class of inhibitors is thought to work by blocking electron flow between ubiquinone and flavin mononucleotide[64-65], so altering the shape of this tunnel could lead to resistance by preventing drug binding and/or allowing electron flow to occur even when drug is bound.

To test the idea of "targeting resistance," we carried out two selection strategies: sequential and simultaneous (Figure 2.4.4). In the sequential selection, we took the 3D7: E182D parasites and selected them with IDI-6273 (a MT inhibitor). In the simultaneous selection, we took 3D7 WT parasites and selected with a combination of Genz-669178 (a WT inhibitor) and IDI-6273 (a MT inhibitor).

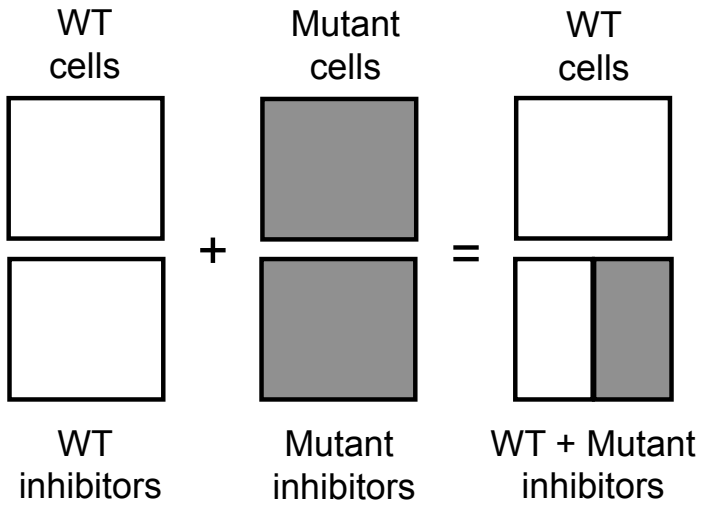

Figure 2.4.4: "Targeting resistance" treatment strategy

SEQUENTIAL PFDHODH INHIBITOR SELECTIONS: MUTANT-TYPE PARASITES

In the sequential selection, drug-resistant parasites emerged in one of four flasks in 41 days (Figure 2.4.4, Table 2.4.3). The three remaining flasks never recovered, indicating that this was not a resistant parasite genome present in the founding population. As

expected, selection with IDI-6273 decreased sensitivity to the selection agent. The sequentially selected parasites showed a 52.8-fold increase in the EC_{50} for IDI-6273, shifting from 48.5 nM to 2.3 uM. Curiously, the sequentially selected line was 4-fold more sensitive to Genz-669178, a WT inhibitor, with EC_{50} values dropping from 31.9 nM to 8.8 nM. This value is similar to the 3D7 parental 3.5 nM. Chloroquine, dihydroartemisinin, and atovaquone - control compounds that are presumably unrelated to pyrimidine synthesis or metabolism - showed small but significant differences, e.g., a 23% increase in sensitivity to chloroquine. Taken together, these results implied that physiological changes affecting multiple pathways had occurred.

PCR sequencing of the *pfdhodh* gene in the sequentially selected line uncovered a novel mutation in codon 182. Surprisingly, codon 182 was now the alternate codon for glutamate, the original WT residue (Figure 2.4.5 C). We called this WT “reversion” line 3D7 E182D: D182E. There are likely to be changes outside of *pfdhodh* as sensitivity to unrelated compounds like chloroquine was also altered, and not all PfDHODH inhibitors returned to WT ranges of sensitivity. Whole-genome sequencing of the 3D7 E182D: D182E line showed a non-synonymous polymorphism of I772V in cytochrome *c* oxidase (PlasmoDB ID: mal_mito_1), which could affect the mitochondrial electrochemical gradient and thus PfDHODH activity or stability. However, this mutation was also present in the 3D7: E182D parent, and so cannot explain the observed differences.

The evolutionary oscillation between glutamate and aspartate at codon 182 suggests that these are two optimal solutions to the fitness-resistance compromise. Nevertheless, there are other solutions, even if they are less easy to reach or provide lower benefit, so sequential cycling between Genz-669178 and IDI-6273 is unlikely to remain effective as other mutants arise and spread or compensatory mutations increase fitness.

A.

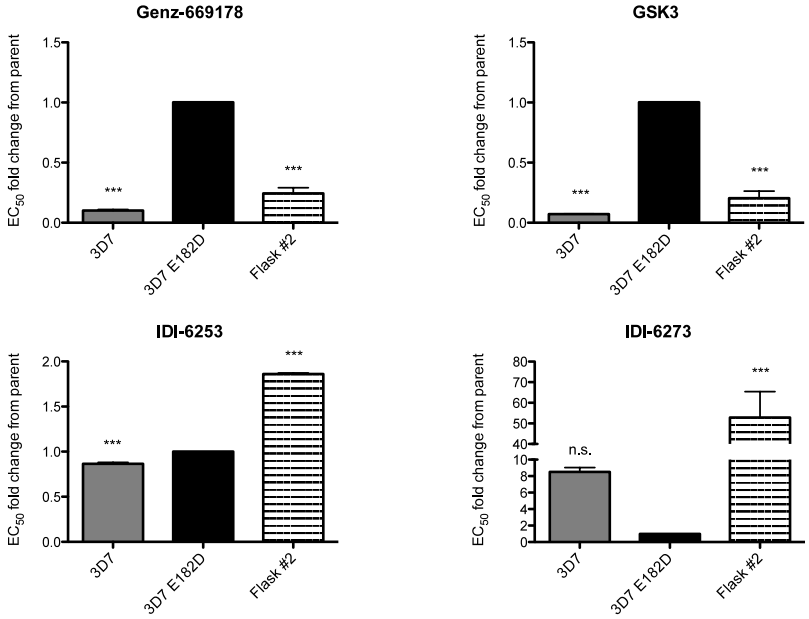

B.

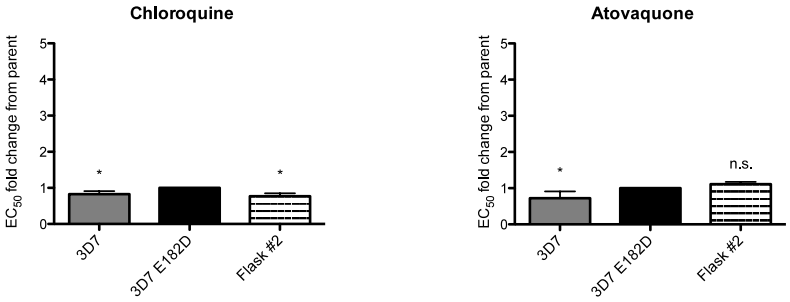

C.

```
3D7                AAATATATTGATGGTGAAATATGTCATGACCTTTT
3D7 E182D          AAATATATTGATGGTGATTATATGTCATGACCTTTT
3D7 E182D: D182E   AAATATATTGATGGTGAGATATGTCATGACCTTTT
                   ********************* *****************
```

Figure 2.4.5: 3D7 E182D: IDI-6273 selection gave reversion to WT protein.

(A). EC_{50} fold shifts relative to the parental selection line show a return to WT-like sensitivity for some PfDHODH inhibitors but not others (e.g., IDI-6273).
(B). The unrelated antimalarial compounds chloroquine and atovaquone show significant differences among the three lines tested, indicating that there are physiological changes beyond PfDHODH point mutations.
(C). PCR sequencing of the PfDHODH gene revealed a novel nucleotide mutation in codon 182, which led to a reversion to the WT protein sequence.

EC_{50} values were calculated using a whole-cell SYBR Green assay. Error bars indicate the standard deviation of three biological replicates, each with triplicate measurements. Significance relative to parental EC_{50} was determined by one-way ANOVA with Dunnett's multiple comparison test. n.s., not significant. *, $p<0.05$. **, $p<0.005$, ***, $p<0.0005$.

Table 2.4.3: 3D7 E182D: IDI-6273 selection data

A.

		EC_{50} fold shift over parent ± s.d.		
		3D7	Parent	Flask #2
PfDHODH allele		WT	E182D	E182D: D182E
PfDHODH WT Inhibitors	Genz-669178	0.10 ± 0.01	1	0.24 ± 0.05
	Genz-668419	0.010 ± 0.01	1	0.25 ± 0.02
PfDHODH Mutant Inhibitors	IDI-6253	0.87 ± 0.01	1	1.86 ± 0.01
	IDI-6273	8.51 ± 0.53	1	52.85 ± 12.62
	GSK-3	0.07 ± 0.07	1	0.20 ± 0.06
Standard Antimalarials	Chloroquine	0.83 ± 0.08	1	0.77 ± 0.08
	Dihydroartemisinin	1.39 ± 0.12	1	0.87 ± 0.04
	Atovaquone	0.72 ± 0.19	1	1.11 ± 0.06

B.

		EC_{50} (nM) ± s.d.		
		3D7	Parent	Flask #2
PfDHODH allele		WT	WT	WT
PfDHODH WT Inhibitors	Genz-669178	3.50 ± 0.23	31. 86 ± 6.09	8.75 ± 0.33
	Genz-668419	7.16 ± 2.11	67.59 ± 23.33	19.03 ± 6.92
PfDHODH Mutant Inhibitors	IDI-6253	5679.9 ± 6760.08	6495.45 ± 7699.76	12134.11 ± 14405
	IDI-6273	450.43 ± 227.67	48.50 ± 28.43	2315.43 ± 516.20
	GSK-3	68.11 ± 11.45	880.47 ± 140.59	198.60 ± 22.03
Standard Antimalarials	Chloroquine	3.05 ± 0.40	3.59 ± 1.05	3.22 ± 0.73
	Dihydroartemisinin	3.18 ± 1.15	2.18 ± 0.49	2.12 ± 0.63
	Atovaquone	0.15 ± 0.07	0.21 ± 0.07	0.24 ± 0.10

(A). EC_{50} fold shifts relative to the parental parasite line demonstrate both increased and decreased sensitivity to different classes of PfDHODH inhibitors.
(B). EC_{50} values demonstrate both increased and decreased sensitivity to different classes of PfDHODH inhibitors.

EC_{50} values were calculated using a whole-cell SYBR Green assay. The s.d. is the standard deviation of three biological replicates, each with triplicate measurements.

While the sequential selections were proceeding, we also performed concurrent WT plus MT inhibitor selections – a test of the "targeting resistance" combination therapy idea. In theory, this combination should suppress the emergence of the targeted alleles, which in this case were WT and E182D.

SIMULTANEOUS PFDHODH INHIBITOR SELECTIONS: "TARGETING RESISTANCE"

We simultaneously selected WT 3D7 parasites with Genz-669178 and IDI-6273. Genz-669178 is a WT inhibitor and IDI-6273 selectively inhibits the PfDHODH E182D (and F227I) mutant. This selection tested the concept of "targeting resistance" – could we force parasites to remain sensitive to the WT PfDHODH inhibitor by blocking their most fit, most favored escape pathway?

We allowed the selection to proceed for 80 days - twice the length necessary for the sequential selection. In keeping with our hypothesis, no resistance was observed (Figure 2.4.6, Table 2.4.4). All recovered parasites remained WT in terms of drug sensitivity to PfDHODH inhibitors and control compounds, and the *pfdhodh* allele remained wild-type.

This selection took one billion parasites through at least 40 generations. Given a nuclear genome of 23.3 megabases, two small organellar genomes in the mitochondria and the apicoplast, and a DNA replication error rate of 1 to 9.7 $x10^{-9}$ per nucleotide per generation [67], this is ample time for every position in the genome to be mutated at least once. Of course, some positions are more susceptible to genomic alterations than others, but 80 days is also in vast excess of the 3 days that most patients take antimalarial therapies. 40 generations is also ample time for the development of resistance through mechanisms other than mutation, e.g., copy number variation and compensatory physiological changes.

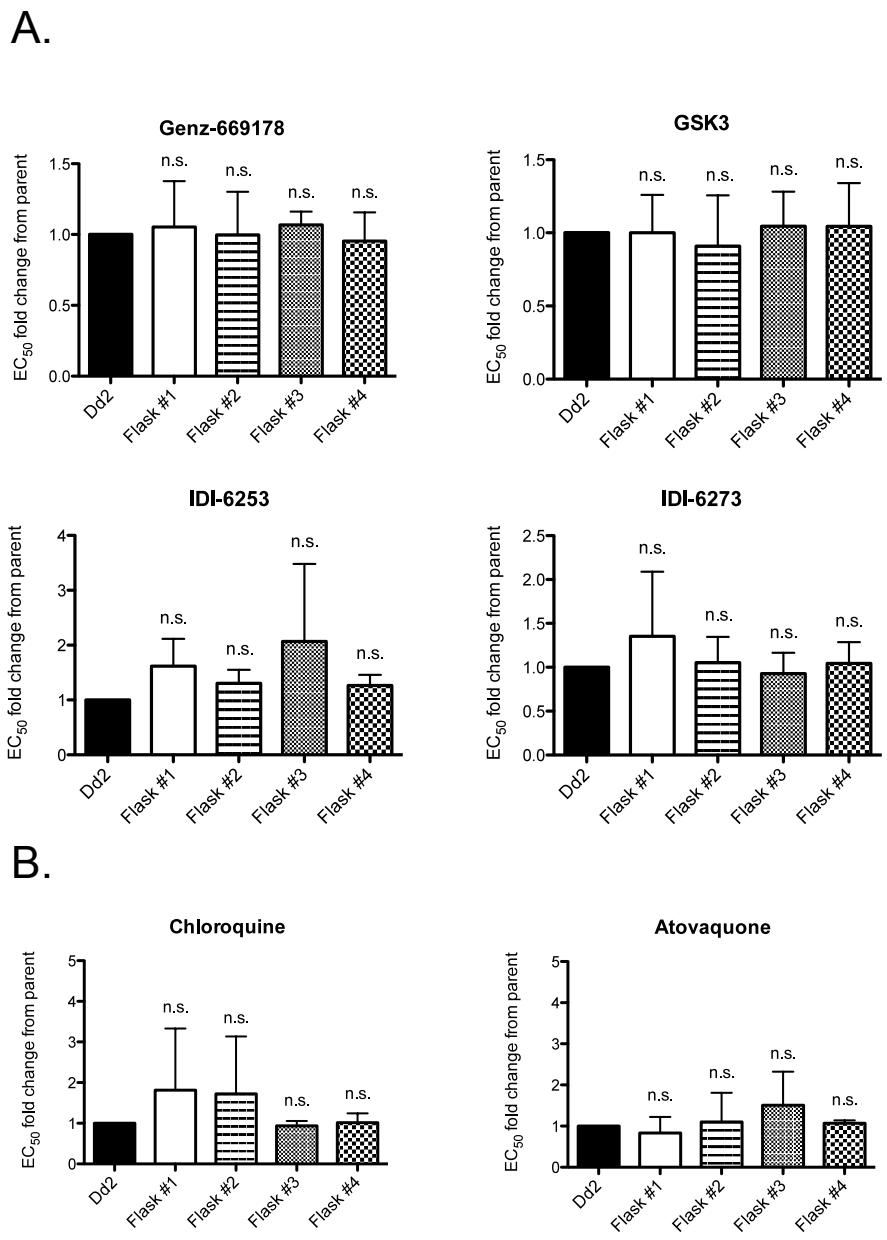

Figure 2.4.6: Dd2: Genz-669178 + IDI-6273 selection gave no resistance

(A). EC_{50} fold shifts relative to the parental selection line show no significant development of resistance.
(B). The unrelated antimalarial compounds chloroquine and atovaquone show no significant differences among the lines tested.

This combination selection proceeded for 80 days (40 generations). EC_{50} values were calculated using a whole-cell SYBR Green assay. Error bars indicate the standard deviation of three biological replicates, each with triplicate measurements. Significance relative to parental EC_{50} was determined by one-way ANOVA with Dunnett's multiple comparison test. n.s., not significant. *, $p<0.05$. **, $p<0.005$, ***, $p<0.0005$.

Table 2.4.4: Dd2: Genz-669178 + IDI-6273 selection results

A.

		EC_{50} fold shift over parent ± s.d.				
		Parent	Flask #1	Flask #2	Flask #3	Flask #4
PfDHODH allele		WT	WT	WT	WT	WT
PfDHODH WT Inhibitors	Genz-669178	1	1.05 ± 0.32	1.00 ± 0.30	1.07 ± 0.09	0.96 ± 0.20
	Genz-668419	1	1.00 ± 0.19	0.94 ± 0.28	1.08 ± 0.12	1.20 ± 0.11
PfDHODH Mutant Inhibitors	IDI-6253	1	1.62 ± 0.50	1.31 ± 0.25	2.07 ± 1.41	1.27 ± 0.19
	IDI-6273	1	1.35 ± 0.74	1.05 ± 0.29	0.93 ± 0.24	1.05 ± 0.24
	GSK-3	1	1.00 ± 0.26	0.91 ± 0.35	1.05 ± 0.24	1.04 ± 0.30
Standard Antimalarials	Chloroquine	1	1.82 ± 1.52	1.72 ± 1.42	0.94 ± 0.12	1.02 ± 0.23
	Dihydroartemisinin	1	0.95 ± 0.35	0.87 ± 0.26	0.98 ± 0.23	1.12 ± 0.17
	Atovaquone	1	0.83 ± 0.39	1.10 ± 0.71	1.51 ± 0.81	1.06 ± 0.08

B.

		EC_{50} (nM) ± s.d.				
		Parent	Flask #1	Flask #2	Flask #3	Flask #4
PfDHODH allele		WT	WT	WT	WT	WT
PfDHODH WT Inhibitors	Genz-669178	3.53 ± 0.36	3.80 ± 1.58	3.60 ± 1.43	3.79 ± 0.65	3.39 ± 0.85
	Genz-668419	5.79 ± 1.50	5.71 ± 1.42	5.38 ± 1.95	6.33 ± 2.14	6.84 ± 1.31
PfDHODH Mutant Inhibitors	IDI-6253	18927.67 ± 13046.72	26476.67 ± 13479.50	22652.00 ± 12847.45	26893.33 ± 9707.35	22290.00 ± 13178.312
	IDI-6273	1189.50 ± 153.44	1665.30 ± 1082.86	1275.85 ± 510.74	1121.15 ± 426.88	1262.100 ± 446.75
	GSK-3	69.81 ± 22.16	66.73 ± 14.83	59.017 ± 11.52	72.28 ± 26.45	73.37 ± 36.28
Standard Antimalarials	Chloroquine	54.33 ± 21.53	81.94 ± 43.02	79.23 ± 40.81	49.20 ± 12.59	52.29 ± 10.41
	Dihydroartemisinin	3.82 ± 1.06	3.395 ± 0.43	3.13 ± 0.05	3.85 ± 1.91	4.29 ± 1.52
	Atovaquone	0.16 ± 0.16	0.093 ± 0.05	0.12 ± 0.06	0.18 ± 0.12	0.18 ± 0.19

(A). EC_{50} fold shifts relative to the parental parasite line show no significant difference.
(B). EC_{50} values for the same data set.
EC_{50} values were calculated using a whole-cell SYBR Green assay. The s.d. is the standard deviation of three biological replicates, each with triplicate measurements.

The promising results from the sequential and simultaneous selections led us to better characterize the E182D mutant line. We wanted to determine if the PfDHODH E182D mutation was sufficient to explain the observed drug sensitivity phenotypes, or if other factors contributed to the phenotype. To address this question, we took two approaches: protein biochemistry and evolutionary competitive growth assays. These strategies allowed us to analyze the PfDHODH protein alone as well as the entire physiological context of the parent and daughter cell lines. Ideally, this would be extended to include allelic replacements of the mutant *pfdhodh* E182D gene in whole parasites.

PURIFIED PFDHODH PROTEIN ACTIVITY AND COMPARISON WITH CELLULAR DATA

We cloned and purified WT and E182D PfDHODH protein, and performed *in vitro* activity assays [65, 49] to determine steady-state kinetic parameters and sensitivity to PfDHODH inhibitors via measurement of orotic acid or a coupled dye, respectively (Figure 2.4.7).

We measured steady-state kinetic parameters for the PfDHODH oxidase reaction, where L-DHO is oxidized to orotic acid by flavin mononucleotide (FMN), and for the ping-pong redox reaction where the reduced FMN is oxidized by respiratory chain ubiquinone (Figure 2.4.7). The steady-state parameters for the PfDHODH WT and E182D proteins (Table 2.4.5) show a 1.8-fold decrease in kcat and a 4.7-fold increase in Km for the L-DHO substrate in the E182D mutant. This would dramatically reduce the catalytic efficiency of the enzyme's oxidase activity. Similarly, the E182D mutant protein had a 6-fold decrease in kcat and a 6.2-fold increase in Km for CoQ_D.

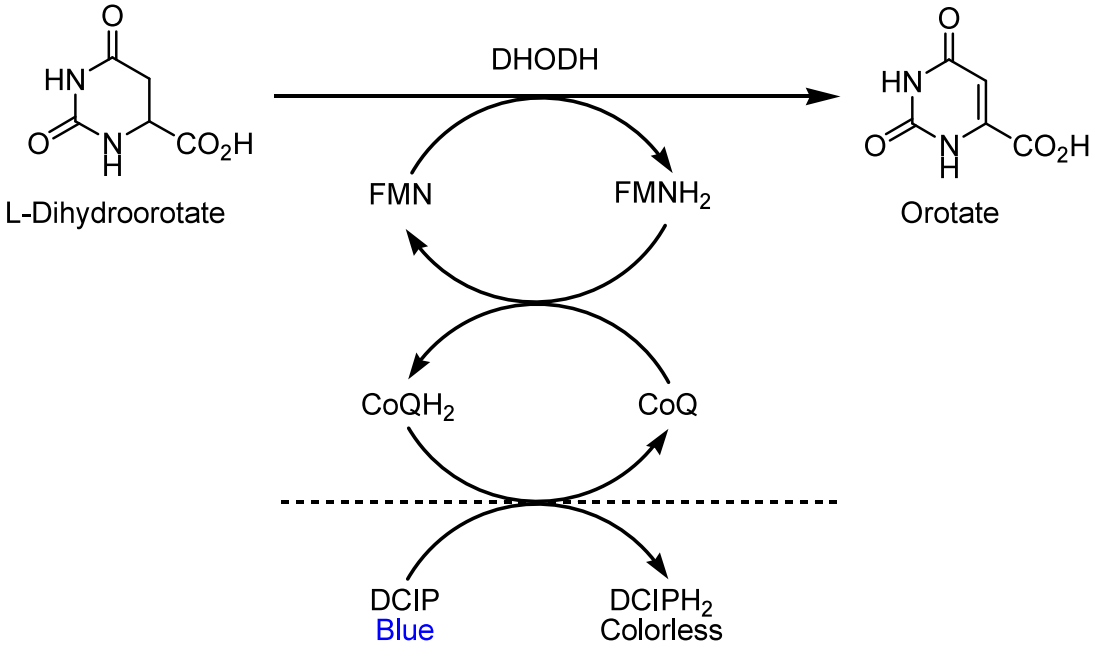

Figure 2.4.7: *In vitro* PfDHODH enzyme activity assays.

The observed decreases in catalytic efficiency for the PfDHODH E182D mutant presumably reduce whole-organism fitness, but the scale of these differences may be insignificant or masked by compensatory mechanisms inside cells.

Table 2.4.5: Steady-state kinetic parameters for WT and E182D PfDHODH protein

PfDHODH allele		WT	E182D
L-DHO	kcat (s^{-1})	1.95 ± 0.32	1.08 ± 0.10
	Km (uM)	19.93 ± 2.71	93.1 ± 31.77
CoQ_D	kcat (s^{-1})	6.99 ± 0.59	1.16 ± 0.004
	Km (uM)	6.29 ± 1.95	38.86 ± 21.53

Steady-state kinetic measurements were performed at 25°C. Errors represent the standard deviation of the fit for three determinations.

We carried out further analysis by measuring the effect of a panel of PfDHODH inhibitors on enzyme activity. *In vitro* protein activity assays recapitulated the results seen in whole-cell assays (Figure 2.4.8, Table 2.4.6): if a compound was more potent against WT than PfDHODH: E182D parasites in whole cell assays, then it was also more potent against the WT than the E182D mutant in protein assays. For example, E182D is resistant to Genz-669178 (Figure 2.4.8 A, rightward shift relative to WT) but sensitized to IDI-6273 (Figure 2.4.8 A, leftward shift relative to WT).

EC_{50} fold changes (Figure 2.4.8 B) show highly significant changes between E182D (bars) and WT (represented by the dotted line at 10^0, one-fold). Note that these changes reflect the trends seen in whole cells, but are often more extreme (Figure 2.4.8 C). This is unsurprising, as *in vitro* protein assays are far simpler than living cells, and do not have the same extent of confounding factors such as plasma membranes, transporters or efflux pumps, off-target protein binding, and so on. The fact that the protein and cell results are largely commensurate indicates that sensitivity or resistance to PfDHODH

inhibitors is principally due to alterations in the *pfdhodh* gene itself. As protein expression in *E.coli* is currently much faster than allelic replacement in *P. falciparum*, protein activity is an ideal method for quickly determining the effect of PfDHODH mutations on drug sensitivity and kinetic parameters.

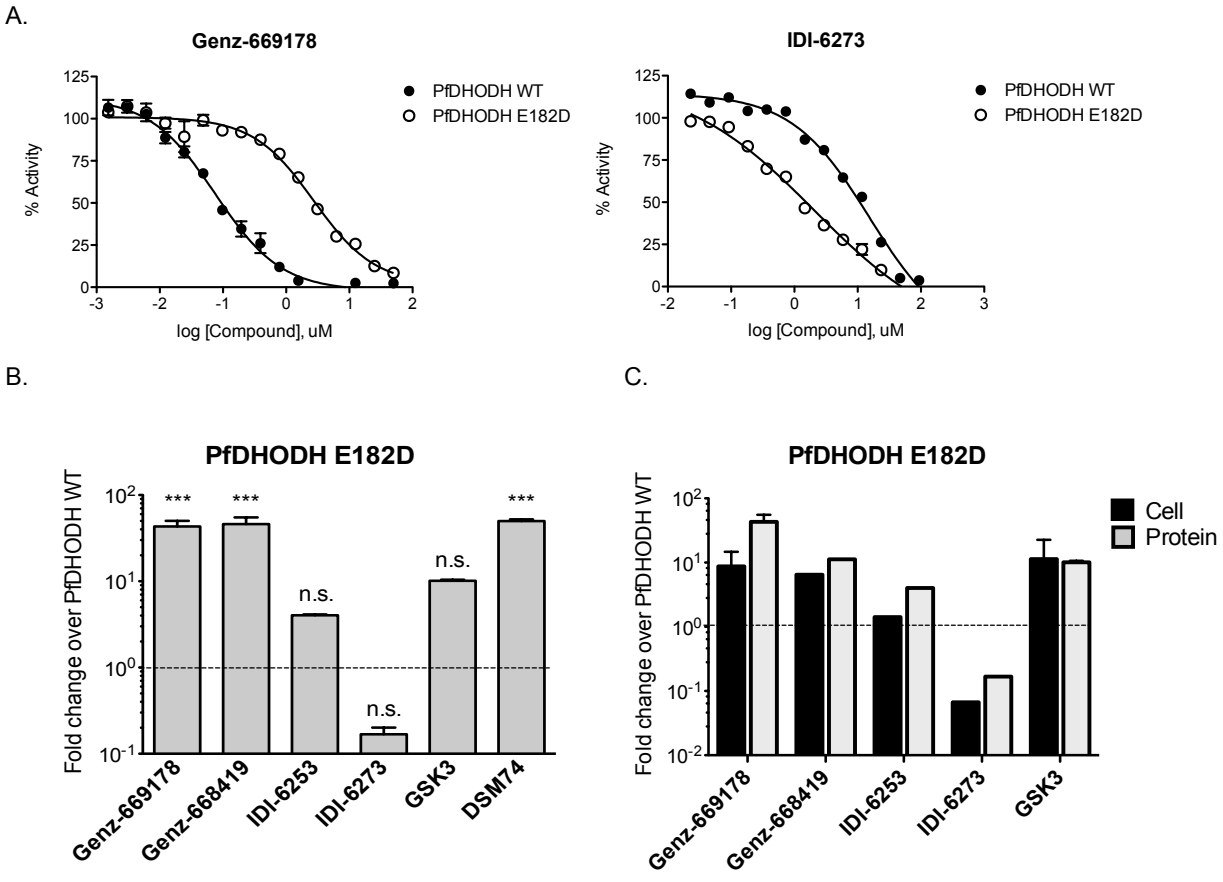

Figure 2.4.8: Recombinant protein *in vitro* activity assays mirror cellular data.

(A). Example EC_{50} curves reflects trends seen in whole-cell assays. Error bars indicate triplicate measurements.
(B). EC_{50} fold changes show significant changes in sensitivity to a panel of PfDHODH inhibitors. Error bars indicate the standard deviation of three biological replicates, each with triplicate measurements.
(C). Protein data mirrors cell data, although the fold changes are more extreme for the *in vitro* protein assays. Error bars indicate the standard deviation of three biological replicates, each with triplicate measurements.
EC_{50} values were calculated using an indirect DCIP-coupled assay. Significance relative to parental EC_{50} was determined by one-way ANOVA with Dunnett's multiple comparison test. n.s., not significant. *, $p<0.05$. **, $p<0.005$, ***, $p<0.0005$.

Table 2.4.6: Inhibition of PfDHODH WT and E182D protein activity

A.

		EC_{50} fold shift over parent ± s.d.	
		Parent	Resistant line
PfDHODH allele		WT	E182D
PfDHODH WT Inhibitors	Genz-669178	1	43.19 ± 12.41
	Genz-668419	1	46.09 ± 15.62
	DSM74	1	49.89 ± 3.97
PfDHODH Mutant Inhibitors	IDI-6253	1	4.04 ± 0.15
	IDI-6273	1	0.17 ± 0.05
	GSK-3	1	10.14 ± 0.54

B.

		EC_{50} (nM) ± s.d.	
		Parent	Resistant line
PfDHODH allele		WT	E182D
PfDHODH WT Inhibitors	Genz-669178	79.50 ± 6.04	3483.33 ± 1290.96
	Genz-668419	144.60 ± 5.54	6722.33 ± 2564.01
	DMS74	381.43 ± 93.07	18783.3 ± 2915.62
PfDHODH Mutant Inhibitors	IDI-6253	3527.67 ± 215.93	14216.67 ± 323.31
	IDI-6273	13493.3 ± 3163.9	2153.00 ± 133.37
	GSK-3	1686.67 ± 459.57	17263.33 ± 5432.9

(A). EC_{50} fold shifts relative to PfDHODH WT shows significant differences.
(B). EC_{50} values for the same data set.
EC_{50} values were calculated using an indirect DCIP-coupled assay. The s.d. is the standard deviation of three biological replicates, each with triplicate measurements.

COMPETITIVE GROWTH ASSAYS: POPULATION DYNAMICS AND EVOLUTIONARY FITNESS

After focusing on molecular details of resistance, we panned out to a population level with competitive growth assays. These assays allow for a quantitative assessment of evolutionary fitness. We performed pairwise assays between the WT 3D7 parental

parasites and two PfDHODH mutants: E182D and the D182E WT revertant, and then analyzed the results with allelic discrimination assays (Figure 2.4.9). In all cases, the WT 3D7 line outcompeted the mutant regardless of the starting inoculum.

Over the course of six generations, the E182D mutant dropped by two-fold Figure 2.4.9 A). In contrast, the D182E revertant decreased by five-fold (Figure 2.4.9 B). This implies that WT is more fit than the E182D mutant, and the E182D mutant is more fit than the D182E revertant. These assays were done without the presence of any drugs. The mutants would presumably have a fitness advantage when WT PfDHODH inhibitors are present, and a disadvantage when mutant PfDHODH inhibitors are present.

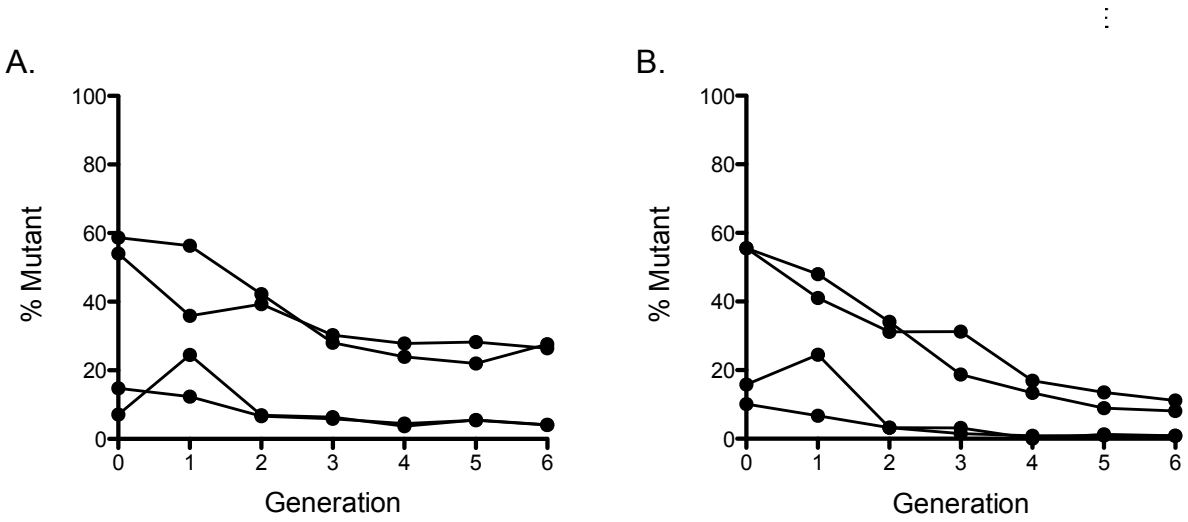

Figure 2.4.9: Pairwise competitions show a mutant fitness defect

(A). The wild-type 3D7 parasite is more fit than the mutant 3D7 E182D.
(B). The wild-type 3D7 parasite is more fit than the wild-type revertant parasite 3D7 E182D: D182E. Thus, the revertant line has changes outside of the *pfdhodh* gene that reduce its fitness, or the alternate glutamate codon compromises PfDHODH function.

Results shown are of competitions done in triplicate, with triplicate allelic discrimination assays performed for each sample. Error bars represent the standard deviation.

It is interesting that the D182E revertant mutant is less fit than the WT. Earlier drug sensitivity data showed that although the protein sequence of the *pfdhodh* gene was the same in these parasite lines, there were significant differences in sensitivity to PfDHODH inhibitors and unrelated antimalarial drugs. There must be changes outside of the *pfdhodh* nucleotide mutation to account for these differences in drug sensitivity and overall competitive fitness. All three lines discussed have a single copy of *pfdhodh* (see Chapter 3). These mutations could potentially lead to different protein levels due to transcriptional or translational control, rare codons, or protein stability. Protein levels could be assessed with a PfDHODH antibody, which we recently obtained as a kind gift from Professor Margaret Phillips. Translational control could be assessed by ribosome footprinting [65].

2.5 Discussion and Future Directions

Drug resistance is an enormous issue for malaria, and we are relying on an increasingly narrow range of artemisinin-based therapies for treatment. Recent reports of potential artemisinin resistance at the Thai-Cambodian border [19] are a serious threat, as resistance from Southeast Asia has spread worldwide for both chloroquine and pyrimethamine [68]. Drug resistance can rapidly compromise the effective useful lifetime of antimalarial agents, and cross-resistance with existing therapies is a major concern as few compounds with novel mechanisms of action are being developed. However, drug resistance emerges in the context of a population and is limited by evolutionary fitness costs. If a parasite is drug-resistant, but pays a heavy fitness price, it is unlikely to be competitively viable. These limitations result in a very small number of mutational escape pathways being heavily favored in *Plasmodium* [27], and likely in many other organisms as well. These escape pathways can be anticipated and blocked.

PfDHODH is a promising novel antimalarial drug target. In this study, we sought to characterize mechanisms of resistance to PfDHODH inhibitors and develop strategies to suppress the emergence and spread of resistance. To do so, we tested resistant parasite lines against a panel of antimalarial agents and identified compounds that were more potent against the mutants than the WT parent. These compounds could be said to have mutually incompatible resistance mechanisms as resistance to one leads to hypersensitivity to the other. The identification of mutant-selective compounds allows us to set a trap: if resistance to one compound results in hypersensitivity to another, then a parasite will be more fit if it retains WT sensitivity. We call this concept “targeting resistance,” and it is an extension of the strong antagonism known as suppression [36].

We demonstrated the efficacy of “targeting resistance” with two selections: in the first, mutant-type 3D7 parasites with a PfDHODH E182D mutation were selected with the mutant-selective compound IDI-6273. The only resistant line to emerge had a novel mutation in *pfdhodh*, and this resulted in a reversion to the WT protein sequence. In the second, WT Dd2 parasites were selected with a combination of Genz-669178 (a WT inhibitor) and IDI-6273 (a mutant inhibitor). No resistance emerged in 80 days. The evolutionary loop between WT and E182D implies that these are both fitness maximums, and thus likely outcomes.

“Targeting resistance” relies on stepwise acquisition of resistance. If the parasite is able to become resistant to both compounds in a single step, targeting resistance would be much more likely to fail. The PfDHODH inhibitors shown all bind the same pocket, although in different ways (see crystallography in Chapter 3). However, this may not be sufficient. An improved combination set would target binding sites that do not influence each other. A distant site on the same target or another target entirely would be ideal.

Identifying compounds that target mutant PfDHODH parasites without necessarily inhibiting mutant PfDHODH directly is part of an ongoing effort from Dr. Amanda Lukens. It will be interesting to see what targets and pathways are represented in the mutant-selective inhibitors. Suppressive combinations would likely include other mitochondrial targets, ubiquinone biosynthesis, or the folate pathway, as these all affect flux through the pyrimidine biosynthetic pathway. General translation is also a possibility, as DHODH inhibition kills cells by arresting translational elongation in the zebrafish neural crest [69]. Another approach to identify suppressive partners would be to screen for compounds that rescue parasites from death due to DHODH inhibition [70].

There is only one known drug-binding site in PfDHODH, but it is a large tunnel and inhibitors that bind sufficiently distinct portions of this site may be less susceptible to cross-resistance. The assays used to identify PfDHODH inhibitors measure activity, not binding to a specific site, so it is possible that a screen will identify compounds with different binding sites.

Another area for improvement would be to identify mutant-specific (rather than mutant-selective) compounds. These efforts are being carried out by Leila Saxby Ross and Dr. Tomoyo Kato. The mutant-selective compounds have relatively little activity against the WT, but it is not negligible. This selective force can lead to resistance developing in the WT population, which would compromise the effectiveness of the mutant-selective compound when needed. The WT population is large and thus has a large potential for diversity. The emerging resistant population is small and thus has relatively little diversity. The less time the minority resistant population is allowed to exist, the less time it has to accumulate diversity (and thus become competitively viable resistant parasites). The goal, therefore, is to neutralize emerging threats as soon as possible, before they have a chance to spread or become more fit through compensatory mutations. Identifying mutant-specific inhibitors would eliminate selective pressure for resistance in the WT population.

The observation of cross-resistance to some PfDHODH inhibitors and hypersensitivity to others implies that the drug-binding site has a limited mutational flexibility, likely limited by fitness constraints. The combination of well-chosen anti-malarial agents active against sensitive and resistant parasites effectively kills parasites in the short-term, and in the long-term, can help shape parasite evolution away from the development of drug resistance.

Chapter Three:

Assessing Resistance Potential of Antimalarials in Development

3.1 ATTRIBUTIONS

Leila S. Ross[1], Amar bir Singh Sidhu[1], Richard Heidebrecht[1,2], Onkar M. P. Singh[3], Paul Rowland3, Francisco-Javier Gamo[4], Maria Jose Lafuente-Monasterio[4], Michael L. Booker[5], Piotrek Sliz[6], Roger C. Wiegand[2], Dyann F. Wirth[1,2]

1. Department of Immunology and Infectious Diseases, Harvard School of Public Health, Boston, MA
2. Infectious Disease Initiative, Broad Institute, Cambridge, MA
3. GlaxoSmithKline, Stevenage, United Kingdom
4. Tres Cantos Medicine Development Campus, GlaxoSmithKline, Tres Cantos, Spain
5. Genzyme Corporation, Waltham, MA
6. Children's Hospital of Boston, Boston, MA

Chemical synthesis was carried out by R.H., F-J.G, M.J.L-M. and M.L.B. M.L.B performed a PfDHODH screen which led to the Genz-666136 series of compounds. F-J.G. and M. J.L-M performed a PfDHODH screen which led to the GSK3 and GSK8 compounds. A.B-S.S performed the selection that resulted in the PfDHODH E182D, PfDHODH F227I, and PfDHODH mutants. L.S.R. performed all other selections shown. L.S.R. performed all parasite proliferation assays shown. L.S.R. performed molecular dynamics simulations in the laboratory of P.S. Cloning, purification, and biochemical assays with recombinant PfDHODH protein were performed by L.S.R. Protein crystallography was performed by O.M.P.S., and the data were collected and structures solved by P.R.

Funding for this work was provided by grants from the Medicines for Malaria Venture, the Bill and Melinda Gates Foundation, the Broad Institute SPARC program, the Genzyme Humanitarian Assistance for Neglected Disease Program, and NIH grant R01 AI093716-01A1.

3.2 INTRODUCTION

Hard-earned lessons from the 1955 Global Malaria Eradication Programme (GMEP) [20] taught us that the largest predictor of success lay in sustained commitment to fine-tuned control programs aimed at total eradication. Merely reducing transmission was not sufficient, and in many cases, a temporary reduction in malaria mortality was paid for dearly when the beaten-down but not eradicated parasites resurged against a now-immunologically naïve population. Mustering the funding, infrastructure, and political will to maintain vigilant surveillance as malaria transmission decreases will be a challenge [71], especially when considering competing health concerns, e.g., HIV-1 and family planning. The island of Aneityum took five years of surveillance after malaria transmission had dropped below detectable levels before both *P. falciparum* and *P. vivax* malaria were declared eradicated and control measures were stopped [72].

Control measures include managing both the mosquito vector and the *Plasmodium* parasite. Vector control is primarily accomplished through insecticide-treated bed nets and indoor residual spraying of insecticides [73]. Many classes of insecticides have been abandoned due to concerns about off-target toxicity, as for DDT [20], or due to resistance in the mosquito, such as in the pyrethroids [71]. Ivermectin is a promising new insecticide [74]. Any malaria control measure must include a robust vector control component. Control measures for the parasite largely consist of antimalarial drugs as no effective vaccine has been developed. Many antimalarial drugs also have issues of resistance and/or toxicity, e.g., primaquine toxicity for people with G6PD deficiency [75].

The cessation of control measures, whether through lack of implementation or lack of effectiveness, is a complex topic. A study of 75 resurgence events between 1930-2000 showed that these resurgences could be attributed to a loss of commitment to control

measures in 91% of cases, of which 57% were due to a lack of funding. Antimalarial drug resistance accounted for 32% of program failures [76]. Money and malaria are inextricably linked, and issues of global poverty cycles, foreign aid dependency, and in-country self-sufficiency are at the fore when discussing the massive scale and long timeframe needed to eradicate malaria.

Part of this is a question of timing: we know that drug resistance can spread locally within a single transmission season, and globally in a few short years [75]. With no effective vaccines, antimalarial drugs are a key intervention, and resistance would defang control efforts. This means that effective interventions must be deployed in a coordinated, saturating, full-scale effort in an attempt to eradicate malaria before resistance compromises the tools used.

It is crucial that malaria control and eradication efforts place considerable effort on strategies to limit and contain resistance in both the parasite and the mosquito vector. This would extend the useful lifetime of antimalarial agents and give eradication programs more time to succeed. Fitness costs in maintaining resistance to the classic antimalarial chloroquine have resulted in sensitivity returning after years of disuse [77], but cycling through existing antimalarials will likely not be sufficient or apply worldwide. Characterizing resistance pathways for antimalarial agents in development will aid in understanding the potential for resistance and developing strategies to protect the efficacy of these drugs before clinical use.

We identified resistance mechanisms of dihydroorotate dehydrogenase (PfDHODH) inhibitors via *in vitro* resistance selections. We then characterized the drug responses of these resistant mutant parasites to a panel of DHODH inhibitors (Figure 3.1.1) and seemingly unrelated control compounds. Most of the resistance appeared to be due to

point mutations in the PfDHODH target. This finding was corroborated by work with purified recombinant wild-type and mutant-type proteins, which showed the same trends in drug sensitivity and resistance. Crystallography of PfDHODH with a variety of inhibitors revealed potential molecular mechanisms of resistance. Several resistant lines had no mutations in the gene *pfdhodh*, and the mechanism(s) of resistance for these are unknown. Targeted sequencing of candidate loci revealed a likely involvement of the folate pathway in one case, but the rest will likely require whole-genome sequencing to generate testable hypotheses.

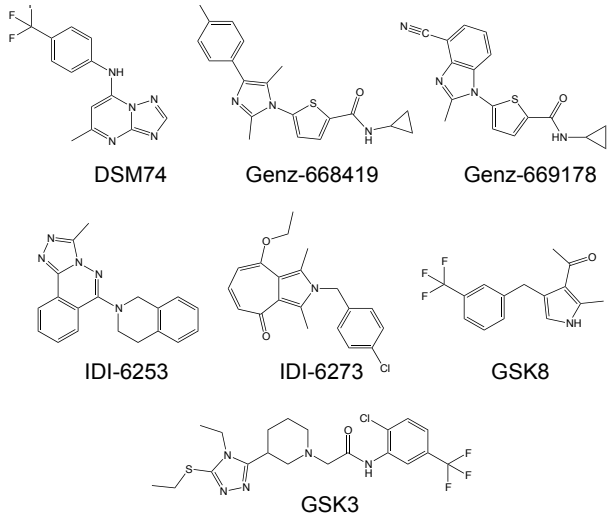

Compound	SMILES
DSM74	FC(F)(F)C1=CC=C(NC2=CC(C)=NC3=NC=NN32)C=C1
Genz-668419	O=C(NC1CC1)C2=CC=C(N3C(C)=C(C4=CC=C(F)C=C4)N=C3C)S2
Genz-669178	O=C(NC1CC1)C2=CC=C(N3C(C=CC=C4C#N)=C4N=C3C)S2
IDI-6253	CC1=NN=C2C3=C(C=CC=C3)C(N4CCC5=C(C=CC=C5)C4)=NN21
IDI-6273	ClC1=CC=C(CN2C(C)=C3C(C=CC=C(OCC)C3=C2C)=O)C=C1
GSK3	CCSC1=NN=C(N1CC)C2CCCN(C2)CC(NC3=C(Cl)C=CC(C(F)(F)F)=C3)=O
GSK8	CC(C1=C(NC=C1CC2=CC=CC(C(F)(F)F)=C2)C)=O

Figure 3.1.1: PfDHODH inhibitors

3.3 MATERIALS AND METHODS

PARASITE CULTURE:

The erythrocytic stages of *P. falciparum* were grown at 37°C in solutions of 4% O+ hematocrit in RPMI 1640 medium (Invitrogen) supplemented with 28 mM $NaHCO_3$, 25 mM HEPES, 5% albumax II (w/v), and 20 µm gentamicin sulfate. Human blood was supplied by Research Blood Components or Interstate Blood Bank. Cultures were grown in a gas mixture of 5% O_2, 5% CO_2, and 90% N_2. Cultures were maintained with media changes every other day and were sub-cultured to maintain parasitemia below 4%. At least 25% of the hematocrit was replaced weekly. Parasite growth was synchronized by treatment with sorbitol [56]. Frozen stocks were prepared using a sterile solution composed of 28% glycerol, 3% sorbitol, and 0.65% sodium chloride. The Dd2 parasite used was MR4 strain MRA-156.

RESISTANCE SELECTION:

Approximately 1 x 10^9 ring stage parasites were treated with ten times the EC_{50} of a compound for two days in four independent flasks. Compound pressure was removed and the cultures were fed on alternate days with compound-free complete RPMI media. Once healthy parasites reappeared in the culture flasks and parasitemia reached 1%-2%, compound exposure was repeated. Selected parasites were cloned by limiting dilution in a 96-well plate with an inoculum of 0.2 infected red blood cells per well. Parasite clones were detected after 2.5 weeks of growth by microscopy.

GENOMIC DNA ANALYSIS:

Genomic DNA was extracted from parasites using the QIAamp blood kit (Qiagen) for sequence analysis of the *pfdhodh* gene (PlasmoDB ID: Pf3D7_0603300). A 2.2 kb fragment encompassing the complete *pfdhodh* ORF was PCR amplified from drug-

resistant clones and parental lines. PCR-amplified fragments were fully sequenced using *pfdhodh*-specific primers.

PfDHODH Forward 5'- GATCCCTAGGATGATCTCTAAATTGAAACCTCAATTTATG -3'
PfDHODH Reverse 5'- GATACTCGAGTTAACTTTTGCTATGCTTTCGGCCAATG -3'
PfDHODH internal 5'- CATTATTTGGATTATATGGTTTTTTTGAATCTTATAATCCTG -3'

The *pfdhodh* gene was amplified with Pfu Ultra II Fusion DNA polymerase (Agilent) with the following conditions: 95°C 120 seconds, 55°C 20 seconds, 60°C 100 seconds, go to step two and repeat 30 times. PCR amplicons were purified with a PCR clean-up kit (Qiagen) and sequenced via Genewiz

IN VITRO DRUG SENSITIVITY AND EC_{50} DETERMINATIONS:

Drug susceptibility was measured using the SYBR Green method [62]. Twelve point curves based on 2-fold dilutions of the test compound were carried out in triplicate and replicated on three different days. EC_{50} values were calculated using the log(inhibitor) vs. response – Variable slope equation in GraphPad Prism (described below):

$$Y = Bottom + \frac{(Top - Bottom)}{1 + 10^{\,Log(IC50 - X) \times\, Hill\ Slope}}$$

Where X = concentration of compound and Y = normalized parasite viability.

MOLECULAR DYNAMICS SIMULATIONS:

PDB ID: 3o8a was used as a scaffold for molecular dynamics simulations. Conformation A was chosen for the disulfide bonds, and conformation B was deleted from the PBD file. The coordinates were prepared with Desmond (Desmond Molecular Dynamics System, versions 2.2 and 3.0, D. E. Shaw Research, New York, NY, 2008 [78]). One microsecond simulations were run on the Orchestra cluster supported by the Harvard Medical School Research Information Technology Group. The simulations used 132 cores in the infiniband-enabled Rehearsal subset of the Orchestra cluster.

SYNTHESIS OF DSM74:

The compound DSM74 was prepared following the literature procedure [63] and was recrystallized from ethanol. ^{1}H NMR spectra matched that reported [43] and HPLC analysis indicated > 95% purity.

SYNTHESIS OF GSK8:

Pentane-2,4-dione (0.206 mL, 2.00 mmol) was added to a solution of 2-propyn-1-amine (0.274 mL, 4.00 mmol) in water (5 mL) and the resulting mixture was stirred at room temperature for 16 hr. The reaction was extracted with dichloromethane and the organic layer was dried over anhydrous Na_2SO_4, filtered, and concentrated under reduced pressure to give 275 mg of (Z)-4-(prop-2-yn-1-ylamino)pent-3-en-2-one (275 mg, 2.005 mmol, 100 % yield) as a yellow oil: ^{1}H-NMR ($CDCl_3$, 400 MHz) *d* 2.02 (s, 3H), 2.28 (t, *J* = 2.4 Hz, 1H), 3.99 (dd, *J* = 6.2, 2.4 Hz, 2H), 5.06 (s, 1H), 10.76 (br. s, 1H). MS: m/e 138 ($M+H^+$). Purity was determined as >95 % by HPLC (308 nm), Rt: 0.95 (Acquity UPLC BEH C18 1.7u 3x50mm, $CH_3CO_2NH_4$ 25mM + 10%ACN at pH 6.6 / ACN).

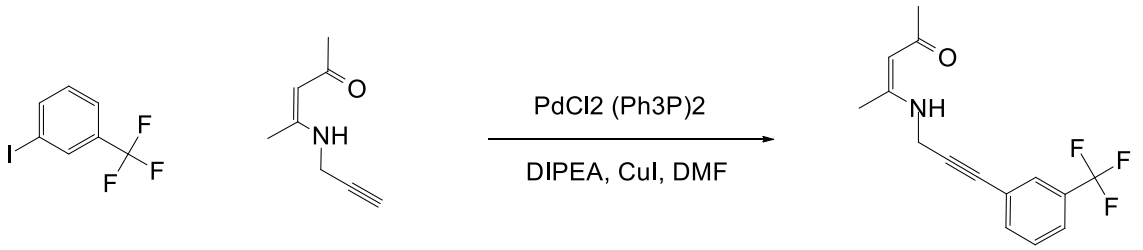

To a solution of (Z)-4-(prop-2-yn-1-ylamino)pent-3-en-2-one (260 mg, 1.895 mmol), CuI (7.22 mg, 0.038 mmol), $PdCl_2$ $(Ph_3P)_2$ (26.6 mg, 0.038 mmol) and DIPEA (3.89 mL,

22.74 mmol) in *N,N*-Dimethylformamide (DMF) (1 mL) under argon atmosphere, 3-iodobenzotrifluoride (0.410 mL, 2.84 mmol) was added and the resultant mixture was stirred at room temperature for 1 h 45 min, the reaction was partitioned between water and EtOAc. The layers were separated and the aqueous was extracted with EtOAc. The combination of the organic layers was washed with aq. 0.5 N HCl and brine. After drying over anhydrous Na2SO4, the organic layer was filtered and concentrated under reduced pressure. The resulting crude was purified by column chromatography (10g, Merck, CyHex:EtOAc gradients from 100:0 to 90:10 to 50:50) to give 365 mg of (Z)-4-((3-(3-(trifluoromethyl)phenyl)prop-2-yn-1-yl)amino)pent-3-en-2-one (365 mg, 1.298 mmol, 68.5 % yield) as a yellow solid: ^{1}H-NMR (CDCl3, 400 MHz) *d* 2.04 (s, 3H), 2.07 (s, 3H), 4.23 (d, *J* = 6.1 Hz, 2H), 5.09 (s, 1H), 7.43 (t, *J* = 7.7 Hz, 1H), 7.58 (m, 2H), 7.67 (s, 1H), 10.87 (br. s, 1H). MS: m/e 282 ($M+H^+$). Purity was determined as > 95 % by HPLC (309 nm), Rt: 1.28 (Acquity UPLC BEH C18 1.7u 3x50mm, $CH_3CO_2NH_4$ 25mM + 10% ACN at pH 6.6 / ACN).

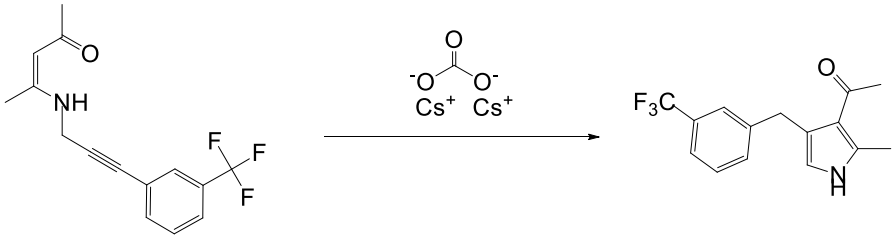

To a solution of 3-iodobenzotrifluoride (100 mg, 0.368 mmol) in anhydrous Dimethyl Sulfoxide (DMSO) (5 mL) under argon atmosphere, cesium carbonate (240 mg, 0.735 mmol) was added and the resultant mixture was stirred at room temperature for 1 h. The reaction was then diluted with EtOAc and 0.5 N aq. HCl. The layers were separated and the aqueous was extracted with EtOAc. The combination of the organic layers was washed with water, then brine, and then dried over anhydrous Na_2SO_4, filtered, and

concentrated under reduced pressure. The resulting crude was purified by column chromatography (dry head, 2g, Isolute, CyHex:EtOAc gradients from 100:0 to 80:20 to 0:100) to give 83 mg of 1-(2-methyl-4-(3-(trifluoromethyl)benzyl)-1H-pyrrol-3-yl)ethanone as a pale brown solid: ^{1}H-NMR (DMSO-D_6, 400 MHz) *d* 2.24 (s, 3H), 2.42 (s, 3H), 4.03 (s, 2H), 6.36, (d, *J* = 3 Hz, 1H), 7.46 (m, 4H), 11.05 (s, 1H). ^{13}C-NMR (DMSO-D_6, 100 MHz) d 15.4, 31.2, 32.9, 120.1, 122.7 (t, *J* = 3.7 Hz), 123.3, 125.0 (q, *J* = 272 Hz), 125.3 (q, J = 3.7 Hz), 129.2 (q, *J* = 31.5 Hz), 129.5,133,2, 135.9, 144.2, 193.9. ^{19}F-NMR (DMSO-D6, 376 MHz) *d* -60.8 (s, 3F). MS: m/e 282 ($M+H^+$). Purity was > 95 % by HPLC (249 nm), Rt: 1.20 (Acquity UPLC BEH C18 1.7u 3x50 mm, $CH_3CO_2NH_4$ 25mM + 10% ACN at pH 6.6 / ACN).

COPY NUMBER VARIATION QUANTITATIVE PCR:

PfDHODH copy number was assessed using the quantitative PCR (qPCR) primers described in Guler 2013 [51] (primers listed below). Two sets of primers were used to amplify regions of PfDHODH. DHODH front produced a 206 bp amplicon starting at nucleotide +656, and DHODH rear produced a 158 bp amplicon starting at nucleotide +1423. Seryl tRNA synthetase and 18s ribosomal RNA were used as reference genes. Power SYBR Green master mix with ROX (Applied Biosystems) was used on a 7900 HT qPCR machine (Applied Biosystems). The qPCR protocol was 95C for 10 minutes, followed by 40 rounds of 95C for 15 seconds and 60C for 1 minute. All experiments were followed by a dissociation curve (90C to 60C in 0.5C steps with 1 second hold at each step), and a 10^6 dilution curve of Dd2 genomic DNA was used to determine the amplification efficiency. Genomic DNA from Dd2 and 3D7 were used as one-copy controls. Selection clones served as the test, and the parent (Dd2 or 3D7) served as the control. Relative copy number was determined for 1 ng of genomic DNA using the $\Delta\Delta C_T$ method [79].

Gene ID	Function	Primer Sequences	Product
PFF0160c	DHODH Front	F-TCCATTCGGTGTTGCTGCAGGATTTGAT R-TCTGTAACTTTGTCACAACCCATATTA	206 bp
	DHODH Rear	F-GTGTTAGCGGAGCAAAACTAAAAG R-ATAATTGACAAACTGAAGCACCTG	158 bp
PF07_0073	Seryl t-RNA Synthetase	F-GGAACAATTCTGTATTGCTTTACC R-AAGCTGCGTTGTTTAAAGCTC	142 bp
MAL13P1.435	18s Ribo-somal RNA	F-ACAATTCATCATATCTTTCAATCGGTA R-GCTGACTACGTCCCTGCCC	69 bp

PFDHODH PLASMID CONSTRUCTION AND MUTAGENESIS:

A synthetic codon-optimized gene encoding residues 159-565 of PfDHODH [41] (Genbank accession No. AY685129) was cloned into a pET28b plasmid with an amino-terminal 6xHistidine tag followed by an rTEV cleavage site as described by Deng et al [64], resulting in pET28b-6xHistidine-rTEV-PfDHODH (codon optimized) del 1-158. The listed mutations were created with the following primers, then cloned into the tagged pET28b construct described above:

L172F Forward 5'-CCTGTACGATATTTTCTTCAAATTTTGTTTGAAGTA-3'
L172F Reverse 5'-GTACTTCAAACAAAATTTGAAGAAAATATCGTACA-3'

E182D Forward 5'-GTACATCGATGGTGACATTTGCCATGACCTG-3'
E182D Reverse 5'-CAGGTCATGGCAAATGTCACCATCGATGTAC-3'

F188I Forward 5'-AGCCATGACCTGATTTTGCTGCTTGG-3'
F188I Reverse 5'-CCAAGCAGCAAAATCAGGTCATGGCT-3'

F188L Forward 5'- ATTTGCCATGACCTGCTGTTGCTGCTTGG-3'
F188L Reverse 5'- CCAAGCAGCAACAGCAGGTCATGGCAAAT-3'

F227I Forward 5'- GTTGCAGCTGGAATCGATAAAAACGGTG-3'
F227I Reverse 5' CACCGTTTTTATCGATTCCAGCTGCAAC-3'

I263F Forward 5'- GAAACCGCGGTTCTTTCGTGACGTC-3'
I263F Reverse 5'-GACGTCACGAAAGAACCGCGGTTTC-3'

L527I Forward 5'-CTTCCGTGTGTCAGATCTATTCGTGCTT-3'
L527I Reverse 5'-AAGCACGAATAGATCTGACACACGGAAG-3'

L531F Forward 5'- GCTCTATTCGTGCTTCGTTTTCAACGGTATG-3'
L531F Reverse 5'- CATACCGTTGAAAACGAAGCACGAATAGAGC-3'

PFDHODH PROTEIN EXPRESSION AND PURIFICATION:

BL21(DE3)Star *Escherichia coli* (Invitrogen) were transformed with WT and mutant PfDHODH expression constructs. Transformed cells were grown in Terrific Broth with 100 µg/mL kanamycin at 37°C and 180 rpm, then dropped to 20°C and induced with 200 µm isopropyl-D-thiogalactoside. Cultures were grown 12-16 hours post-induction, then pelleted by centrifugation at 10,000*x g* and frozen at -80°C for later use. For purification, conical tubes of frozen cell pellets were thawed in 25°C water. Thawed pellets were then resuspended in buffer A (100 mM HEPES pH 8.0, 150 mM NaCl, 10% glycerol, 0.05% Thesit). The cells were lysed by sonication on ice (Branson digital sonifer 450, 5 minutes at 40% amplitude with a pattern of 5 seconds on and 10 seconds off). The cell lysate was clarified by centrifugation at 40,000*x g* for 45 minutes at 4°C, then filtered through a 0.45 µm filter. The clarified and filtered lysate was applied to a HisPrep FF 16/10 column (GE Healthcare) pre-equilibrated with buffer A on an AKTA Purifier FPLC. The column was washed with 30 cV of buffer A, then eluted with stepwise increments of buffer B (100 mM HEPES pH 8.0, 150 mM NaCl, 10 glycerol, 0.05% Thesit, 400 mM imidazole). The eluted protein was concentrated by centrifugation in concentrator spin columns (Pierce), then injected into a HiLoad 16/60 Superdex 200 size exclusion column pre-equilibrated with running buffer (10 mM HEPES pH 7.8, 100 mM NaCl, 5% glycerol, 1 mM *N,N*-dimethyldodecylamine *N*-oxide, 10 mM DTT). Fractions containing PfDHODH were pooled and concentrated. Protein concentration was assessed by Bradford assay (Pierce). Catalytically active protein concentration was assessed by boiling 50 µLof protein, clarifying by centrifugation for 10 minutes at 13,200*x g*, and then measuring absorbance of the cleared supernatant at 445 nm to determine the flavin mononucleotide concentration (ε_{445} = 12.5 mM^{-1} cm^{-1}). Aliquots of protein were flash-frozen in liquid nitrogen, then stored at -80°C.

PFDHODH BIOCHEMICAL ASSAYS:

Substrate-dependent inhibition of recombinant PfDHODH protein was assessed in an *in vitro* assay in 60 µLvolumes in 384-well clear plates (Corning 3702). A 16-point dilution series of inhibitor concentrations were assayed against 2-10 nM protein with 500 µm L-dihydroorotate substrate (L-DHO, excess), 18 mM dodecylubiquinone electron acceptor (CoQ_D, ~ Km), and 100 µm 2,6-dichloro-indophenol indicator dye in DHODH assay buffer (100 mM HEPES pH 8.0, 150 mM NaCl, 5% glycerol, 0.5% Triton X-100). Assays were incubated at 25°C for twenty minutes, then assessed by measuring the absorbance at 600 nM in a SpectraMax M5 plate reader. Molecular oxygen, which can act as an electron acceptor in this reaction, was depleted through the addition of 0.1 mg/mL of glucose oxidase, 0.02 mg/mL of catalase, and 50 mM glucose, followed by incubation at 25°C for five minutes prior to assay assembly. Data were normalized to 1% DMSO and excess inhibitor (500 nM Genz-669178 unless another compound was appropriate).

PFDHODH CRYSTALLOGRAPHY:

Wild-type PfDHODH protein was produced as described above by GlaxoSmithKline (Stevenage, United Kingdom). Protein-compound complexes were formed by mixing 50 µLof protein (in size exclusion buffer at ~10 mg/mL) with 1 µL of 500 mM *N,N*-dimethyldodecylamine *N*-oxide (LDAO), 0.5 µLof 200 mM L-dihydroorotate, and 0.5 µLof 200 mM compound. Complexes were allowed to form at room temperature for five minutes before being distributed into hanging drop or paraffin oil immersion microbatch trays by hand. 1 µLof protein-compound complex was mixed with 1 µLof precipitant in each drop. All trays were incubated at 20°C. Crystals were harvested from the following conditions for structure determination via synchrotron:

WT PfDHODH, Genz-669178: 0.2M LiCl + 24% PEG 3350

WT PfDHODH, IDI-6253: 0.2M LiCl + 20% PEG 3350

WT PfDHODH, IDI-6273: 0.1M MES pH 6.5 + 20% PEG 3350

STATISTICAL ANALYSES:

EC_{50} data are shown as mean ± standard deviation and were analyzed by one-way ANOVA with Dunnett's multiple comparison *post hoc* test (for three or more groups) or a two-tailed t-test (for two groups) via Graph Pad Prism 5.0d Software. Differences were considered significant for $P < 0.05$.

3.4 RESULTS

PROPOSED RESISTANCE MECHANISMS TO PFDHODH INHIBITORS

We sought to deeply sample resistance pathways to PfDHODH inhibitors, and did so through a comprehensive set of *in vitro* drug resistance selections. Earlier selections (described in Chapter 2) had shown that the PfDHODH mutations E182D, F227I, and L531F each gave resistance to PDHODH inhibitors. Examination of crystal structures (Figure 3.4.1) showed that these residues were all in or near the species-selective drug-binding site, but did not appear to make direct contact with bound inhibitors.

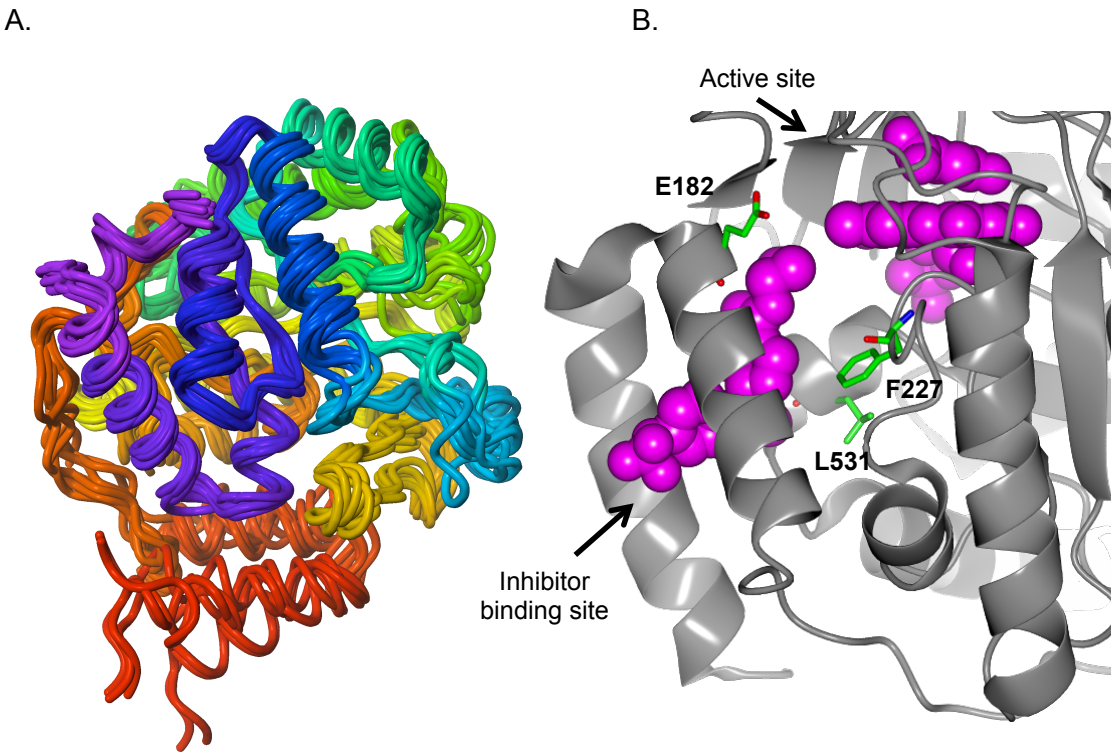

Figure 3.4.1: Lid dynamics and observed resistance mutations in PfDHODH

(A). Overlay of molecular dynamics simulations at 1, 350, 750, and 1000 nanoseconds. The α1- α2 helix lid (in red) shows more mobility than the rest of the protein.
(B). Observed resistance mutations: F188, L172, F227, L531, L527, E182, I263. All mutations observed in PfDHODH were near the α1- α2 helix lid or electron tunnel.
All images shown are of PDB ID: 3o8a and were generated with CCP4mg [66].

All three resistance mutations appeared to be important in holding the α1- α2 helix lid to the main body of the protein. Crystal structures showed sparse contacts holding the lid to the body of the protein. Molecular dynamics simulations (Figure 3.4.1 A) corroborated the idea that the lid was loosely associated: the lid was by far the most mobile portion of the protein, and was held by a limited number of hydrogen bonds and hydrophobic interactions. The lid defines the PfDHODH inhibitor binding pocket and is the entrance to the presumed tunnel for electron flow between respiratory chain ubiquinone and the flavin mononucleotide cofactor. Given this, we proposed that mutations that weakened lid binding were potential drug resistance sites. Compromising lid binding would presumably affect the binding of ubiquinone in addition to that of PfDHODH inhibitors, so some theoretically possible mutations might result in non-viable parasites. PfDHODH amplification or a resistance pathway unrelated to the target gene were also logical resistance options. We chose to focus on single nucleotide polymorphisms (SNPs) and gene amplification in PfDHODH both for ease of detection and because in our hands, they were the most likely outcome.

Resistance Selections: An Overview

We carried out a variety of resistance selections. Intermittent pulse selections (Figure 3.4.1 A) gave more consistently successful results than applying constant drug pressure. We used this intermittent pulse strategy in three ways (Figure 3.4.1 B, C): primary selection, where a wild-type (WT) parasite is treated with a WT PfDHODH inhibitor; sequential selection, where the resultant mutant parasites are treated with a mutant inhibitor; and simultaneous selection, where WT parasites are treated with a combination of WT and mutant inhibitors. The simultaneous selection is a test of the “targeting resistance” concept and should suppress the emergence of resistance.

A.

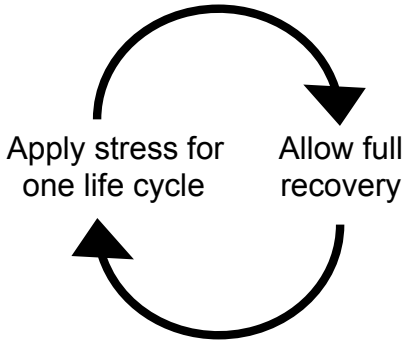

B.

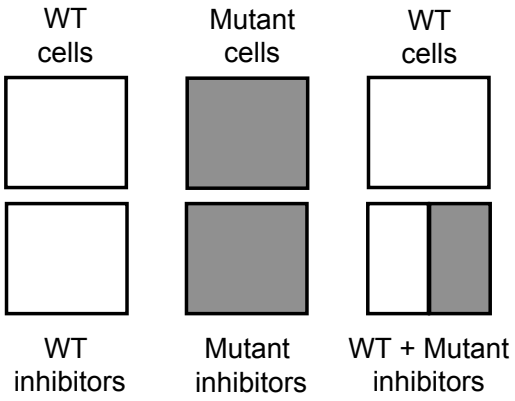

C.

Type of selection	Expected results
Primary	Resistance
Sequential	Return to wild-type or development of further resistance
Simultaneous	Suppression of resistance

D.

Type of selection	Observed results
Primary	Resistance (F188I, Fi88L, E182D, F227I, L531F)
Sequential	Return to WT (D182E) or more mutations (L172F, L527I)
Simultaneous	Fewer cases of resistance (I263F) or none at all

Figure 3.4.2: Drug resistance selection strategies used and expectations

(A). Repeated intermittent pulse selections: short-term stress and recovery cycles.
(B). The selections used different parasite lines, inhibitors, and inhibitor combinations.
(C). Expected results from different selection strategies.
(D). Observed results were consistent with the hypotheses.

Observed resistance mutations (Figure 3.4.2 D) were largely consistent with our hypothesis, but led to a refinement of the model: resistance mutations appear to line both lid-body interactions and the presumed ubiquinone-FMN electron transfer tunnel. This, coupled with the observation that triazolopyrimidine inhibitors appear to block electron flow from FMN to ubiquinone, but not from FMN to inorganic oxidants like

atmospheric oxygen or ferricyanide [65], led to the following model: PfDHODH inhibitor resistance mutations disrupt electron flow between ubiquinone and FMN, and they may do so by either disrupting the lid-body interactions that create the electron tunnel, or by directly impeding electron flow in a normally-formed tunnel.

Overall, we were able to raise resistant mutants to nearly every PfDHODH inhibitor tested (Table 3.4.1). In several cases, similar or even the same *pfdhodh* mutation occurred in independent cultures. This is further evidence that a small number of resistance pathways are heavily favored by evolution. For example, the selection of Dd2 parasites (MR4 strain MRA-156) with Genz-669178 led to the highly similar *pfdhodh* mutations F188I and F188L in independent flasks. Selection of the Dd2-PfDHODH F227I mutant line with IDI-6253 gave an L527I mutation in all four flasks. Note that this mutation gave low-level resistance to PfDHODH inhibitors, but was not statistically significant. Perhaps L527I is a compensatory mutation that increases the fitness of the F227I mutant. Combination therapy led to fewer resistant populations (independent flasks) than monotherapy. The selection of 3D7 E182D with IDI-6273 and the selection of Dd2 with the combination of Genz-669178 and IDI-6273 were discussed in Chapter 2 and will not be discussed in detail.

Selections which gave resistance were subjected to copy number variation quantitative PCR for *pfdhodh*. No selections with mutations in *pfdhodh* had copy number variation, but several resistant lines with no mutations in *pfdhodh* had gene amplifications (Table 3.4.1). These observations are consistent with the Guler 2013 study demonstrating that nonspecific gene amplification is the initial step in resistance to triazolopyrimidine PfDHODH inhibitors [51], and the amplifications are primed for mutation. Thus, selections with amplified *pfdhodh* should be continued to identify more mutational resistance.

Table 3.4.1: Summary of resistance selection results

Selection Information					PfDHODH locus		
Parasite Line	Drug(s)	Culture	Resistance	Candidate for WGS	Residue	Nucleotide	Copy #
3D7	Genz-669178	1	Y	Y	WT		2
		2	Y	Y	WT		1
		3	Y	Y	WT		1
		4	N	N	WT		n.d.
3D7 E182D	IDI-6273	1	N	N	WT		n.d.
		2	Y	N	D182E	T546G	1
		3	N	N	WT		n.d.
		4	N	N	WT		n.d.
Dd2	Genz-669178	1	N	N	WT		n.d.
		2	Y	N	F188I	T562A	1
		3	N	Y	WT		n.d.
		4	Y	N	F188L	T564A	1
Dd2 F227I	IDI-6253	1	Y*	N	L527I	T1579A	1
		2	Y*	N	L527I	T1579A	1
		3	Y*	N	L527I	T1579A	1
		4	Y*	N	L527I	T1579A	1
Dd2 F227I	IDI-6273	1	N	Y	F227I		1
		2	Y	Y	F227I		2
		3	Y	Y	F227I		2
		4	N	Y	F227I		1
Dd2 F227I	GSK3	1	Y	N	L172F	A516T	1
		2	Y	N	L172F	A516T	1
		3	Y	N	L172F	A516T	1
		4	Y	N	L172F	A516T	1
Dd2	Genz-669178 + IDI-6253	1	N	N	WT		n.d.
		2	Y	Y	WT		4
		3	N	N	WT		n.d.
		4	N	N	WT		n.d.
Dd2	Genz-669178 + IDI-6273	1	N	N	WT		n.d.
		2	N	N	WT		n.d.
		3	N	N	WT		n.d.
		4	N	N	WT		n.d.
Dd2	Genz-669178 + GSK3	1	Y	N	I263F	A787T	1
		2	N	N	WT		n.d.
		3	N	N	WT		n.d.
		4	N	N	WT		n.d.

The selections all took between six to ten weeks to yield stable resistance (Figure 3.4.3 A), meaning that parasite lines maintained resistance after being frozen and revived in culture. The number of drug pulses required (Figure 3.4.3 B) ranged from a single pulse (3D7 E182D: IDI-6273) to eleven (3D7: Genz-669178).

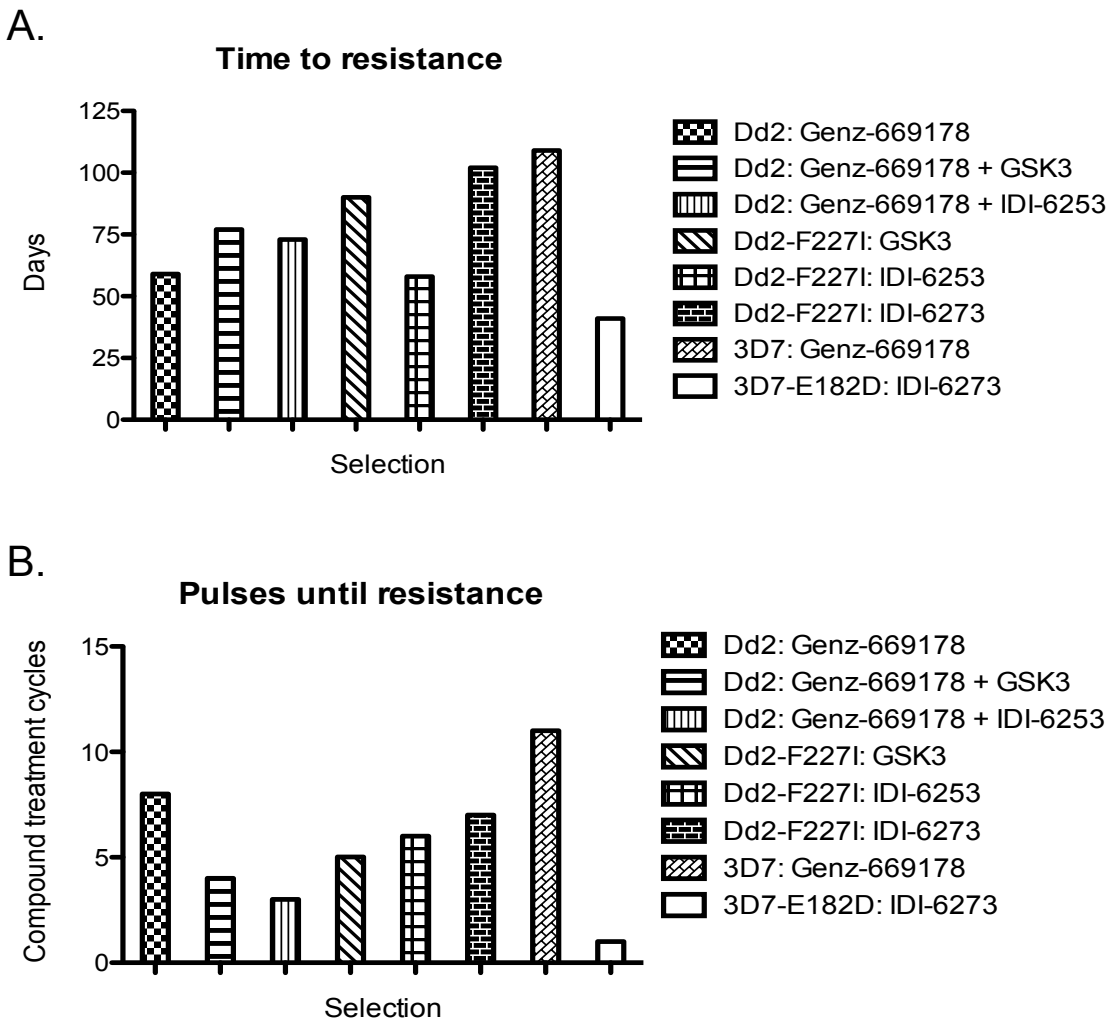

Figure 3.4.3: Parameters of successful resistance selections

(A). Time to resistance varied from 6 to 10 weeks.
(B). The number of stress pulse cycles until resistance developed ranged from 1 to 11. The Dd2: Genz-669178 + IDI-6273 selection did not develop resistance and is not shown on these charts.

INDIVIDUAL DRUG RESISTANCE SELECTIONS

The 3D7: Genz-669178 selection gave significant resistance to the selecting agent in two of four flasks (Figure 3.4.4 A). Curiously, it also gave resistance to structurally

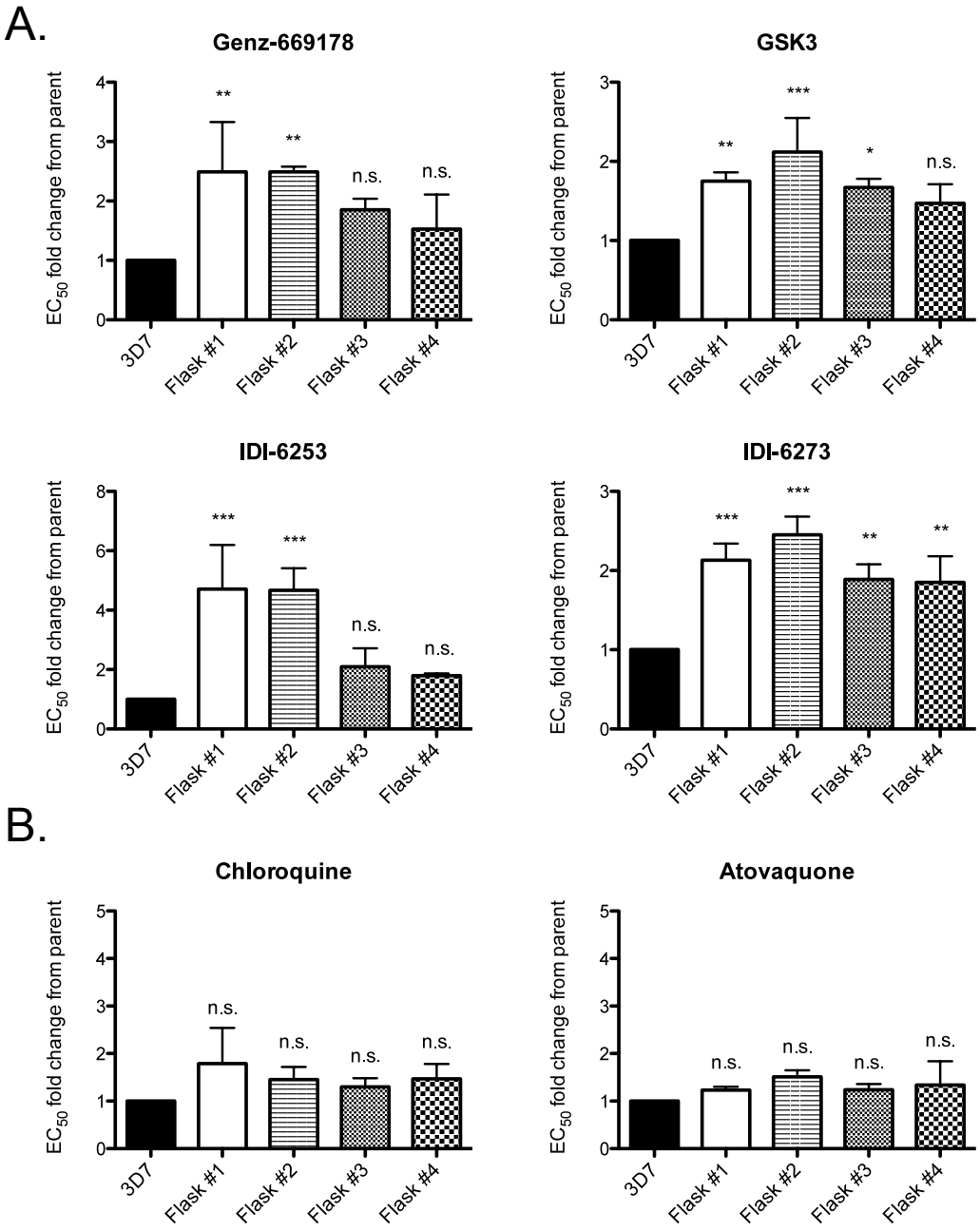

Figure 3.4.4: The 3D7: Genz-669178 selection gave resistance to PfDHODH inhibitors of several structural classes

(A). EC_{50} fold shifts relative to the parental selection line show significant development of resistance for four structural classes of PfDHODH inhibitors.
(B). The unrelated antimalarial compounds chloroquine and atovaquone show no significant differences among the lines tested.

EC_{50} values were calculated using a whole-cell SYBR Green assay. Error bars indicate the standard deviation of three biological replicates, each with triplicate measurements.

unrelated PfDHODH inhibitors, but not to antimalarial agents with unrelated mechanisms of action (Figure 3.4.4 B). There were no mutations in *pfdhodh*. As sensitivity to unrelated antimalarial agents was decreased (though not significantly so), this may be a non-specific resistance due to efflux pumps. Culture #1 had two copies of the WT *pfdhodh* gene, but had similar drug sensitivities to cultures without gene amplification.

Table 3.4.2: 3D7: Genz-669178 selection results

		EC_{50} fold shift over parent ± s.d.				
		Parent	Flask #1	Flask #2	Flask #3	Flask #4
PfDHODH allele		WT	2 copies of WT	WT	WT	WT
PfDHODH WT Inhibitors	Genz-669178	1	2.49 ± 0.84	2.49 ± 0.09	1.85 ± 0.19	1.53 ± 0.58
	Genz-668419	1	2.22 ± 0.72	3.24 ± 1.65	2.06 ± 0.43	1.48 ± 0.54
PfDHODH Mutant Inhibitors	IDI-6253	1	4.71 ± 1.49	4.67 ± 0.74	2.10 ± 0.62	1.80 ± 0.07
	IDI-6273	1	2.13 ± 0.21	2.45 ± 0.23	1.89 ± 0.19	1.85 ± 0.33
	GSK-3	1	1.75 ± 0.11	2.12 ± 0.43	1.68 ± 0.11	1.47 ± 0.24
Standard Antimalarials	Chloroquine	1	1.79 ± 0.75	1.45 ± 0.27	1.30 ± 0.18	1.47 ± 0.31
	Dihydroartemisinin	1	1.41 ± 0.27	1.55 ± 0.37	1.35 ± 0.26	1.53 ± 0.29
	Atovaquone	1	1.24 ± 0.07	1.51 ± 0.14	1.24 ± 0.12	1.34 ± 0.50

B.

		EC_{50} (nM) ± s.d.				
		Parent	Flask #1	Flask #2	Flask #3	Flask #4
PfDHODH allele		WT	2 copies of WT	WT	WT	WT
PfDHODH WT Inhibitors	Genz-669178	6.29 ± 5.45	18.61 ± 21.35	15.89 ± 14.15	12.11 ± 11.43	11.67 ± 13.71
	Genz-668419	5.36 ± 3.48	10.93 ± 6.16	13.94 ± 2.82	10.94 ± 7.69	8.33 ± 7.45
PfDHODH Mutant Inhibitors	IDI-6253	16924.33 ± 6982.80	85876.66 ± 87359.51	88806.66 ± 80102.39	35316.66 ± 20068.73	30603.33 ± 13421.49
	IDI-6273	480.90 ± 68.57	1025.86 ± 181.84	1169.67 ± 90.72	901.13 ± 85.18	886.40 ± 159.79
	GSK-3	64.78 ± 21.47	111.89 ± 29.45	141.20 ± 66.97	107.12 ± 28.61	93.72 ± 25.72
Standard Antimalarials	Chloroquine	6.00 ± 1.62	9.92 ± 2.87	8.72 ± 2.87	7.72 ± 1.780	8.48 ± 1.04
	Dihydroartemisinin	2.39 ± 1.40	3.15 ± 1.62	3.56 ± 2.26	3.01 ± 1.52	3.89 ± 2.53
	Atovaquone	0.15 ± 0.06	0.19 ± 0.09	0.23 ± 0.10	0.19 ± 0.09	0.22 ± 0.17

(A). EC_{50} fold shifts relative to the parental parasite line show significant differences in sensitivity to a variety of PfDHODH inhibitors, although the *pfdhodh* allele was wild-type. (B). EC_{50} values for the same data set.
EC_{50} values were calculated using a whole-cell SYBR Green assay. The s.d. is the standard deviation of three biological replicates, each with triplicate measurements.

A similar selection, using Dd2 as the WT selection line and again using Genz-669178 as the selection agent, gave starkly different results (Figure 3.4.5, Table 3.4.3).

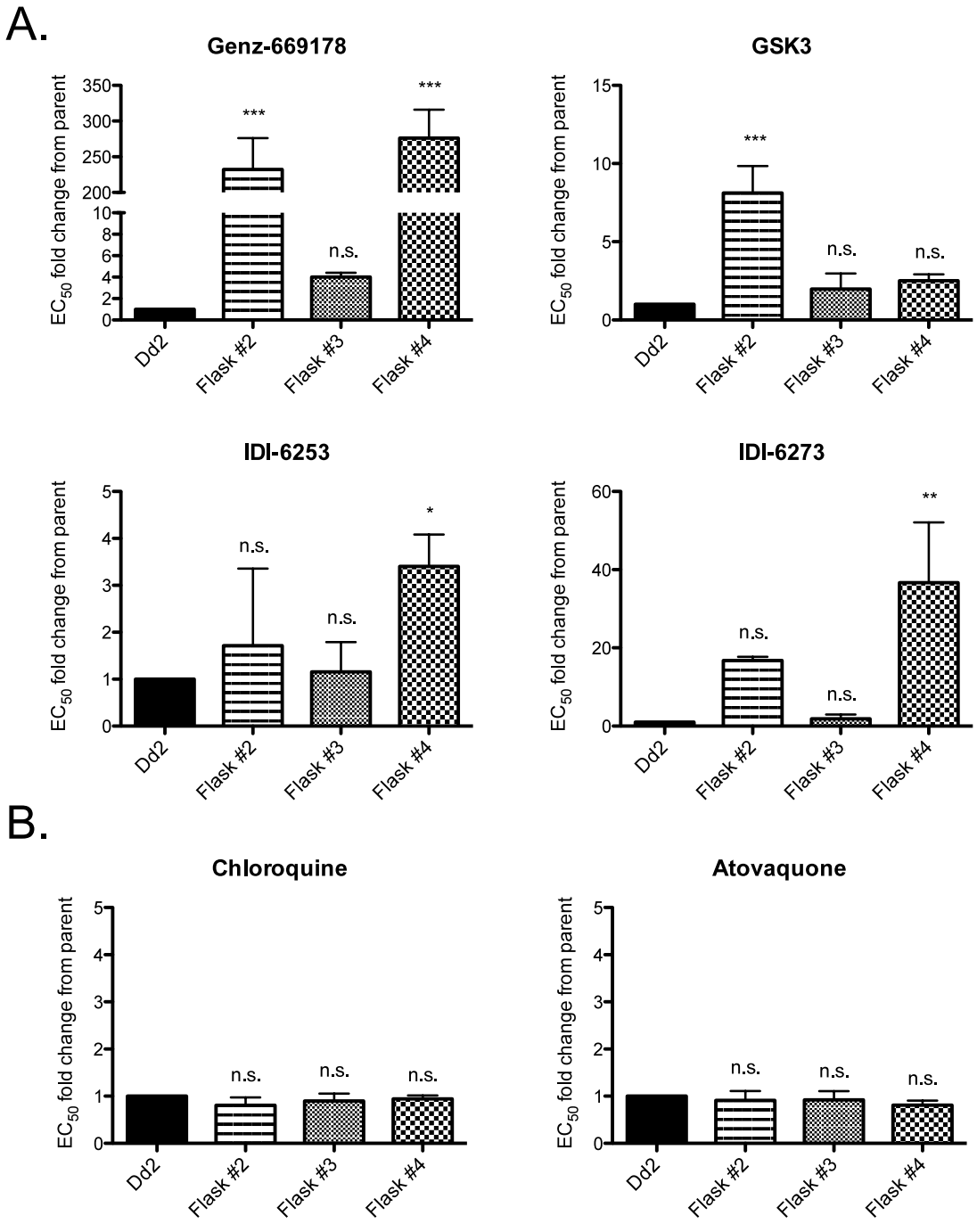

Figure 3.4.5: The Dd2: Genz-669178 selection gave resistance to PfDHODH inhibitors of several structural classes

(A). EC_{50} fold shifts relative to the parental selection line show highly significant resistance for the selecting agent in two of three flasks (flask #1 did not recover). (B). The unrelated antimalarial compounds chloroquine and atovaquone show no significant differences among the lines tested.

EC_{50} values were calculated using a whole-cell SYBR Green assay. Error bars indicate the standard deviation of three biological replicates, each with triplicate measurements.

The 3D7 selection gave low-level resistance with no discernable changes in *pfdhodh*. In contrast, the Dd2 selection gave two separate lines with highly significant resistance and one line with medium-level resistance (and one flask that never recovered). The two highly resistant lines developed strikingly similar mutations in *pfdhodh*, indicating a evolutionary fitness maximum for resistance.

Table 3.4.3: Dd2: Genz-669178 selection results

A.

		EC_{50} fold shift over parent ± s.d.			
		Parent	Flask #2	Flask #3	Flask #4
PfDHODH allele		WT	F188I	WT	F188L
PfDHODH WT Inhibitors	Genz-669178	1	210.59 ± 43.93	4.01 ± 0.39	276.22 ± 39.75
	Genz-668419	1	61.75 ± 10.44	3.34 ± 1.06	38.02 ± 4.60
PfDHODH Mutant Inhibitors	IDI-6253	1	16.77 ± 1.64	1.16 ± 0.63	3.40 ± 0.68
	IDI-6273	1	16.77 ± 0.97	1.84 ± 0.63	36.69 ± 35.37
	GSK-3	1	8.12 ± 1.73	1.98 ± 0.99	2.49 ± 0.42
Standard Antimalarials	Chloroquine	1	0.80 ± 0.17	0.90 ± 0.16	0.95 ± 0.07
	Dihydroartemisinin	1	0.63 ± 0.37	0.59 ± 0.15	0.89 ± 0.17
	Atovaquone	1	0.91 ± 0.20	0.92 ± 0.18	0.81 ± 0.09

B.

		EC_{50} (nM) ± s.d.			
		Parent	Flask #2	Flask #3	Flask #4
PfDHODH allele		WT	F188I	WT	F188L
PfDHODH WT Inhibitors	Genz-669178	2.50 ± 0.70	1556 ± 892	10.83 ± 3.88	700.43 ± 256.71
	Genz-668419	4.44 ± 0.70	708 ± 296	17.66 ± 4.55	169.37 ± 34.85
PfDHODH Mutant Inhibitors	IDI-6253	32753.67 ± 41203.66	16257 ± 6025	54133.33 ± 42312.46	142925.0 ± 128516.66
	IDI-6273	1197.67 ± 740.44	67316 ± 76212	3626.67 ± 2670.44	57043.67 ± 77167.70
	GSK-3	59.25 ± 27.21	1104 ± 490	108.23 ± 71.88	140.37 ± 49.62
Standard Antimalarials	Chloroquine	3.81 ± 0.57	5.5 ± 6.0	2.45 ± 0.95	3.34 ± 0.55
	Dihydroartemisinin	77.35 ± 53.36	83 ± 58	73.08 ± 47.74	71.70 ± 49.13
	Atovaquone	0.16 ± 0.06	0.24 ± 0.02	0.15 ± 0.03	0.13 ± 0.06

(A). EC_{50} fold shifts relative to the parental parasite line show significant differences in sensitivity to a variety of PfDHODH inhibitors. Note the two highly similar mutations in PfDHODH: F188I and F188L. These gave similar, but not the same, sensitivity changes. (B). EC_{50} values for the same data set.

EC_{50} values were calculated using a whole-cell SYBR Green assay. The s.d. is the standard deviation of three biological replicates, each with triplicate measurements.

Flask #2, which developed an F188I mutation in PfDHODH, became 210-fold resistant to Genz-669178, with EC_{50} values rising from 7.4 nM to 1556 nM. Flask #4, which gained an F188L mutation in PfDHODH, became 276-fold resistant to Genz-669178, with EC50 values rising from 2.5 nM to 700 nM. Curiously, even though leucine and isoleucine are very similar residues, F188I was 3.3-fold more resistant to GSK3 than F188L (8.12 versus 2.49-fold, respectively). Flask #3 gained a borderline significant 4-fold resistance to Genz-669178, rising from an EC_{50} of 2.5 nM to 10.8 nM. No mutations were found in *pfdhodh*, so this is a whole-genome sequencing candidate. No significant changes in sensitivity were observed for the unrelated antimalarial drugs chloroquine, atovaquone, or dihydroartemisinin. (Note: parental Dd2 data is shown for a paired assay with flasks #3 and #4, but Dd2 and flask #2 were run in a separate set of assays. Thus, the fold changes and EC_{50} values shown will not match for flask #2).

After selecting two WT parasite lines (3D7 and Dd2) with WT PfDHODH inhibitors, we selected mutant parasite lines (PfDHODH E182D or F227I) with mutant-selective inhibitors. No mutant-selective inhibitors were found for PfDHODH L531F in the small set tested, so no selections were done with this mutant line. The selection of parasite line 3D7 E182D with compound IDI-6273 was discussed in Chapter 2.

The first mutant parasite-mutant inhibitor selection was parasite Dd2 F227I with compound GSK3 (Figure 3.4.6, Table 3.4.4). Each of the four independent selections gave rise to the same PfDHODH mutation: L172F. This indicates a fitness maximum. Note that all selections were started from early freezes of the same clonal parasite line, so it is unlikely that L172F arising in all four flasks is a founder effect. This mutation was not seen in other Dd2 F227I selections. All of the selected flasks gave similar, though not identical, results. This may be due to other physiological changes in the lines.

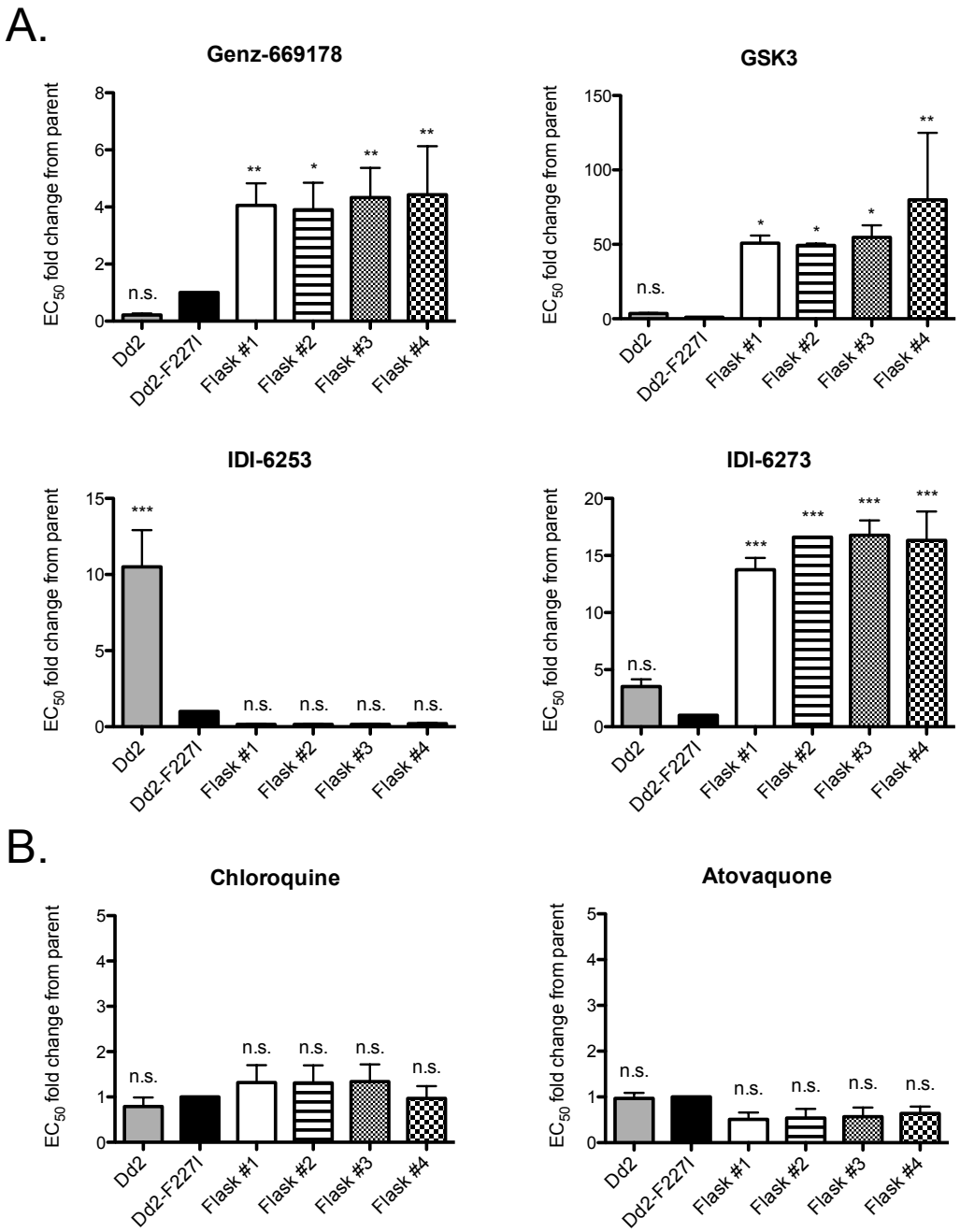

Figure 3.4.6: The Dd2 F227I: GSK3 selection gave resistance to PfDHODH inhibitors of several structural classes

(A). EC_{50} fold shifts relative to the parental selection line show highly significant resistance in all four selection flasks. These did not revert to WT-like sensitivity (Dd2). (B). The unrelated antimalarial compounds chloroquine and atovaquone show no significant differences among the lines tested.

EC_{50} values were calculated using a whole-cell SYBR Green assay. Error bars indicate the standard deviation of three biological replicates, each with triplicate measurements.

As expected, this selection led to resistance to the selecting agent, with GSK3 EC_{50} values increasing at least 50-fold for all four flasks. Sensitivity to unrelated PfDHODH inhibitors was also affected: Genz-669178 became 4-fold less effective, IDI-6273 became ~15-fold less effective, and IDI-6253 became 5-to-6-fold more effective. Unrelated control compounds showed no significant changes, although all four flasks gained a borderline significant two-fold sensitivity to atovaquone.

Table 3.4.4: Dd2 F227I: GSK3 selection results

A.

		EC_{50} fold shift over parent ± s.d.				
		Parent	Flask #1	Flask #2	Flask #3	Flask #4
PfDHODH allele		F227I	L172F + F227I	L172F + F227I	L172F + F227I	L172F + F227I
PfDHODH WT Inhibitors	Genz-669178	1	4.06 ± 0.77	3.9 ± 0.95	4.33 ± 1.04	4.43 ± 1.7
	Genz-668419	1	1.52 ± 0.29	2.17 ± 1.09	1.62 ± 0.38	2.0 ± 0.67
PfDHODH Mutant Inhibitors	IDI-6253	1	0.16 ± 0.04	0.16 ± 0.03	0.16 ± 0.04	0.2 ± 0.05
	IDI-6273	1	13.76 ± 1.03	16.6 ± 3.58	16.77 ± 1.31	16.32 ± 2.54
	GSK-3	1	50.81 ± 5.07	49.28 ± 1.22	54.63 ± 8.24	79.9 ± 45.05
Standard Antimalarials	Chloroquine	1	1.32 ± 0.38	1.31 ± 0.39	1.34 ± 0.38	0.97 ± 0.27
	Dihydroartemisinin	1	0.75 ± 0.18	0.75 ± 0.16	0.82 ± 0.16	1.26 ± 0.77
	Atovaquone	1	0.51 ± 0.15	0.54 ± 0.20	0.57 ± 0.20	0.64 ± 0.15

B.

		EC_{50} (nM) ± s.d.				
		Parent	Flask #1	Flask #2	Flask #3	Flask #4
PfDHODH allele		F227I	L172F + F227I	L172F + F227I	L172F + F227I	L172F + F227I
PfDHODH WT Inhibitors	Genz-669178	889.57 ± 1422.39	168.81 ± 136.04	182.79 ± 80.58	317.53 ± 108.45	308.77 ± 125.90
	Genz-668419	469.50 ± 436.47	209.99 ± 161.40	392.97 ± 269.84	331.43 ± 51.21	367.70 ± 34.2
PfDHODH Mutant Inhibitors	IDI-6253	7747 ± 12596	4585.0 ± 3650.51	6181.1 ± 6529.28	7519.67 ± 3643.4	6466.33 ± 1866.32
	IDI-6273	3207 ± 684.48	455.75 ± 192.97	1415.23 ± 1639.20	533.07 ± 192.54	580.10 ± 159.87
	GSK-3	610.53 ± 916.66	2663.90 ± 2128.88	2676.68 ± 2273.74	3724.33 ± 575.48	3824.33 ± 1048.05
Standard Antimalarials	Chloroquine	155.44 ± 87.39	174.41 ± 83.39	173.05 ± 80.63	200.27 ± 45.30	171.27 ± 72.99
	Dihydroartemisinin	13.78 ± 3.71	10.68 ± 0.81	10.88 ± 1.72	10.36 ± 1.50	11.51 ± 0.52
	Atovaquone	0.44 ± 0.12	0.24 ± 0.098	0.24 ± 0.08	0.21 ± 0.02	0.22 ± 0.03

(A). EC_{50} fold shifts relative to the parental parasite line show significant differences in sensitivity to a variety of PfDHODH inhibitors. All four flasks gained a PfDHODH L172F mutation, and had similar, but not identical, drug sensitivity profiles.
(B). EC_{50} values for the same data set.

EC_{50} values were calculated using a whole-cell SYBR Green assay. The s.d. is the standard deviation of three biological replicates, each with triplicate measurements.

Selection of the Dd2 F227I parasite line with the mutant-selective compound IDI-6253 also led to one mutation arising and dominating in all four independent flasks. In this case, the mutation was PfDHODH L527I. Although this mutation is in the presumed ubiquinone binding pocket, no statistically significant resistance was observed for PfDHODH inhibitors or for unrelated antimalarial compounds, and this mutation did not restore “WT” Dd2 levels of sensitivity (Figure 3.4.7, Table 3.4.5). However, it should be noted that this selection gained borderline significant 3 to 4-fold resistance to the selecting agent, IDI-6253. It is difficult to reach significance with small-scale resistance due to the inherent variability between assays that use human blood from different donors. This data would likely reach significance with further biological replicates.

These results imply that the F227I + L527I combination has a benefit over the F227I parent that is unrelated to PfDHODH inhibitor resistance – or that the 3 to 4-fold resistance seen is actually significant in a biological sense. L527I may be a compensatory mutation that increases the fitness of the parent line. It is highly unlikely that the same mutation occurred in all four flasks and outcompeted all other potential alleles without a clear benefit. Competitive growth assays of F227I versus F227I + L527I (with and without drug present) would help clarify the role of this mutation. One possibility is that the double-mutant parasites grow better when there is no drug pressure – faster cycle times, larger burst size, and so on. Residues F227 and L527 and quite close to each other (see Figure 3.4.2 B). It is plausible that the original F227I mutation reduced a favorable, stabilizing hydrophobic interaction with spatial neighbor L527. This may have been alleviated when both residues were mutated to isoleucines, as “isoleucine zipper”-type hydrophobic interactions are likely stronger than isoleucine-leucine interactions.

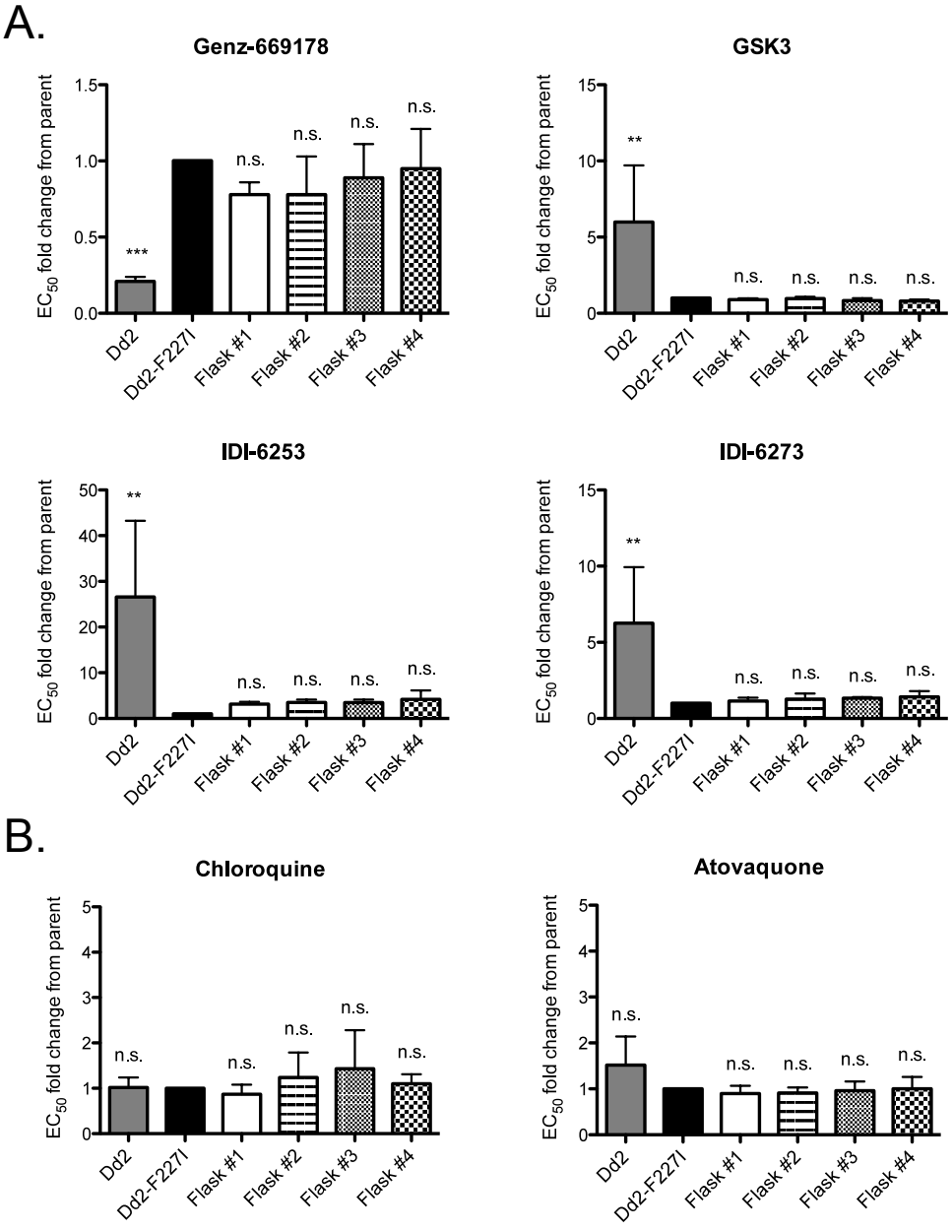

Figure 3.4.7: The Dd2 F227I: IDI-6253 selection did not give significant resistance

(A). EC_{50} fold shifts relative to the parental selection line show low-level, non-significant resistance. All four flasks gained an L527I mutation in PfDHODH.
(B). The unrelated antimalarial compounds chloroquine and atovaquone show no significant differences among the lines tested.

EC_{50} values were calculated using a whole-cell SYBR Green assay. Error bars indicate the standard deviation of three biological replicates, each with triplicate measurements.

Table 3.4.5: Dd2-F227: IDI-6253 selection results

A.

		EC_{50} fold shift over parent ± s.d.				
		Parent	Flask #1	Flask #2	Flask #3	Flask #4
PfDHODH allele		F227I	F227I + L527I	F227I + L527I	F227I + L527I	F227I + L527I
PfDHODH WT Inhibitors	Genz-669178	1	0.78 ± 0.08	0.78 ± 0.25	0.89 ± 0.22	0.95 ± 0.26
	Genz-668419	1	0.68 ± 0.13	0.71 ± 0.20	0.78 ± 0.09	0.89 ± 0.27
PfDHODH Mutant Inhibitors	IDI-6253	1	3.13 ± 0.52	3.51 ± 0.64	3.48 ± 0.66	4.18 ± 1.96
	IDI-6273	1	1.14 ± 0.23	1.27 ± 0.39	1.33 ± 0.08	1.42 ± 0.38
	GSK-3	1	0.89 ± 0.09	0.97 ± 0.11	0.83 ± 0.16	0.81 ± 0.10
Standard Antimalarials	Chloroquine	1	0.97 ± 0.14	0.98 ± 0.04	1.09 ± 0.17	1.38 ± 0.51
	Dihydroartemisinin	1	0.87 ± 0.21	1.24 ± 0.55	1.43 ± 0.85	1.10 ± 0.21
	Atovaquone	1	0.90 ± 0.17	0.81 ± 0.12	0.96 ± 0.20	1.36 ± 0.46

B.

		EC_{50} (nM) ± s.d.				
		Parent	Flask #1	Flask #2	Flask #3	Flask #4
PfDHODH allele		F227I	F227I + L527I	F227I + L527I	F227I + L527I	F227I + L527I
PfDHODH WT Inhibitors	Genz-669178	40.52 ± 20.52	32.54 ± 19.85	34.78 ± 28.78	38.77 ± 29.50	36.73 ± 15.31
	Genz-668419	108.30 ± 11.83	74.40 ± 19.92	77.29 ± 28.34	84.81 ± 19.07	97.12 ± 30.63
PfDHODH Mutant Inhibitors	IDI-6253	199.94 ± 147.57	237.42 ± 187.78	287.30 ± 271.22	273.33 ± 217.49	255.30 ± 139.12
	IDI-6273	1062.27 ± 721.25	3463.67 ± 2823.82	3869.67 ± 3172.65	3922.67 ± 2923.38	4378.00 ± 2770.89
	GSK-3	32.36 ± 31.17	29.00 ± 27.56	33.15 ± 33.71	29.00 ± 29.47	26.95 ± 26.29
Standard Antimalarials	Chloroquine	83.35 ± 86.94	62.45 ± 52.54	90.88 ± 82.22	98.36 ± 83.14	103.10 ± 122.37
	Dihydroartemisinin	6.22 ± 6.06	6.40 ± 6.06	6.12 ± 5.16	6.92 ± 6.37	7.50 ± 5.71
	Atovaquone	0.26 ± 0.20	0.25 ± 0.23	0.21 ± 0.16	0.23 ± 0.13	0.32 ± 0.21

(A). EC_{50} fold shifts relative to the parental parasite line show significant differences in sensitivity to a variety of PfDHODH inhibitors. All four flasks gained a PfDHODH L527I mutation, and had similar, but not identical, drug sensitivity profiles.
(B). EC_{50} values for the same data set.

EC_{50} values were calculated using a whole-cell SYBR Green assay. The s.d. is the standard deviation of three biological replicates, each with triplicate measurements.

For the last single-drug selection, the Dd2 F227I line was selected with the mutant-selective compound IDI-6273. This did not result in resistance to the selective agent, but curiously gave resistance to the structurally unrelated WT PfDHODH inhibitor Genz-669178 (Figure 3.4.8, Table 3.4.6). In flasks #2 and #3, the EC50 for Genz-669178 increased 3.6-fold, rising from 3.4 μm to ~10 uM. Although these changes are small, the error was small enough to declare this highly significant.

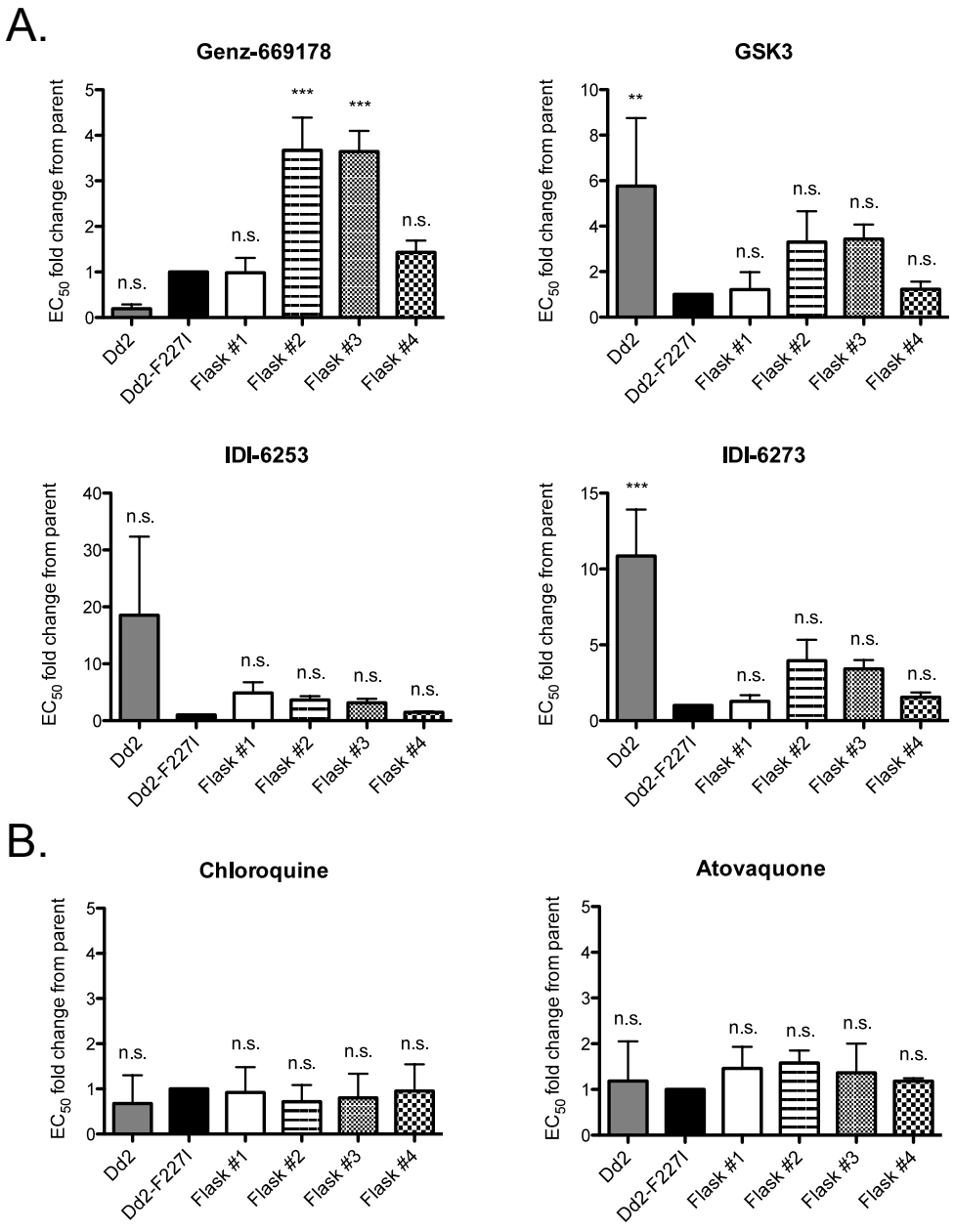

Figure 3.4.8: The Dd2 F227I: IDI-6273 selection gave highly significant resistance not to the selecting agent, but to the unrelated Genz-669178

(A). EC_{50} fold shifts relative to the parental selection line show highly significant resistance to Genz-669178 in flasks #2 and #3, and non-significant resistance to other PfDHODH inhibitors.
(B). The unrelated antimalarial compounds chloroquine and atovaquone show no significant differences among the lines tested.

EC_{50} values were calculated using a whole-cell SYBR Green assay. Error bars indicate the standard deviation of three biological replicates, each with triplicate measurements.

Table 3.4.6: Dd2 F227I: IDI-6273 selection results

A.

		EC_{50} fold shift over parent ± s.d.				
		Parent	Flask #1	Flask #2	Flask #3	Flask #4
PfDHODH allele		F227I	F227I	2 copies of F227I	2 copies of F227I	F227I
PfDHODH WT Inhibitors	Genz-669178	1	0.99 ± 0.33	3.67 ± 0.72	3.64 ± 0.46	1.43 ± 0.26
	Genz-668419	1	0.87 ± 0.21	3.16 ± 0.88	3.28 ± 0.67	1.41 ± 0.35
PfDHODH Mutant Inhibitors	IDI-6253	1	1.26 ± 1.89	3.95 ± 0.68	3.41 ± 0.69	1.54 ± 0.18
	IDI-6273	1	4.87 ± 0.42	3.64 ± 1.38	3.15 ± 0.57	1.47 ± 0.32
	GSK-3	1	1.21 ± 0.77	3.31 ± 1.35	3.44 ± 0.64	1.23 ± 0.33
Standard Antimalarials	Chloroquine	1	0.92 ± 0.56	0.72 ± 0.37	0.80 ± 0.53	0.95 ± 0.59
	Dihydroartemisinin	1	1.79 ± 0.08	0.95 ± 0.37	1.30 ± 0.70	1.49 ± 0.42
	Atovaquone	1	1.48 ± 0.47	1.08 ± 0.27	1.39 ± 0.64	1.84 ± 0.42

B.

		EC_{50} (nM) ± s.d.				
		Parent	Flask #1	Flask #2	Flask #3	Flask #4
PfDHODH allele		F227I	F227I	2 copies of F227I	2 copies of F227I	F227I
PfDHODH WT Inhibitors	Genz-669178	3388.17 ± 5765.55	2175.97 ± 3620.64	9675.98 ± 16382.01	10651.11 ± 18038.40	4187.34 ± 7081.33
	Genz-668419	2853.54 ± 4839.72	2014.08 ± 3320.25	8802.49 ± 14967.7	9712.78 ± 16484.7	4518.03 ± 7694.92
PfDHODH Mutant Inhibitors	IDI-6253	357.29 ± 279.31	1701.65 ± 1454.72	970.83 ± 1010.02	1120.44 ± 919.23	1373.73 ± 1665.02
	IDI-6273	103.67 ± 39.91	172.79 ± 117.64	333.35 ± 156.53	338.86 ± 75.73	146.77 ± 26.62
	GSK-3	43.55 ± 54.03	80.94 ± 109.23	159.41 ± 211.43	172.60 ± 232.55	54.86 ± 72.41
Standard Antimalarials	Chloroquine	1442.44 ± 2303.53	143.89 ± 664.27	198.12 ± 632.37	208.97 ± 535.37	229.11 ± 568.62
	Dihydroartemisinin	143.89 ± 245.04	198.12 ± 337.92	208.97 ± 357.26	229.11 ± 392.09	277.26 ± 474.74
	Atovaquone	224.96 ± 389.51	255.35 ± 442.03	376.21 ± 651.41	341.64 ± 591.54	257.08 ± 445.10

(A). EC_{50} fold shifts relative to the parental parasite line show significant differences in sensitivity to a variety of PfDHODH inhibitors. All four flasks gained a PfDHODH L527I mutation, and had similar, but not identical, drug sensitivity profiles.
(B). EC_{50} values for the same data set.

EC_{50} values were calculated using a whole-cell SYBR Green assay. The s.d. is the standard deviation of three biological replicates, each with triplicate measurements.

No significant changes in sensitivity were observed for other PfDHODH inhibitors or unrelated control compounds. However, the same 3 to 4-fold decreases in sensitivity are seen for all PfDHODH inhibitors tested in flasks #2 and #3. Flasks #2 and #3 both had a two-fold amplification of *pfdhodh* F227I, which would explain their low-level resistance to PfDHODH inhibitors but not unrelated antimalarial drugs such as chloroquine.

Combination selection of the WT Dd2 parasite line with Genz-669178 and GSK3 (Figure 3.4.9, Table 3.4.7) led to significant resistance in one of four independent selections.

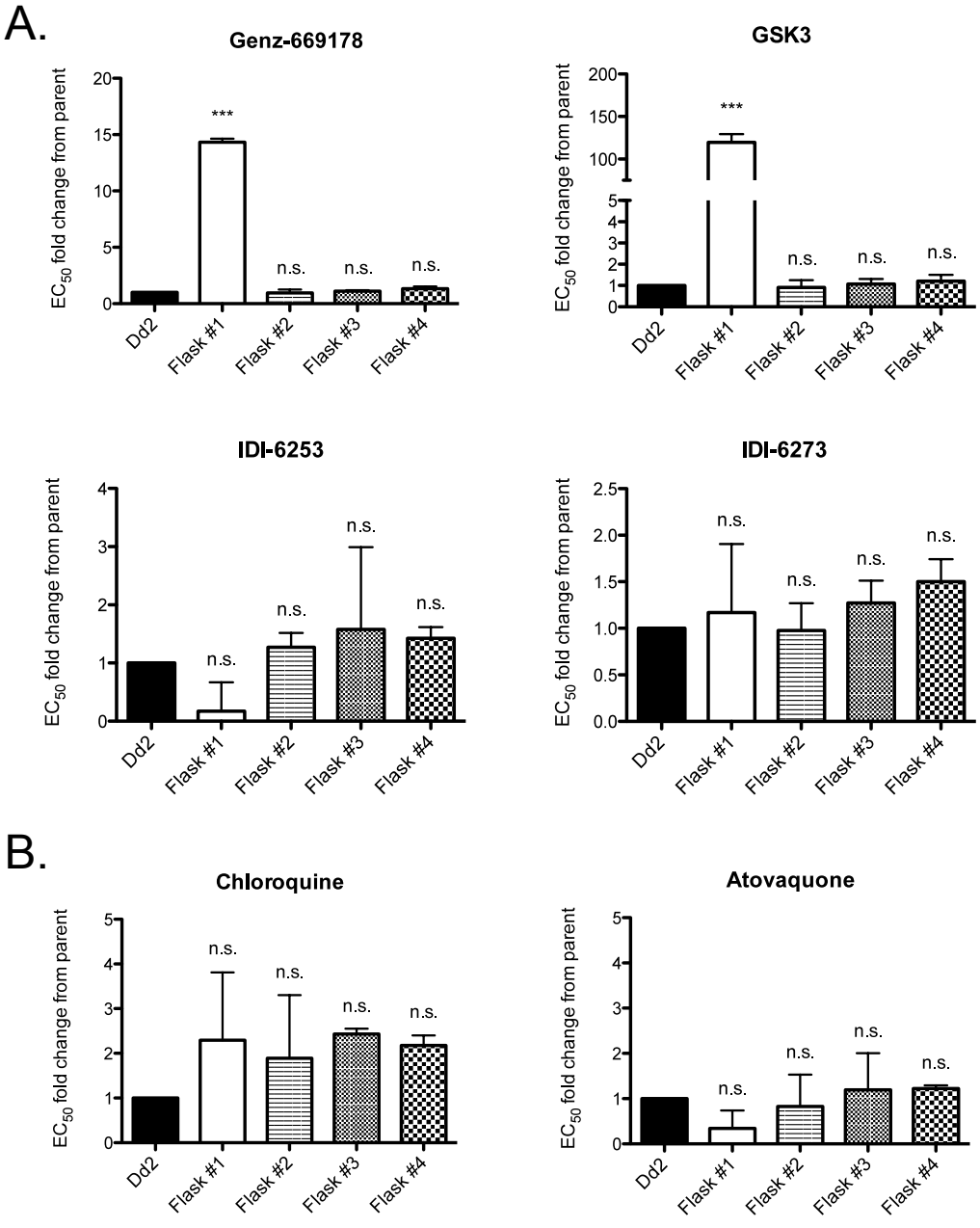

Figure 3.4.9: The Dd2: Genz-669178 + GSK3 combination selection gave highly significant resistance to both selection agents in one of four selections

(A). EC_{50} fold shifts relative to the parental selection line show highly significant resistance to both selection agents in flask #1, which gained a PfDHODH I263F mutation. (B). The unrelated antimalarial compounds chloroquine and atovaquone show no significant differences among the lines tested.

EC_{50} values were calculated using a whole-cell SYBR Green assay. Error bars indicate the standard deviation of three biological replicates, each with triplicate measurements.

Table 3.4.7: Dd2: Genz-669178 + GSK3 combination selection results

A.

		EC_{50} fold shift over parent ± s.d.				
		Parent	Flask #1	Flask #2	Flask #3	Flask #4
PfDHODH allele		WT	I263F	WT	WT	WT
PfDHODH WT Inhibitors	Genz-669178	1	14.32 ± 0.32	0.96 ± 0.30	1.10 ± 0.09	1.33 ± 0.20
	Genz-668419	1	18.94 ± 0.19	0.87 ± 0.28	0.98 ± 0.12	1.01 ± 0.11
PfDHODH Mutant Inhibitors	IDI-6253	1	0.17 ± 0.50	1.27 ± 0.25	1.58 ± 1.41	1.42 ± 0.19
	IDI-6273	1	1.17 ± 0.74	0.98 ± 0.29	1.27 ± 0.24	1.50 ± 0.24
	GSK-3	1	119.64 ± 9.88	0.90 ± 0.35	1.07 ± 0.24	1.21 ± 0.30
Standard Antimalarials	Chloroquine	1	2.29 ± 1.52	1.89 ± 1.42	2.43 ± 0.12	2.18 ± 0.23
	Dihydroartemisinin	1	0.97 ± 0.61	0.97 ± 0.30	1.18 ± 0.35	1.07 ± 0.50
	Atovaquone	1	0.95 ± 0.35	0.81 ± 0.26	0.99 ± 0.23	0.95 ± 0.17

B.

		EC_{50} (nM) ± s.d.				
		Parent	Flask #1	Flask #2	Flask #3	Flask #4
PfDHODH allele		WT	I263F	WT	WT	WT
PfDHODH WT Inhibitors	Genz-669178	3.53 ± 0.36	50.98 ± 14.27	3.78 ± 1.60	4.37 ± 2.14	5.50 ± 4.25
	Genz-668419	5.79 ± 1.5	110.23 ± 36.83	5.28 ± 1.25	5.81 ± 1.31	6.60 ± 3.88
PfDHODH Mutant Inhibitors	IDI-6253	18927.67 ± 13046.72	1189.50 ± 1418.32	22091.67 ± 12599.00	28728.33 ± 19614.32	26994.33 ± 61.01
	IDI-6273	1189.50 ± 153.44	18927.67 ± 228.40	1159.50 ± 118.90	1514.00 ± 197.99	1789.00 ± 284.26
	GSK-3	69.81 ± 22.16	9787.67 ± 5.86	59.70 ± 13.87	69.52 ± 19.70	86.39 ± 61.01
Standard Antimalarials	Chloroquine	54.33 ± 22.16	54.33 ± 61.20	86.83 ± 45.69	113.51 ± 65.95	96.24 ± 61.73
	Dihydroartemisinin	3.82 ± 1.06	3.50 ± 0.88	3.04 ± 0.67	3.73 ± 0.88	3.67 ± 2.00
	Atovaquone	0.16 ± 0.16	0.05 ± 0.03	0.093 ± 0.05	0.15 ± 0.10	0.17 ± 0.14

(A). EC_{50} fold shifts relative to the parental parasite line show significant differences in sensitivity to a variety of PfDHODH inhibitors in one of four flasks.
(B). EC_{50} values for the same data set.

EC_{50} values were calculated using a whole-cell SYBR Green assay. The s.d. is the standard deviation of three biological replicates, each with triplicate measurements.

This selection treated a WT parasite with both WT and mutant-type PfDHODH inhibitors – a test of the “targeting resistance” concept discussed in Chapter 2. None of the four selection flasks showed resistance at 50 days. Extension of the selections to 80 days, however, led to substantial resistance to both selecting compounds in one of four flasks. While this finding certainly weakens the argument for targeting resistance, the lengthy treatment required and the fact that only one of four flasks gained resistance suggests that it is more difficult for the parasite to become resistant to this combination than either drug alone.

Flask #1 gained an I263F mutation in PfDHODH. This selected line gained 14.3-fold resistance to Genz-669178, with an EC_{50} rising from 3.5 nM to 51 nM. A 19-fold resistance was observed for the structurally similar compound Genz-668419. A striking 120-fold increase in EC_{50} was seen for GSK3, rising from 68.91 nM to 9789.87 nM. This selected line gained a borderline significant 5-fold sensitivity to IDI-6253. No changes were seen in sensitivity to unrelated antimalarial compounds.

The combination selection of Dd2 parasites with Genz-669178 and IDI-6253 gave similar results: in 80 days, one of four independent selections gave rise to resistance (Figure 3.4.10, Table 3.4.8). In this case, there was a four-fold amplification of *pfdhodh* with no mutations in the gene. The resistance observed was small – only 2 to 3-fold – but applied to a variety of PfDHODH inhibitor structural classes. Curiously, these resistant parasites became hypersensitive to a variety of "unrelated" compounds. For instance, the EC_{50} for chloroquine dropped 10-fold, going from 46.59 nM to 2.6 nM. This resembles the change between parasite lines Dd2 (chloroquine resistant) and 3D7 (chloroquine sensitive). It is unlikely that this flask is a 3D7 contaminant as we have no 3D7-based lines with the same drug sensitivity profile. Analysis of an extended set of unrelated antimalarials showed a folate pathway alteration (Table 3.4.8 C), although it is unclear if these changes are related to resistance or are merely coincidental.

The folate pathway is required for pyrimidine biosynthesis as a source of one-carbon units. Testing sensitivity to folate pathway inhibitors suggested that the resistant line has wild-type dihydropterate synthase (DHS, targeted by sulfadoxine), but mutant bifunctional dihydrofolate reductase-thymidylate synthase (DHFR-TS, targeted by pyrimethamine and cycloguanil). The sensitivity to sulfadoxine was unchanged. Pyrimethamine sensitivity increased 100-fold, and cycloguanil sensitivity increased a staggering 588-fold.

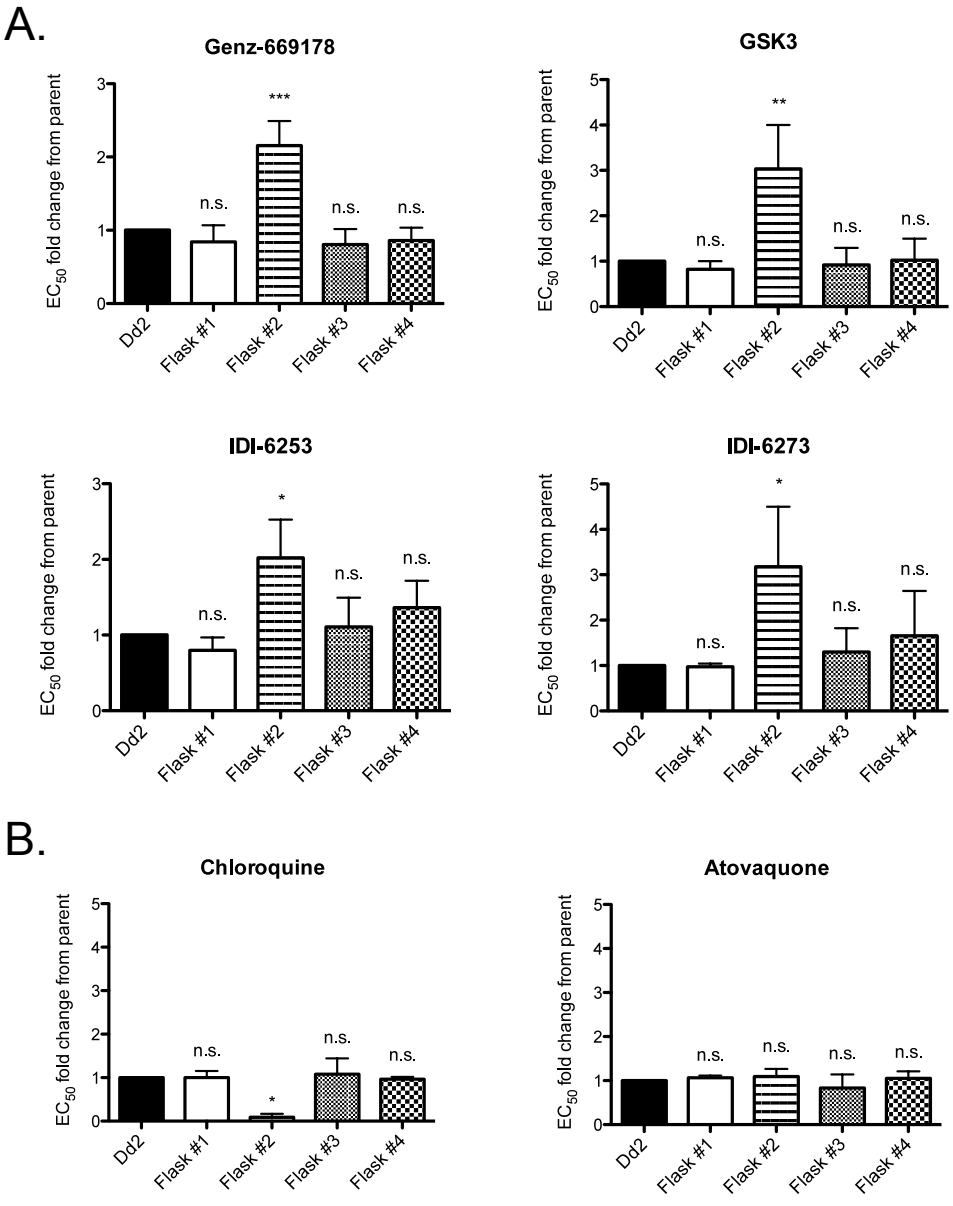

Figure 3.4.10: The Dd2: Genz-669178 + IDI-6253 combination selection gave significant resistance to multiple PfDHODH inhibitors in one of four selections

(A). EC_{50} fold shifts relative to the parental selection line show highly significant resistance to both selection agents in flask #2, which had no mutations in *pfdhodh.* (B). The unrelated antimalarial compounds atovaquone shows no significant differences among the lines tested, but flask #2 became hypersensitive to chloroquine.

EC_{50} values were calculated using a whole-cell SYBR Green assay. Error bars indicate the standard deviation of three biological replicates, each with triplicate measurements.

Table 3.4.8: Dd2: Genz-669178 + IDI-6253 selection results

A.

		EC_{50} fold shift over parent ± s.d.				
		Parent	Flask #1	Flask #2	Flask #3	Flask #4
PfDHODH allele		WT	WT	4 copies of WT	WT	WT
PfDHODH WT Inhibitors	Genz-669178	1	0.84 ± 0.23	2.16 ± 0.34	0.81 ± 0.21	0.86 ± 0.18
	Genz-668419	1	0.96 ± 0.12	2.42 ± 0.61	0.98 ± 0.10	1.05 ± 0.31
PfDHODH Mutant Inhibitors	IDI-6253	1	0.80 ± 0.17	2.02 ± 0.50	1.11 ± 0.39	1.36 ± 0.36
	IDI-6273	1	0.97 ± 0.07	3.18 ± 1.32	1.30 ± 0.53	1.65 ± 1.00
	GSK-3	1	0.82 ± 0.18	3.03 ± 0.97	0.92 ± 0.38	1.02 ± 0.48
Standard Antimalarials	Chloroquine	1	1.00 ± 0.15	0.09 ± 0.08	1.08 ± 0.36	0.97 ± 0.05
	Dihydroartemisinin	1	1.19 ± 0.79	2.00 ± 1.88	1.08 ± 0.72	1.01 ± 0.32
	Atovaquone	1	1.06 ± 0.05	1.10 ± 0.17	0.83 ± 0.31	1.05 ± 0.16

B.

		EC_{50} (nM) ± s.d.				
		Parent	Flask #1	Flask #2	Flask #3	Flask #4
PfDHODH allele		WT	WT	4 copies of WT	WT	WT
PfDHODH WT Inhibitors	Genz-669178	3.13 ± 0.36	2.66 ± 0.95	6.75 ± 1.38	2.57 ± 0.93	2.73 ± 0.83
	Genz-668419	5.27 ± 0.95	5.00 ± 0.40	12.59 ± 3.30	5.11 ± 0.72	5.42 ± 1.36
PfDHODH Mutant Inhibitors	IDI-6253	21151.00 ± 13882.82	16270.00 ± 10629.67	41983.33 ± 28762.27	26143.00 ± 22082.52	27352.00 ± 19706.17
	IDI-6273	756.65 ± 765.59	762.75 ± 797.97	1896.45 ± 1430.55	1182.15 ± 1389.96	1630.80 ± 2015.54
	GSK-3	57.30 ± 17.66	44.95 ± 2.55	162.43 ± 13.08	48.97 ± 9.93	54.32 ± 14.13
Standard Antimalarials	Chloroquine	46.59 ± 32.40	46.94 ± 36.45	2.60 ± 0.76	42.64 ± 20.04	45.51 ± 31.51
	Dihydroartemisinin	3.09 ± 2.06	3.58 ± 1.82	5.73 ± 2.40	3.22 ± 2.85	3.13 ± 0.60
	Atovaquone	0.10 ± 0.06	0.10 ± 0.06	0.11 ± 0.07	0.087 ± 0.08	0.10 ± 0.04

C.

		EC_{50} fold shift over parent ± s.d.				
		Parent	Flask #1	Flask #2	Flask #3	Flask #4
PfDHODH allele		WT	WT	4 copies of WT	WT	WT
Standard Antimalarials	Chloroquine	1	1.00 ± 0.15	0.09 ± 0.08	1.08 ± 0.36	0.97 ± 0.05
	Pyrimethamine	1	0.58 ± 0.38	0.0098 ± 0.0005	0.47 ± 0.23	0.94 ± 0.46
	Cycloguanil	1	1.14 ± 0.30	0.0017 ± 0.0002	0.89 ± 0.13	0.89 ± 0.09
	Sulfadoxine	1	0.80 ± 0.49	0.72 ± 0.28	0.70 ± 0.26	0.74 ± 0.32

(A). EC_{50} fold shifts relative to the parental parasite line show significant differences in sensitivity to a variety of PfDHODH inhibitors in one of four flasks.
(B). EC_{50} values for the same data set.
(C). EC50 fold shifts for a set of unrelated antimalarials and folate pathway inhibitors.

EC_{50} values were calculated using a whole-cell SYBR Green assay. The s.d. is the standard deviation of three biological replicates, each with triplicate measurements.

Targeted DNA sequencing confirmed these inferences: DHS was wild-type, and DHFR-TS was mutant. The mutant DHFR-TS residues involved in clinically observed pyrimethamine and cycloguanil sensitivity are well characterized [80]. The typical DHFR-

TS pattern of mutations in the resistant Dd2 line relative to the sensitive 3D7 line (N51I, C59S, S108N) was slightly altered to N51I, C59S, and S108R. This S108R mutation might increase the efficiency of the enzyme, which could increase the cellular supply of methyl-tetrahydrofolate. Methyl-tetrahydrofolate is an essential source of one-carbon units when converting dUMP to dCTP in pyrmidine biosynthesis. Thus, a more efficient folate pathway could at least theoretically alleviate low-level PfDHODH inhibition.

It is less clear how chloroquine sensitivity might be related to PfDHODH inhibitors. Although nucleotides get the vast majority of attention, it is worth noting that vitamin B1 (thiamine) is also a pyrimidine, and so also requires PfDHODH activity. Vitamin B1 is an essential cofactor in many cellular processes, including glucose and amino acid metabolism, and the genes necessary for both scavenge and biosynthesis are present in *Plasmodium spp*. [81]. Importantly, scavenging is not sufficient, and depleting thiamine from parasite growth media is detrimental. It has not gone unnoticed that the thiamine biosynthetic pathway is essential in malaria parasites and not present in humans, and a recent effort showed that oxythiamine, a thiamine analog, was lethal to *P. falciparum* in culture [82]. It is plausible that a reduced vitamin B1 pool affects chloroquine sensitivity – e.g., slowing down glucose metabolism would decrease both cellular ATP and the flux through the pentose phosphate shunt, which would alter the redox status of the parasite. One of the main armaments against oxidative damage is glutathione. Glutathione has also been shown to degrade non-polymerized ferriprotoporphyrin IX ("free heme") – it is thought that chloroquine works mainly through interrupting the polymerization of the free-radical producing free heme into the more inert form hemozoin [83]. Thus, reducing sugar metabolism would decrease cellular NADPH, which would lead to an over-reliance on glutathione for preventing oxidative damage. If the glutathione pools were sufficiently

shunted towards fighting oxidative damage and away from detoxifying free heme, this could potentiate the efficacy of chloroquine.

Assessing Target Responsibility via Purified Protein

These drug resistance selections were characterized by looking for changes in drug sensitivity and/or the target *pfdhodh*. Drug resistance, of course, may be due to other factors than mutations or copy number variation in the presumed target. However, there is not yet a robust and cost-effective methodology for determining mechanisms of drug resistance in a large number of parasite lines. Classic population genetics strategies like linkage mapping are still in use, but making genetic crosses in malaria is experimentally arduous and requires the use and potential sacrifice of non-human primates [84]. It is highly unlikely that existing crosses (from controlled primate infections of isolated from human patients) would have resistance to PfDHODH inhibitors, as these drugs are not yet in clinical use.

Genome-wide tools such as whole genome sequencing and microarrays can generate a long list of candidate genomic regions, but following up on those candidates is difficult due to the relative genetic intractability of *P. falciparum* (never mind that of *P. vivax*, which has yet to be successfully cultured long-term in a lab setting). In-progress advances in transfection and recombination technology – zinc finger nucleases [85], TALENS [86], and the RNA-guided CRISPR/Cas9 system [87, 88] – may change this. The gold standard and eventual goal is to do allelic replacements to determine if mutations in *pfdhodh* are responsible for the observed changes in drug sensitivity. As current techniques would take 6-12 months to generate PfDHODH allelic replacement parasites, we decided to focus on protein biochemistry.

We cloned, expressed, and purified a total of 11 DHODH proteins in *Escherichia coli* (Figure 3.4.11). These included WT and all observed mutant PfDHODH proteins as well as the WT proteins from *P. vivax* and *H. sapiens*. Class II DHODH proteins are inactive without the cognate FMN cofactor. Some of the mutants – particularly L531F and all F227I-containing mutants – had only ~5% catalytically competent protein. This may have relevance to their *in vivo* activity, with the caveat that expression of a truncated form of the enzyme in a recombinant host might not reflect native expression parameters.

A.

B.

DHODH protein	[Protein], mg/mL	[FMN], uM	[Active protein], mg/mL	% Catalytically Competent Protein
Pf WT	3.04	2.80	1.27	42.03
Pf E182D	4.25	1.81	0.82	19.47
Pf F227I	28.21	0.80	0.36	1.29
Pf L531F	7.73	0.61	0.27	3.62
Pf F188I	1.48	1.20	0.54	37.0
Pf F188L	5.57	4.90	2.23	40.19
Pf I263F	2.78	3.46	1.58	56.90
Pf L172F + F227I	4.76	1.17	0.53	11.24
Pf L527I + F227I	7.37	0.85	0.38	5.28
Pv WT	1.62	1.20	0.54	33.80
Hs WT	1.47	2.85	1.30	88.57

C.

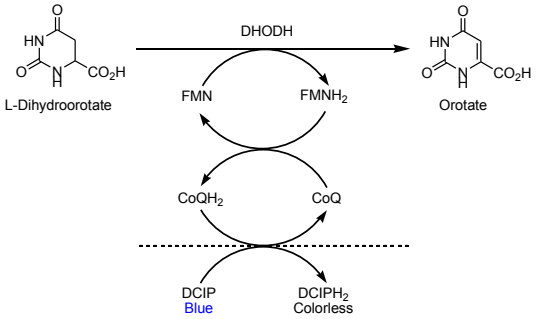

Figure 3.4.11: Production and use of recombinant DHODH proteins

(A). Purification resulted in a clean, single band by Coomassie staining (shown: PfDHODH I263F, 45 kDa).
(B). The yield of protein (and catalytically competent protein with a flavin mononucleotide cofactor) varied widely between different constructs. However, we were able to obtain sufficient active protein for all 11 constructs.
(C). The *in vitro* reaction catalyzed by DHODH protein. This can either be measured through direct observation of orotic acid product or through a coupled DCIP dye.

Protein activity assays showed large differences in sensitivity to PfDHODH inhibitors (Figure 3.4.12, Figure 3.4.13, Table 3.4.10). These differences are shown as fold changes over WT PfDHODH (represented by the dotted line at $10^0 = 1$).

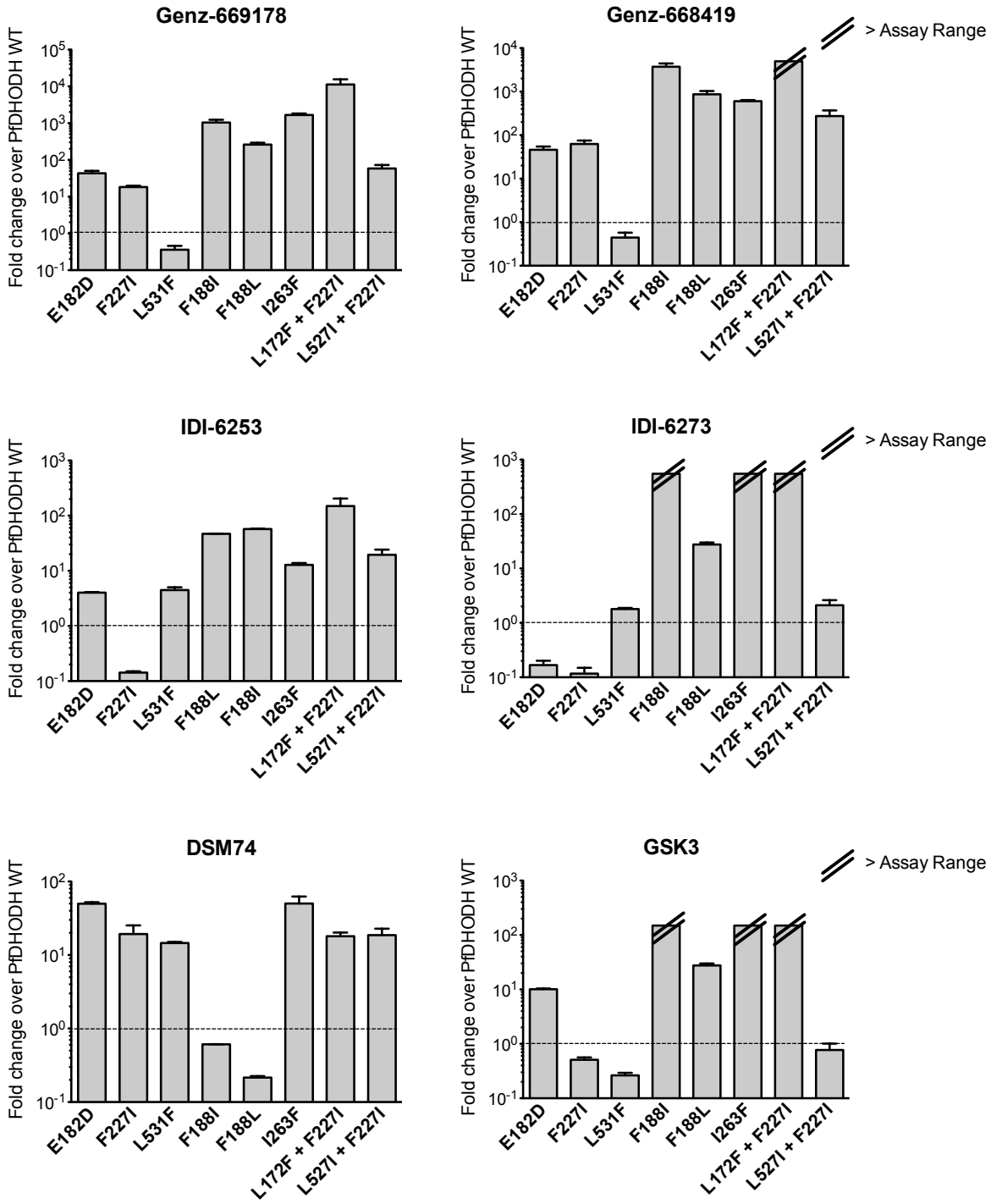

Figure 3.4.12: Inhibition of recombinant DHODH proteins *in vitro*

In general, the protein data showed dramatic changes in sensitivity (note the $\log_{10}$ scale and μm numbers, in contrast to the linear scale an nM numbers for cell data). In some

cases, the proteins were not sufficiently inhibited by the maximum allowable concentration of drug in the assay (2 mM), and these were referred to as “out of range” of the assay. This was largely due to solubility and reaching concentrations of DMSO that would affect enzyme activity (~8% by volume). Note that of the compounds shown, only IDI-6253 inhibited human DHODH (data not shown), and it did so with a nearly identical EC_{50} to the *P. falciparum* enzyme.

Some of the proteins were hypersensitive to PfDHODH inhibitors: E182D was 5.9-fold more sensitive than WT to IDI-6273. F227I was 7 and 8-fold more sensitive to IDI-6253 and IDI-6273, respectively, and 2-fold more sensitive to GSK3. Hypersensitivity was not, however, the most common observation – that was resistance on a dramatic scale.

E182D was 40 to 50-fold resistant to the WT PfDHODH inhibitors Genz-669178, Genz-668419, and DSM74. F188I and F188L were also 50-fold resistant to triazolopyrimidines like DSM4, but were hundreds to thousands-fold more resistant to alkylthiophenes like Genz-669178. The addition of either L172F or L527I to F227I considerably increased resistance to a variety of inhibitors: e.g., F227I was 62.7-fold resistant to Genz-668419, but L527I + F227I was 273.9-fold resistant and L172F + F227I was immeasurably resistant (at least 5000-fold, with the assay limited by compound solubility). L531F, originally isolated as a triazolopyrimidine-resistant line (selected with compound DSM74), was more sensitive to alkylthiophene PfDHODH inhibitors like Genz-669178 and Genz-668419.

The purified protein and cell data largely show the same upward and downward trends in drug sensitivity (Figure 3.4.14). This mirroring indicates that mutations in *pfdhodh* are major factors, if not necessarily the only factor, in determining sensitivity to PfDHODH inhibitors. Confirming this concept with allelic replacements in cells would be ideal, but

for now, purifying protein is a much faster option for testing the effect of different mutations on protein stability, activity, and sensitivity to inhibitors. Efforts to utilize new allelic replacement strategies (such as the use of zinc finger nucleases) are in progress.

The protein data was more extreme than the cell data, and the EC_{50} values did not match perfectly. For example, the EC_{50} of Genz-669178 was 17.9 nM in WT Dd2 cells, and 79.5 nM in WT protein. (Note that the observed values for the protein assays depend on the amount of protein used, much like how copy number variation can affect cellular data, and it is difficult to match the concentration of purified protein in a well with the concentration of protein in a cell in the same assay volume). The Genz-669178 EC_{50} rose to 38.4 nM for E182D cells, and 3483 nM for E182D protein. Thus, E182D is resistant to Genz-669178, but the cells had an 8.7-fold increase and the purified protein had a more extreme 43.2-fold increase.

It is not surprising that the *in vitro* protein activity assay showed larger changes than in cell-based assays. Cells have many complicating factors that are not present in *in vitro* protein assays – biological membranes, alternate targets or non-specific protein binding, efflux mechanisms, and drug metabolism. The PfDHODH *in vitro* protein activity assay distills the reaction to its bare components, but the buffer used is certainly different than *Plasmodium* cytosol, and the reactions are run at 25°C (rather than the 37C-42°C of a febrile infected person or the constant 37°C of blood-stage culture).

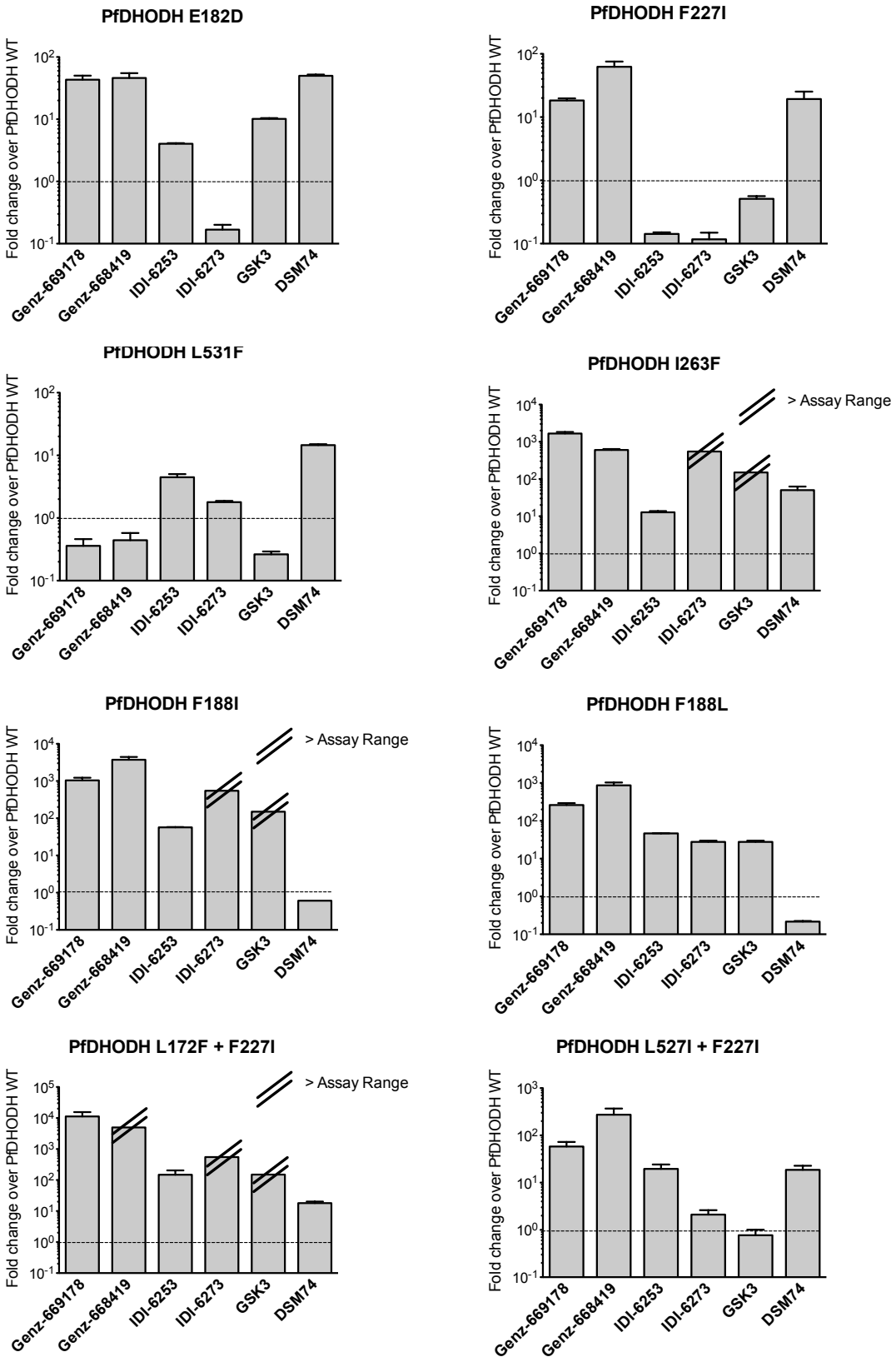

Figure 3.4.13: Inhibition of recombinant DHODH proteins, organized by residue

Table 3.4.9: DHODH protein inhibition values

A.

PfDHODH allele		EC_{50} fold shift over parent ± s.d.							
		E182D	F227I	L531F	F188I	F188L	I263F	L172F + F227I	L527I + F227I
PfDHODH WT Inhibitors	Genz-669178	43.19 ± 12.41	18.31 ± 2.63	0.36 ± 0.17	1041.13 ± 331.86	261.22 ± 56.29	1677.15 ± 266.08	11244.65 ± 7365.47	58.39 ± 25.19
	Genz-668419	46.09 ± 15.62	62.72 ± 22.19	0.44 ± 0.24	3753.11 ± 1182.62	873.17 ± 284.61	606.33 ± 54.72	> 5000	273.88 ± 166.53
	DSM74	49.89 ± 3.97	19.29 ± 10.40	14.62 ± 0.83	57.16 ± 2.09	46.78 ± 0.76	12.82 ± 1.76	149.58 ± 97.23	19.54 ± 8.10
PfDHODH Mutant Inhibitors	IDI-6253	4.04 ± 0.15	0.14 ± 0.01	4.48 ± 0.95	> 550	> 550	> 550	> 550	2.11 ± 0.88
	IDI-6273	0.17 ± 0.05	0.12 ± 0.06	1.80 ± 0.15	> 150	27.72 ± 4.04	> 150	> 150	0.77 ± 0.41
	GSK-3	10.14 ± 0.54	0.51 ± 0.09	0.26 ± 0.05	0.61 ± 0.002	0.22 ± 0.02	50.25 ± 21.51	18.024 ± 3.91	18.67 ± 7.21

B.

PfDHODH allele		EC_{50} (uM) ± s.d.			
		WT	E182D	F227I	L531F
PfDHODH WT Inhibitors	Genz-669178	0.08 ± 0.006	3.48 ± 1.29	1.47 ± 0.33	0.029 ± 0.01
	Genz-668419	0.14 ± 0.006	6.72 ± 2.56	8.99 ± 2.93	0.06 ± 0.03
	DSM74	0.38 ± 0.09	18.78 ± 2.92	6.71 ± 2.73	5.58 ± 0.32
PfDHODH Mutant Inhibitors	IDI-6253	3.52 ± 0.22	14.22 ± 0.32	0.50 ± 0.019	15.81 ± 3.36
	IDI-6273	13.49 ± 31.64	2.15 ± 0.13	1.70 ± 1.02	24.26 ± 1.98
	GSK-3	1.69 ± 0.46	17.26 ± 5.43	0.89 ± 0.37	0.044 ± 0.06

PfDHODH allele		EC_{50} (uM) ± s.d.					
		WT	F188I	F188L	I263F	L172F + F227I	L527I + F227I
PfDHODH WT Inhibitors	Genz-669178	0.08 ± 0.006	82.77 ± 26.383	20.77 ± 4.48	133.33 ± 21.15	893.95 ± 585.56	4.64 ± 2.00
	Genz-668419	0.14 ± 0.006	542.7 ± 171.00	126.26 ± 41.15	87.68 ± 7.91	> 2000	39.60 ± 24.08
	DSM74	0.38 ± 0.09	21.80 ± 0.79	17.85 ± 0.29	4.89 ± 0.66	57.05 ± 37.09	7.45 ± 3.09
PfDHODH Mutant Inhibitors	IDI-6253	3.52 ± 0.22	> 2000	> 2000	> 2000	> 2000	7.45 ± 3.09
	IDI-6273	13.49 ± 31.64	> 2000	374.07 ± 54.54	> 2000	> 2000	10.41 ± 5.53
	GSK-3	1.69 ± 0.46	1.03 ± 0.003	0.36 ± 0.03	84.76 ± 36.28	30.4 ± 6.59	31.49 ± 12.17

(A). EC_{50} fold shifts relative to the WT PfDHODH protein show significant differences in sensitivity to a variety of PfDHODH inhibitors.
(B). EC_{50} values for the first set of selection mutants (selected by Amar bir Singh Sidhu).
(C). EC_{50} values for the expanded set of selection mutants (selected by Leila Saxby Ross).

EC_{50} values were calculated using an indirect DCIP-coupled reaction. The s.d. is the standard deviation of three biological replicates, each with triplicate measurements.

In a few cases, the protein and cell data did not match up. The I263F and L172F + F227I mutant parasites were both more sensitive to the compound IDI-6253 than the WT parasites. Nevertheless, both proteins were highly resistant, and L172F + F227I was insensitive to even 2 mM of this compound. Given the concordance of the rest of the data, this may reflect actual biology and not be an artifact. If so, it is difficult to explain unless factors outside of the target PfDHODH are involved in resistance.

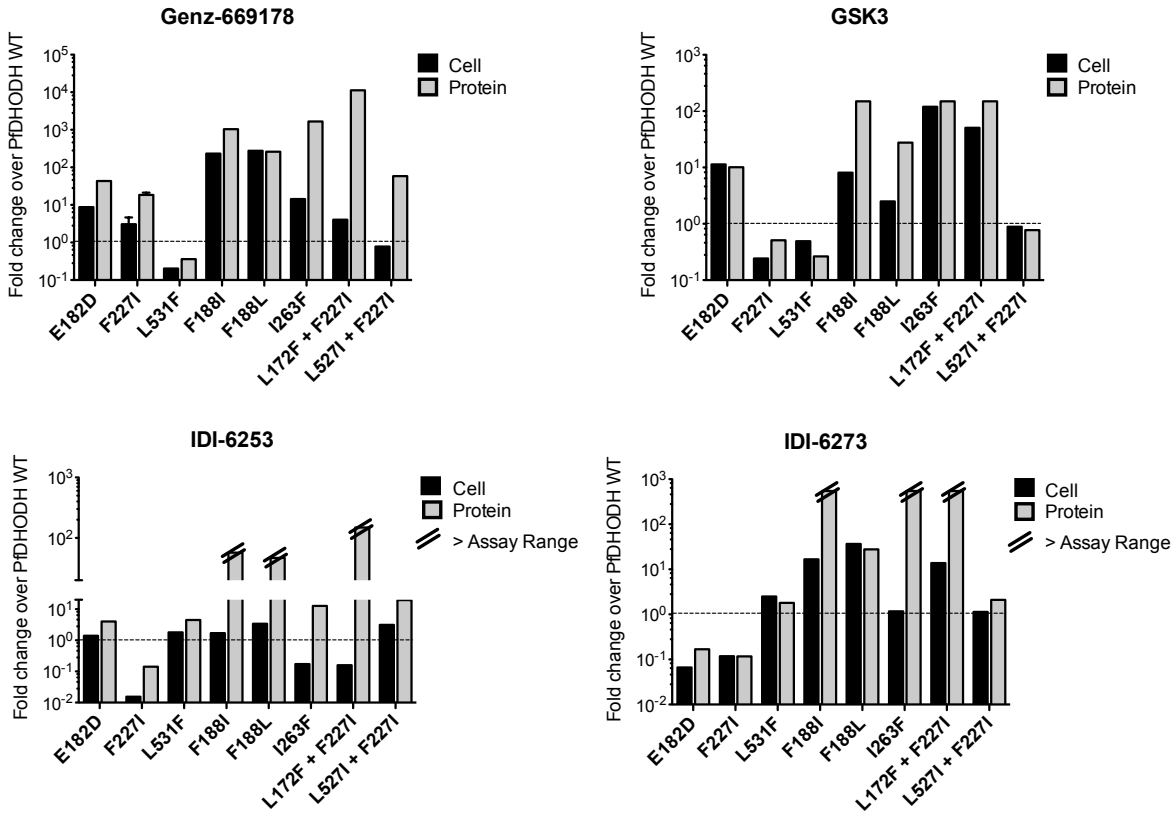

Figure 3.4.14: Protein activity data mirrors cell data

CRYSTALLOGRAPHY

In an effort to further our understanding of the molecular details of drug resistance, we collaborated with Dr. Onkar M.P. Singh and Dr. Paul Rowland at GlaxoSmithKline (Stevenage, United Kingdom) to determine the high-resolution crystal structures of PfDHODH bound to different inhibitors (Table 3.4.10, Figure 3.4.15, Figure 3.4.16, Figure 3.4.17, Figure 3.4.18, Figure 3.4.19). Attempts to crystallize E182D and F227I mutant proteins failed, and no other mutants were tried. The failure of the mutant proteins may be due to several factors. First, the quality of the preparation may not have been sufficient for crystallography. The same procedure was followed for both WT and mutant protein preparation, but what sufficed for the WT will not necessarily suffice for the mutants. Addition of another purification step (weak anion exchange with DEAE resin,

pH 8.0) did not improve crystallography attempts. Second, the mutant proteins often had lower flavin mononucleotide (FMN) loads than the WT (see Figure 3.4.11 B). If the proteins with and without FMN bound have different conformations, having a larger minority population could disrupt orderly packing. Finally, this may reflect actual biology. The model for how these mutations lead to resistance is that they weaken the interactions holding the α1- α2 helix lid to the body of the protein, which disrupts electron transfer between FMN and ubiquinone either directly or by disrupting formation of the electron tunnel. The mutants are more floppy than the WT and less likely to crystallize. This may reflect overall stability – although these mutants all support viable parasites.

In contrast, the WT PfDHODH protein crystallized with a variety of DHODH inhibitors. The alkylthiophene Genz-669178 was co-crystallized with WT PfDHODH protein with a resolution of 2.0 Å and an R-free of 0.19. Once published, this would be the highest resolution PfDHODH structure available. Co-crystals of the mutant-selective inhibitors IDI-6253 and IDI-6273 were also solved. These had lower resolution – 2.7 Å and 2.8 Å, respectively – but due to the rigid rings, the orientation of the inhibitors in the drug-binding pocket is unambiguous.

Table 3.4.10: Crystallography parameters

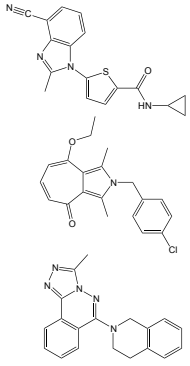

Compound	Resolution	R	R-free	Space group	Number of molecules
Genz-669178	2.0	0.170	0.190	C2	2
IDI-6273	2.8	0.171	0.230	$P2_1$	2
IDI-6253	2.7	0.194	0.268	$P2_1$	2

An overlay of the structures (Figure 3.4.15) showed that there is considerable plasticity in the binding pocket, as was observed by Deng et al [64]. Structurally distinct PfDHODH inhibitors bound in the same pocket, but with quite disparate orientations. Some commonalities include a small, hydrophobic moiety positioned near the FMN cofactor and a hydrogen bond to R265. Note that these commonalities likely mimic how the native ubiquinone binds, but there is no ubiquinone co-crystal structure to confirm this. Surprisingly, most of the residues lining the binding pocket do not move as different ligands bind. Only two – H185 and F188 – had substantial movement. Note that mutation of F188 gave substantial resistance to a variety of PfDHODH inhibitors. H185 mutants were not recovered in the resistance selections discussed here, but we believe that they would also lead to resistance.

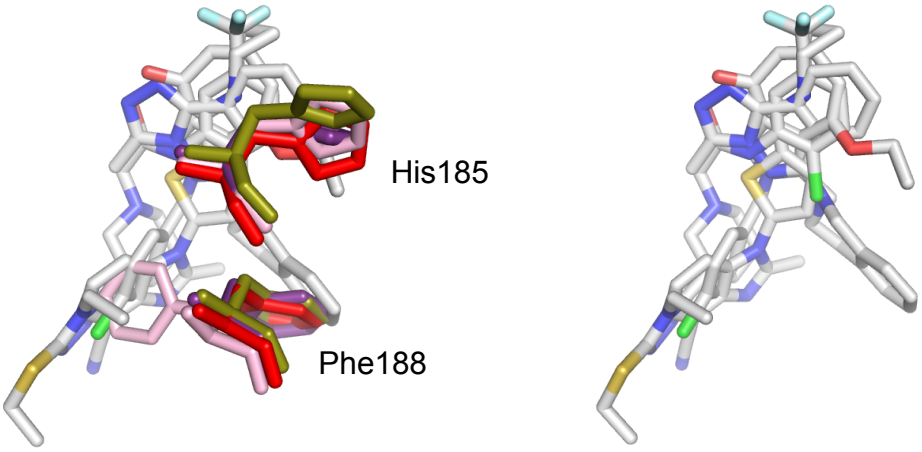

Figure 3.4.15: PfDHODH inhibitors bind in widely different modes
The residues H185 and F188 move substantially to accommodate different ligands. Image provide by Dr. Paul Rowland.

The co-crystal structure of PfDHODH with Genz-669178 (Figure 3.4.16, Figure 3.4.17) was similar to the alkylthiophene Genz-667348 (PDB ID: 3o8a [44]), but had an increased

resolution of 2.0 Å. At the protein level, E182D gives 43.19-fold resistance, F227I gives 18.31-fold resistance, F188I gives 1041-fold resistance, F188L gives 261-fold resistance, I263F gives 1677-fold resistance, L172F + F227I gives 1244.65-fold resistance, and L527I + F227I gives 58.39-fold resistance. L531F gives 3-fold sensitivity.

All of these residues are close to the Genz-669178 ligand and many are also involved in holding the lid to the body of the protein. Resistance could be explained by steric interruptions of ligand binding, or through a weakened lid-body interaction that reduces the amount of time the binding pocket exists. The sensitivity seen with the L531F mutation may be due to gaining a positive *pi* stacking or edge-to-face interaction between phenylalanine and the ligand. This could increase the binding affinity and thus reduce the inhibitor EC_{50}.

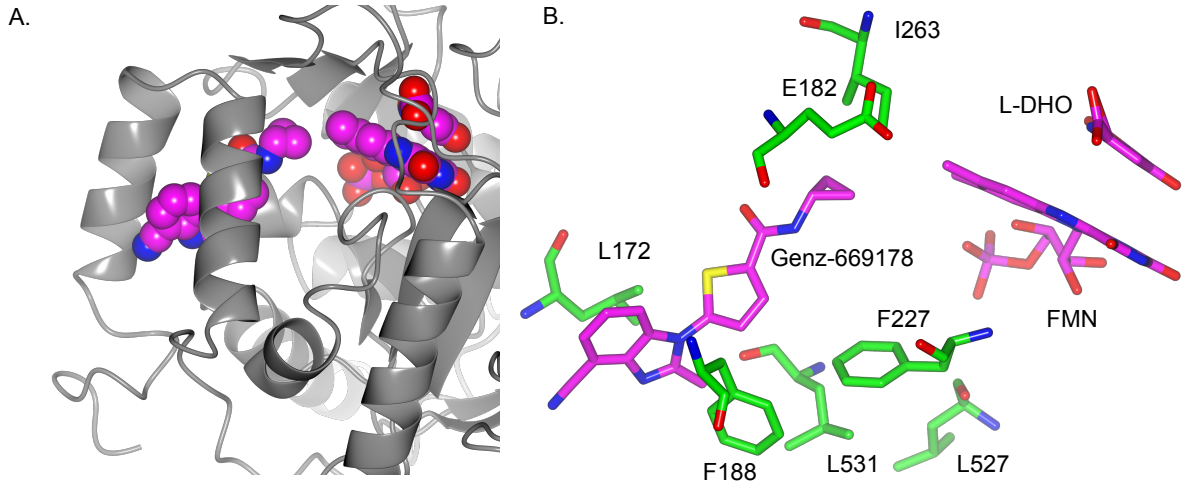

Figure 3.4.16: Co-crystal of PfDHODH with Genz-669178

A). Ribbon diagram of the α1- α2 helix lid for orientation.
(B). All resistance mutations observed for PfDHODH inhibitors. All mutations other than L531F give PfDHODH inhibitor resistance. Although L531F was isolated as a resistant mutant, it is three-fold more sensitive to wild-type PfDHODH inhibitors.
Images made with CCP4mg [66] using coordinates 4dtjm.

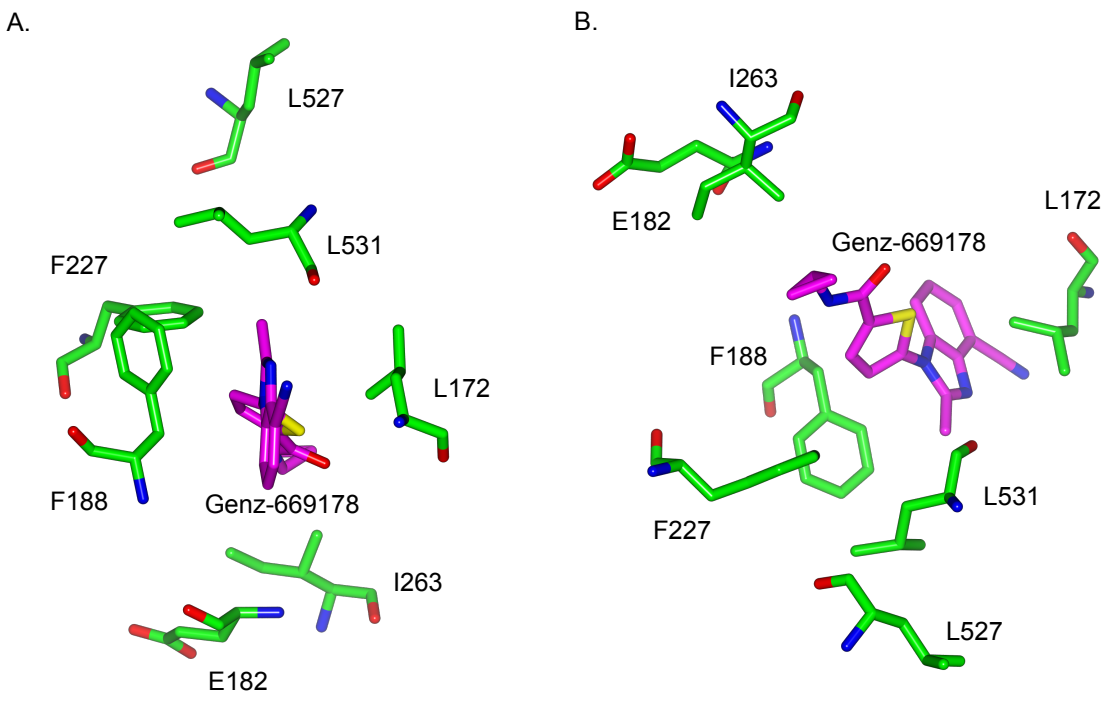

Figure 3.4.17: Resistance residues line portions of the inhibitor binding site

(A). Diagram of resistance mutations in relation to Genz-669178, an alkylthiophene. (B). Orthogonal view. Resistance mutations surround the inhibitor, and appear to form spatial groups, e.g., F227 and F188, E182 and I263, L527 and L531.
Images made with CCP4mg [66] using coordinates 4dtjm (PfDHODH with Genz-669178).

PfDHODH was crystallized with compound IDI-6253, which is a mutant-selective inhibitor (Figure 3.4.18). At the protein level, E182D, L531F, and the combination L527I + F227I gave low-level resistance of 2 to 5-fold magnitude. In contrast, F227I gave 6-fold sensitivity, and high-level resistance (>550-fold) was observed for F188I, F188L, I263F, and the combination L172F + F227I.

It is interesting to consider the F227I mutation: alone, it gives sensitivity. When paired with L172F, it gives high-level resistance. When paired with L527I, it gives low-level resistance. L172F is too distant to have a direct interaction with F227I – although it is possible that when no ligand is bound, the lid helices are packed more tightly against the

body of the protein. In either case, the bulkiness of the L172F exchange may alter helix packing and thus change the binding pocket in a way that leads to resistance.

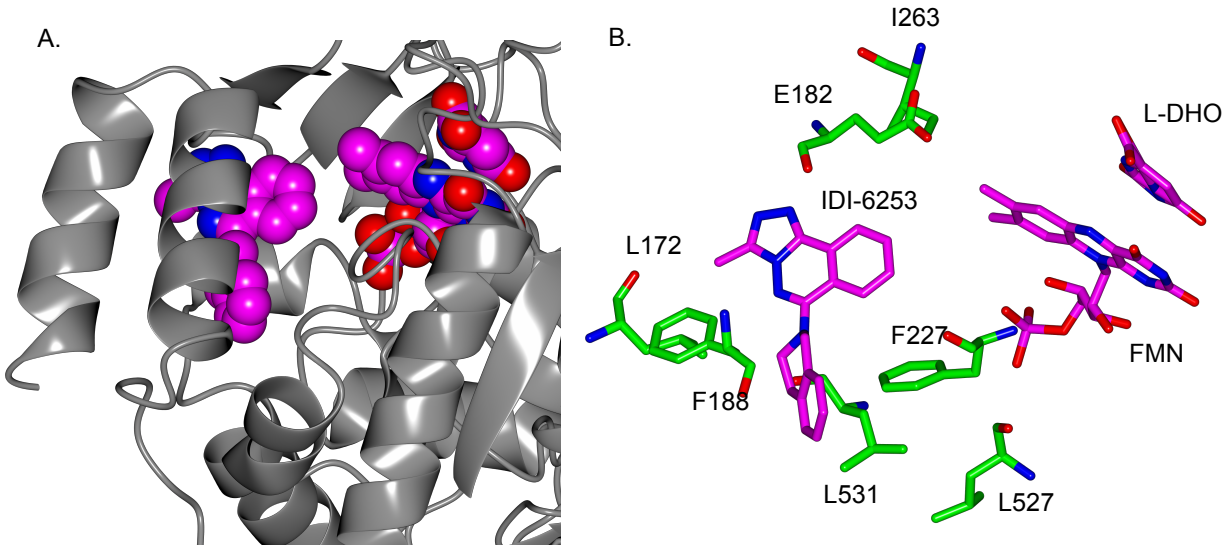

Figure 3.4.18: Co-crystal of PfDHODH with IDI-6253

(A). Ribbon diagram of the α1- α2 helix lid for orientation.
(B). All resistance mutations observed for PfDHODH inhibitors. L527I gives resistance to IDI-6253. F227I gives sensitivity.
Images made with CCP4mg [66] using coordinates 2ihho.

IDI-6253 is quite close to F227, so the F227I mutation may lead to sensitivity by reducing steric clashes (rather than favorable *pi-pi* interactions) and allowing a better fit. L527 is spatially close to F227, and a direct interaction is plausible. The combination of L527I + F227I may lead to a stronger interaction between the two residues in an isoleucine zipper, and this may change the binding pocket in a way that favors resistance.

Finally, PfDHODH was crystallized with IDI-6273, a mutant-selective inhibitor (Figure 3.4.19). At the protein level, E182D and F227I both gave ~6-fold sensitivity. As for IDI-6253, F227 is very close, so mutation to a smaller residue may reduce steric clashes. It

is less clear how E182D leads to sensitivity. L531F and the combination L527I + F227I had little effect.

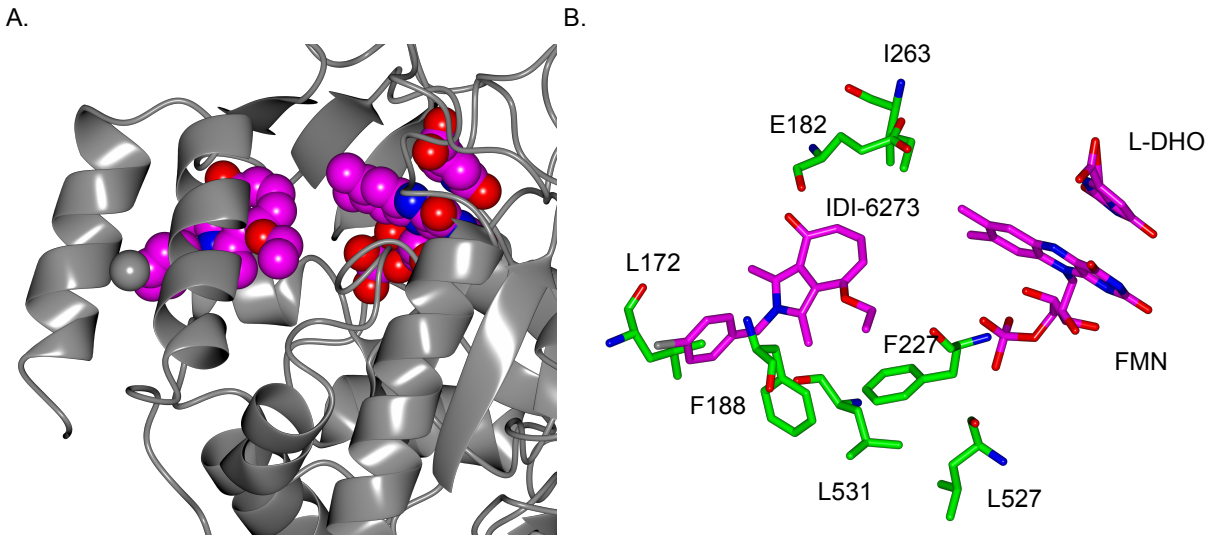

Figure 3.4.19: Co-crystal of PfDHODH with IDI-6273

(A). Ribbon diagram of the α1- α2 helix lid for orientation.
(B). All resistance mutations observed for PfDHODH inhibitors. L172F gives 15-fold resistance to IDI-6273. E182D and F227I give hypersensitivity.
Images made with CCP4mg [66] using coordinates 2ihho.

Curiously, F188L gave 27.7-fold resistance, whereas the sister mutation F188I gave >550 fold resistance. As these often had differing impact on the potency of different PfDHODH inhibitors, solving crystal structures of F188I and F188L would be informative for fine-tuned detail about the drug-binding site. I263F and the combination L172F + F227I both gave >550-fold resistance.

3.5 DISCUSSION AND FUTURE DIRECTIONS

This study focused on cataloging potential mechanisms of resistance to a small panel of structurally unrelated PfDHODH inhibitors, with an eye on developing strategies to suppress and contain these mechanisms should these compounds ever be developed into drugs. This was accomplished through *in vitro* drug resistance selections. We used an intermittent pulse strategy, which allows for recovery between stresses. Continuous selection with PfDHODH inhibitors tends to give gene amplification rather than point mutations [51]. Using this approach, we discovered several mutations in PfDHODH, the target gene: L172F, F188I, F188L, E182D, F227I, I263F, L527I, and L531F, as well as several instances of copy number variation in *pfdhodh*. Resistant cell lines with no discernable alterations to *pfdhodh* sequence or copy number will be subjected to whole-genome sequencing. Overall, the simultaneous use of a wild-type and mutant-type inhibitor lead to much less resistance (16%) than the use of a single drug in a primary or sequential selection (60-75%) (Figure 3.5.1).

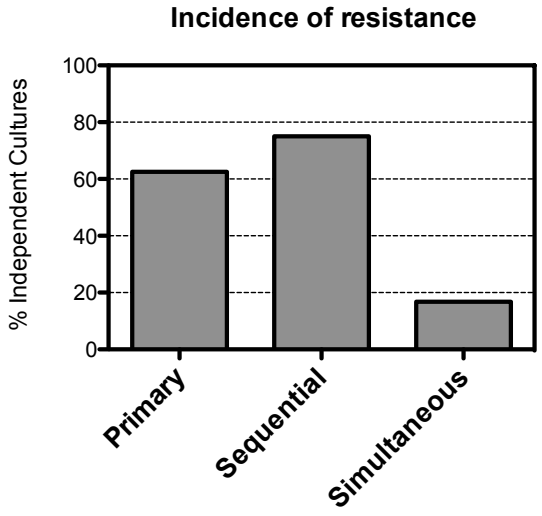

Figure 3.5.1: Selection with two drugs simultaneously led to fewer instances of resistance than selection with a single drug

Although these selected cell lines undoubtedly have mutations in addition to those in *pfdhodh*, the observed changes in drug sensitivity were largely recapitulated by *in vitro* assays with purified recombinant protein. This mirroring indicates that the mutations in PfDHODH are the driving force behind resistance, and also implies that purified protein can be used to predict the effect of different mutations in parasites. Producing protein is substantially faster and cheaper than doing drug resistance selections or making allelic replacements in parasites. Two caveats are that not all proteins will be able to be expressed, and that successful expression does not guarantee that the protein is sufficiently functional in cells to support viability.

Determining the steady state kinetic parameters for all of the mutant proteins (as in Chapter 2) would help gauge the consequences of different mutations – e.g., a mutation which dramatically changes the Km or kcat for the substrate or cofactors likely has larger fitness repercussions than a more mild mutation. Pre-steady state measurements and more detailed enzymology could help explain detailed points about the catalysis of oxidative and reductive half-reactions [65] and the mode of inhibitor action. Although crystallography of the E182D and F227I mutant proteins failed, it may be worth pursuing crystallography further with these and other mutants. A WT structure with ubiquinone bound, rather than a PfDHODH inhibitor, would also be useful. Computational modeling has been surprisingly predictive with PfDHODH, and would likely be continued to guide medicinal chemistry efforts for greater selectivity and potency.

Protein can also be used as a proxy for determining compound susceptibility in *Plasmodium* species that do not have *in vitro* culture systems. In the case of *P. vivax*, PvDHODH was similarly sensitive to the six inhibitors shown, with all falling within 10-fold of the PfDHODH values (Figure 3.5.1).

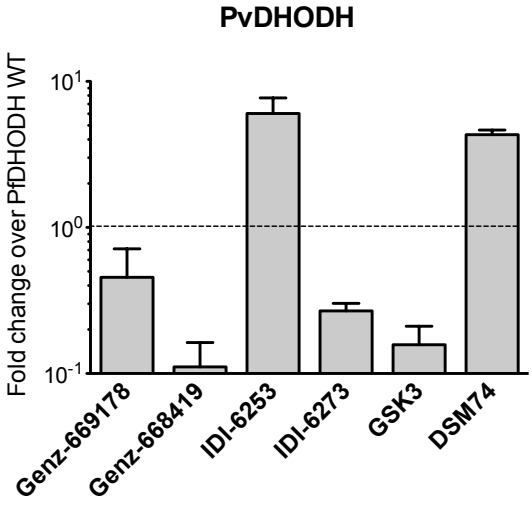

Figure 3.5.2: *P. vivax* PvDHODH protein is sensitive to PfDHODH inhibitors

We are also working on complementary approaches in whole cells. Allelic replacements of the mutant *pfdhodh* genes would give parasites with different *pfdhodh* alleles in isogenic backgrounds. These parasite lines would be ideal for both testing drug sensitivity and for doing competitive growth assays (with and without a variety of drugs). While the growth habits (cycle time, burst size) of individual parasite lines could be characterized by FACS, we believe that it is unlikely to find gross differences, and that pairwise competitive growth provides a more sensitive measure of evolutionary fitness. As many of the mutations of interest are close to the amino-terminus of *pfdhodh*, traditional allelic replacement techniques are unlikely to succeed, and alternate strategies such as zinc finger nucleases or a cas9-based system are being pursued.

As the *P. falciparum* mitochondria is thought to be mainly important for its role in supplying reduced ubiquinone to PfDHODH [89], it is quite possible that mutations in *pfdhodh* and other resistance mechanisms would alter mitochondrial physiology. Mitochondrial function could be assessed by measuring the consumption of oxygen,

production of pyrimidines, and level of reactive oxygen species. A more global metabolomics project could provide this information and more.

Chapter Four:

Concluding Remarks and Future Directions

Malaria is both preventable and curable, and yet there are hundreds of millions of infections and an estimated 600,000 malaria-related deaths every year [1]. Malaria control programs rely on a combination of vector control with insecticides and bednets and disease control with antimalarial drugs. No effective vaccine exists, and humans only build short-term, partial immunity through natural exposure. Our long co-evolution with malaria parasites has left traces in both genomes: in humans, alleles for potentially deleterious hemoglobinopathies such as sickle cell anemia and the alpha and beta thalessemias are more common in areas with malaria transmission, likely because these alleles offer some degree of protection from severe malaria. In *Plasmodium*, the use of antimalarial drugs has led to selective sweeps, leading to changes in population structure and the rise and spread of drug-resistant parasites [15].

Malaria parasites are highly adaptable, and drug pressure can lead to resistance nearly simultaneous with introduction [23, 75]. Resistance is reported for nearly every antimalarial in use, including worrisome reports of delayed clearance with artemisinin-based combination therapies (ACTs), which form the backbone of most modern control programs [19]. The armament of antimalarial agents is limited, with a heavy reliance on a small number of chemical scaffolds and biological targets [13]. Cross-resistance of antimalarials in development with therapeutics in clinical use is a major concern.

Drug resistance, however, is not necessarily inevitable or permanent. As with any trait, the evolution and spread of resistance is shaped and restricted by fitness considerations. If a resistant parasite is not competitively viable, it will not spread or be maintained in a population. In 1993, faced with an efficacy of less than 50%, Malawi phased out chloroquine and started using sulfadoxine-pyrimethamine instead. Over the course of eight years, the molecular marker for chloroquine resistance – specific mutations in

pfcrt1 – dropped to undetectable levels. This suggests that the fitness cost of the mutant *pfcrt1* was high enough to drive it out of the parasite population once the selecting force was removed. It also implies that chloroquine could potentially be used again [77].

Evolutionary oscillations between sensitive and resistant parasites can also occur on much smaller timescales through the use of suppressive combination therapy. Synergistic combinations tend to be favored for their short-term potency. Synergy, however, heavily selects for drug resistance, as parasites resistant to one of the two compounds used have a tremendous fitness advantage over the sensitive parent [90]. In contrast, strong antagonism ("suppression") rewards sensitivity rather than resistance: resistance to one compound results in a fitness disadvantage, and the resistant line will be outcompeted by the sensitive parent. Suppressive combinations thus select away from resistance. Conceptually, suppressive combinations often work by having two compounds which in some way mask each other's effects: perhaps the pathways they affect can compensate for each other, or their targets are not available at the same time. When resistance to one compound develops, the resistant parasites are now subject to the full force of the second compound. If this disadvantage is sufficiently large, then the sensitive parasites are more fit than the resistant ones, and the resistant parasites will be outcompeted.

For example, in *Escherichia coli*, inhibitors of protein and DNA synthesis have suppressive interactions: cells grow faster in this combination than with each drug alone. Molecularly, this is because ribosomal genes are not directly regulated by DNA stress. This leads to a non-optimal excessively high rate of protein synthesis relative to DNA replication, which takes resources away from other necessary cellular processes and is thus a fitness disadvantage [37].

In Chapter 2, we described “targeting resistance,” a type of suppressive combination therapy that pairs inhibitors for the sensitive and resistant forms of a single target. We demonstrated that both sequential and simultaneous use of these inhibitors maintained or directed evolution towards a WT, sensitive allele for the target. These results were promising, but the fact that the WT and mutant-type inhibitors target the same binding pocket (though not the exact same site in that pocket) is a weakness. This is being addressed by Dr. Amanda Lukens through screening for compounds that inhibit the mutant parasite lines from a large collection of malaria-active compounds (instead of the small, biased set of DHODH inhibitors this study was started with). Ideally, this screen would identify compounds in unrelated pathways such that the binding pockets are unrelated and thus less likely to fail in one swoop. Another weakness is that the mutant-type inhibitors are selective, but not specific. Future work includes identifying and developing specific compounds with no residual activity against the WT.

We would also like to further explore the evolutionary aspects of drug resistance: this could be accomplished retrospectively through sequencing saved selection time points to chart the rise and fall of different alleles. This could be done on a whole-genome scale or with quantitative PCR for select individual alleles. The most interesting time points would be before official resistance, as there are likely multiple resistant parasite types competing with each other until one dominates the culture. It would be interesting to identify the unsuccessful minor variants and speculate as to why they were marginalized.

If allelic replacement is successful, competitive growth assays with sensitive and resistant parasites with isogenic backgrounds would allow a fine-tuned description of fitness costs and benefits. This could be extended to include conditions with a variety of drugs and other stresses, such as febrile temperatures, to model some of the stresses inside a human infection.

In Chapter 3, we used *in vitro* selection, protein activity assays, and crystallography for an in-depth characterization of potential resistance mechanisms for PfDHODH inhibitors. The goal is to identify the small number of fitness-resistance maximums that the parasite is likely to take in order to design strategies for resistance control. This could extend the useful lifetime of DHODH inhibitors. Future work includes identifying the most fit of the resistance mutants, which can be approximated *in vitro* through competitive growth assays under a variety of conditions, and identifying inhibitors specific for those mutants.

The efforts of the United States' Office of Malaria Control in War Areas, the precursor to the Center for Disease Control and Prevention, reduced malaria in the United States (Figure 4.1), and eventually led to eradication with the National Malaria Eradication Program campaign between 1947-1952 [91].

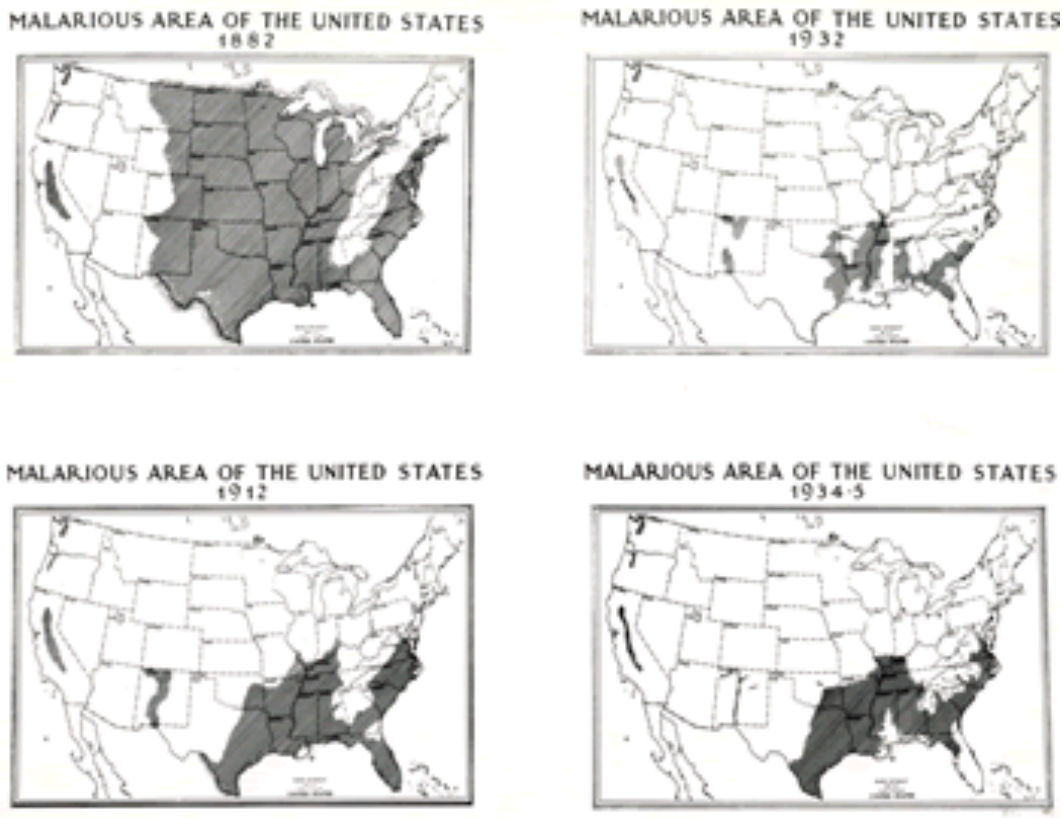

Figure 4.1: The distribution of malaria in the United States of America, 1882-1935 (The Center for Disease Control and Prevention [91])

The success of the United States' National Malaria Eradication Program, which relied heavily on vector control through the use of the insecticide DDT and draining or otherwise compromising mosquito breeding sites, led to the World Health Organization-led 1955 Global Malaria Eradication Programme (GMEP). GMEP successfully eradicated malaria from many countries. However, GMEP was abandoned after 14 years with the acknowledgement that the current tools – the insecticide DDT and the antimalarial drugs chloroquine and pyrimethamine – were no longer effective, and that political will and financial support were dwindling. In areas where eradication was not complete, GMEP may actually have been harmful as the parasite population rebounded against a now-immunologically naïve population, and malaria often returned in epidemics [20].

Studies of parasite resurgences show that the number one factor is the cessation of control programs due to a lack of funding [76]. If sufficient funds are later obtained, there is a large risk that the previously effective tools have reduced efficacy or are even obsolete due to drug resistance. Given that drug resistance rapidly compromises insecticides and antimalarial agents, new strategies are needed to both understand how resistance develops and how to counter it in the field. The studies presented here suggest that suppressive drug combinations, particularly in the form of "targeting resistance," may extend the useful lifetime of antimalarials and thus give eradication a better chance of success.

Studies of small-scale eradication, such as on the island of Aneityum, have shown that community partnership and education are essential, as extensive and long-term coordination and cooperation are required to eliminate malaria [72]. Mass drug administration, particularly for vulnerable pregnant women and young children, was combined with vigorous vector control through the use of indoor residual spraying, bed

net use, and the drainage of standing water. *P. falciparum* was declared eliminated one year after no transmission was observed. *P. vivax* took five years.

This extensive follow-up time will be a challenge – how do you convince people and governments to continue with malaria interventions when transmission is decreasing or even stopped for several years? There are many competing priorities, but a relaxation of control measures could lead to a resurgence in malaria cases – and having to restart the clock. Sustaining financial commitment and the communal responsibility to prevent, diagnose, and treat malaria infection will require much more than bench science.

Eradication is still possible. We have the tools – for now. We need to make more tools, and to develop strategies to protect their effectiveness. We also need a massive and sustained intersection of control measures, and these will require funding, political and social will, and education of the public [92]. These measures must be completed before resistance renders them useless, and must be unrelenting even as transmission and perceived risk decrease.

References

1. Organization, W. H., World Malaria Report 2012. **2012**.

2. Prudencio, M.; Rodriguez, A.; Mota, M. M., The silent path to thousands of merozoites: the Plasmodium liver stage. *Nature reviews. Microbiology* **2006,** *4* (11), 849-56.

3. Portugal, S.; Carret, C.; Recker, M.; Armitage, A. E.; Goncalves, L. A.; Epiphanio, S.; Sullivan, D.; Roy, C.; Newbold, C. I.; Drakesmith, H.; Mota, M. M., Host-mediated regulation of superinfection in malaria. *Nature medicine* **2011,** *17* (6), 732-7.

4. Cowman, A. F.; Berry, D.; Baum, J., The cellular and molecular basis for malaria parasite invasion of the human red blood cell. *The Journal of cell biology* **2012,** *198* (6), 961-71.

5. Hisaeda, H.; Yasutomo, K.; Himeno, K., Malaria: immune evasion by parasites. *The international journal of biochemistry & cell biology* **2005,** *37* (4), 700-6.

6. Shikani, H. J.; Freeman, B. D.; Lisanti, M. P.; Weiss, L. M.; Tanowitz, H. B.; Desruisseaux, M. S., Cerebral malaria: we have come a long way. *The American journal of pathology* **2012,** *181* (5), 1484-92.

7. Suh, K. N.; Kain, K. C.; Keystone, J. S., Malaria. *CMAJ : Canadian Medical Association journal = journal de l'Association medicale canadienne* **2004,** *170* (11), 1693-702.

8. Liu, Z.; Miao, J.; Cui, L., Gametocytogenesis in malaria parasite: commitment, development and regulation. *Future microbiology* **2011,** *6* (11), 1351-69.

9. Killeen, G. F.; Seyoum, A.; Sikaala, C.; Zomboko, A. S.; Gimnig, J. E.; Govella, N. J.; White, M. T., Eliminating malaria vectors. *Parasites & vectors* **2013,** *6*, 172.

10. Agnandji, S. T.; Lell, B.; Fernandes, J. F.; Abossolo, B. P.; Methogo, B. G.; Kabwende, A. L.; Adegnika, A. A.; Mordmuller, B.; Issifou, S.; Kremsner, P. G.; Sacarlal, J.; Aide, P.; Lanaspa, M.; Aponte, J. J.; Machevo, S.; Acacio, S.; Bulo, H.; Sigauque, B.; Macete, E.; Alonso, P.; Abdulla, S.; Salim, N.; Minja, R.; Mpina, M.; Ahmed, S.; Ali, A. M.; Mtoro, A. T.; Hamad, A. S.; Mutani, P.; Tanner, M.; Tinto, H.; D'Alessandro, U.; Sorgho, H.; Valea, I.; Bihoun, B.; Guiraud, I.; Kabore, B.; Sombie, O.; Guiguemde, R. T.; Ouedraogo, J. B.; Hamel, M. J.; Kariuki, S.; Oneko, M.; Odero, C.; Otieno, K.; Awino, N.; McMorrow, M.; Muturi-Kioi, V.; Laserson, K. F.; Slutsker, L.; Otieno, W.; Otieno, L.; Otsyula, N.; Gondi, S.; Otieno, A.; Owira, V.; Oguk, E.; Odongo, G.; Woods, J. B.; Ogutu, B.; Njuguna, P.; Chilengi, R.; Akoo, P.; Kerubo, C.; Maingi, C.; Lang, T.; Olotu, A.; Bejon, P.; Marsh, K.; Mwambingu, G.; Owusu-Agyei, S.; Asante, K. P.; Osei-Kwakye, K.; Boahen, O.; Dosoo, D.; Asante, I.; Adjei, G.; Kwara, E.; Chandramohan, D.; Greenwood, B.; Lusingu, J.; Gesase, S.; Malabeja, A.; Abdul, O.; Mahende, C.; Liheluka, E.; Malle, L.; Lemnge, M.; Theander, T. G.; Drakeley, C.; Ansong, D.; Agbenyega, T.; Adjei, S.; Boateng, H. O.; Rettig, T.; Bawa, J.; Sylverken, J.; Sambian, D.; Sarfo, A.; Agyekum, A.; Martinson, F.; Hoffman, I.; Mvalo, T.; Kamthunzi, P.; Nkomo, R.; Tembo, T.; Tegha, G.; Tsidya, M.; Kilembe, J.; Chawinga, C.; Ballou, W. R.; Cohen, J.; Guerra, Y.; Jongert, E.; Lapierre, D.; Leach, A.; Lievens, M.; Ofori-Anyinam, O.; Olivier, A.; Vekemans, J.; Carter, T.; Kaslow, D.; Leboulleux, D.; Loucq, C.; Radford, A.; Savarese, B.; Schellenberg, D.;

Sillman, M.; Vansadia, P., A phase 3 trial of RTS,S/AS01 malaria vaccine in African infants. *N Engl J Med* **2012,** *367* (24), 2284-95.

11. Daubenberger, C. A., First clinical trial of purified, irradiated malaria sporozoites in humans. *Expert review of vaccines* **2012,** *11* (1), 31-3.

12. Gosling, R. D.; Okell, L.; Mosha, J.; Chandramohan, D., The role of antimalarial treatment in the elimination of malaria. *Clinical microbiology and infection : the official publication of the European Society of Clinical Microbiology and Infectious Diseases* **2011,** *17* (11), 1617-23.

13. Schlitzer, M., Malaria chemotherapeutics part I: History of antimalarial drug development, currently used therapeutics, and drugs in clinical development. *ChemMedChem* **2007,** *2* (7), 944-86.

14. Rocco, F., *The miraculous fever-tree : malaria, medicine and the cure that changed the world*. HarperCollins: London, UK, 2003; p xix, 348 p, [16] p. of plates.

15. Wootton, J. C.; Feng, X.; Ferdig, M. T.; Cooper, R. A.; Mu, J.; Baruch, D. I.; Magill, A. J.; Su, X. Z., Genetic diversity and chloroquine selective sweeps in Plasmodium falciparum. *Nature* **2002,** *418* (6895), 320-3.

16. Ge, H. Z. H. B. J. F., Jin., Si Ku Quan Shu (Emergency Prescriptions Kept Up One's Sleeve). **340 A.D.**

17. Tu, Y., The development of new antimalarial drugs: qinghaosu and dihydro-qinghaosu. *Chinese medical journal* **1999,** *112* (11), 976-7.

18. Wright, C. W.; Linley, P. A.; Brun, R.; Wittlin, S.; Hsu, E., Ancient Chinese methods are remarkably effective for the preparation of artemisinin-rich extracts of Qing Hao with potent antimalarial activity. *Molecules* **2010,** *15* (2), 804-12.

19. Dondorp, A. M.; Nosten, F.; Yi, P.; Das, D.; Phyo, A. P.; Tarning, J.; Lwin, K. M.; Ariey, F.; Hanpithakpong, W.; Lee, S. J.; Ringwald, P.; Silamut, K.; Imwong, M.; Chotivanich, K.; Lim, P.; Herdman, T.; An, S. S.; Yeung, S.; Singhasivanon, P.; Day, N. P.; Lindegardh, N.; Socheat, D.; White, N. J., Artemisinin resistance in Plasmodium falciparum malaria. *N Engl J Med* **2009,** *361* (5), 455-67.

20. Najera, J. A.; Gonzalez-Silva, M.; Alonso, P. L., Some Lessons for the Future from the Global Malaria Eradication Programme (1955-1969). *PLoS medicine* **2011,** *8* (1).

21. Sachs, J.; Malaney, P., The economic and social burden of malaria. *Nature* **2002,** *415* (6872), 680-5.

22. Ekland, E. H.; Fidock, D. A., In vitro evaluations of antimalarial drugs and their relevance to clinical outcomes. *International journal for parasitology* **2008,** *38* (7), 743-7.

23. Chiodini, P. L.; Conlon, C. P.; Hutchinson, D. B.; Farquhar, J. A.; Hall, A. P.; Peto, T. E.; Birley, H.; Warrell, D. A., Evaluation of atovaquone in the treatment of patients with

uncomplicated Plasmodium falciparum malaria. *The Journal of antimicrobial chemotherapy* **1995,** *36* (6), 1073-8.

24. Nzila, A.; Mwai, L., In vitro selection of Plasmodium falciparum drug-resistant parasite lines. *The Journal of antimicrobial chemotherapy* **2010,** *65* (3), 390-8.

25. Witkowski, B.; Berry, A.; Benoit-Vical, F., Resistance to antimalarial compounds: methods and applications. *Drug resistance updates : reviews and commentaries in antimicrobial and anticancer chemotherapy* **2009,** *12* (1-2), 42-50.

26. Nygaard, S.; Braunstein, A.; Malsen, G.; Van Dongen, S.; Gardner, P. P.; Krogh, A.; Otto, T. D.; Pain, A.; Berriman, M.; McAuliffe, J.; Dermitzakis, E. T.; Jeffares, D. C., Long- and short-term selective forces on malaria parasite genomes. *PLoS genetics* **2010,** *6* (9).

27. Costanzo, M. S.; Hartl, D. L., The evolutionary landscape of antifolate resistance in Plasmodium falciparum. *Journal of genetics* **2011,** *90* (2), 187-90.

28. Costanzo, M. S.; Brown, K. M.; Hartl, D. L., Fitness trade-offs in the evolution of dihydrofolate reductase and drug resistance in Plasmodium falciparum. *PloS one* **2011,** *6* (5), e19636.

29. Sarafianos, S. G.; Das, K.; Hughes, S. H.; Arnold, E., Taking aim at a moving target: designing drugs to inhibit drug-resistant HIV-1 reverse transcriptases. *Current opinion in structural biology* **2004,** *14* (6), 716-30.

30. Shah, N. P.; Nicoll, J. M.; Nagar, B.; Gorre, M. E.; Paquette, R. L.; Kuriyan, J.; Sawyers, C. L., Multiple BCR-ABL kinase domain mutations confer polyclonal resistance to the tyrosine kinase inhibitor imatinib (STI571) in chronic phase and blast crisis chronic myeloid leukemia. *Cancer cell* **2002,** *2* (2), 117-25.

31. Quintas-Cardama, A.; Kantarjian, H.; Cortes, J., Flying under the radar: the new wave of BCR-ABL inhibitors. *Nature reviews. Drug discovery* **2007,** *6* (10), 834-48.

32. Rosenbloom, D. I.; Hill, A. L.; Rabi, S. A.; Siliciano, R. F.; Nowak, M. A., Antiretroviral dynamics determines HIV evolution and predicts therapy outcome. *Nature medicine* **2012**.

33. Fischbach, M. A., Combination therapies for combating antimicrobial resistance. *Current opinion in microbiology* **2011,** *14* (5), 519-23.

34. Chait, R.; Vetsigian, K.; Kishony, R., What counters antibiotic resistance in nature? *Nat Chem Biol* **2012,** *8* (1), 2-5.

35. Yeh, P. J.; Hegreness, M. J.; Aiden, A. P.; Kishony, R., Drug interactions and the evolution of antibiotic resistance. *Nature reviews. Microbiology* **2009,** *7* (6), 460-6.

36. Chait, R.; Craney, A.; Kishony, R., Antibiotic interactions that select against resistance. *Nature* **2007,** *446* (7136), 668-71.

37. Bollenbach, T.; Quan, S.; Chait, R.; Kishony, R., Nonoptimal microbial response to antibiotics underlies suppressive drug interactions. *Cell* **2009,** *139* (4), 707-18.

38. Pinto, P.; Dougados, M., Leflunomide in clinical practice. *Acta Reumatol Port* **2006,** *31* (3), 215-24.

39. Ng, S. B.; Buckingham, K. J.; Lee, C.; Bigham, A. W.; Tabor, H. K.; Dent, K. M.; Huff, C. D.; Shannon, P. T.; Jabs, E. W.; Nickerson, D. A.; Shendure, J.; Bamshad, M. J., Exome sequencing identifies the cause of a mendelian disorder. *Nat Genet* **2010,** *42* (1), 30-5.

40. Aravind, L.; Iyer, L. M.; Wellems, T. E.; Miller, L. H., Plasmodium biology: genomic gleanings. *Cell* **2003,** *115* (7), 771-85.

41. Hurt, D. E.; Widom, J.; Clardy, J., Structure of Plasmodium falciparum dihydroorotate dehydrogenase with a bound inhibitor. *Acta crystallographica. Section D, Biological crystallography* **2006,** *62* (Pt 3), 312-23.

42. Fishwick, C. W.; Bedingfield, P.; Cowen, D.; Acklam, P. A.; Cunningham, F.; Parsons, M.; McConkey, G. A.; Johnson, A. P., Factors influencing the specificity of inhibitor binding to the human and malaria parasite dihydroorotate dehydrogenases. *J Med Chem* **2012**.

43. Gujjar, R.; Marwaha, A.; El Mazouni, F.; White, J.; White, K. L.; Creason, S.; Shackleford, D. M.; Baldwin, J.; Charman, W. N.; Buckner, F. S.; Charman, S.; Rathod, P. K.; Phillips, M. A., Identification of a metabolically stable triazolopyrimidine-based dihydroorotate dehydrogenase inhibitor with antimalarial activity in mice. *J Med Chem* **2009,** *52* (7), 1864-72.

44. Booker, M. L.; Bastos, C. M.; Kramer, M. L.; Barker, R. H., Jr.; Skerlj, R.; Sidhu, A. B.; Deng, X.; Celatka, C.; Cortese, J. F.; Guerrero Bravo, J. E.; Crespo Llado, K. N.; Serrano, A. E.; Angulo-Barturen, I.; Jimenez-Diaz, M. B.; Viera, S.; Garuti, H.; Wittlin, S.; Papastogiannidis, P.; Lin, J. W.; Janse, C. J.; Khan, S. M.; Duraisingh, M.; Coleman, B.; Goldsmith, E. J.; Phillips, M. A.; Munoz, B.; Wirth, D. F.; Klinger, J. D.; Wiegand, R.; Sybertz, E., Novel inhibitors of Plasmodium falciparum dihydroorotate dehydrogenase with anti-malarial activity in the mouse model. *J Biol Chem* **2010,** *285* (43), 33054-64.

45. Phillips, M. A.; Rathod, P. K., Plasmodium dihydroorotate dehydrogenase: a promising target for novel anti-malarial chemotherapy. *Infectious disorders drug targets* **2010,** *10* (3), 226-39.

46. Rodrigues, T.; Lopes, F.; Moreira, R., Inhibitors of the mitochondrial electron transport chain and de novo pyrimidine biosynthesis as antimalarials: The present status. *Current medicinal chemistry* **2010,** *17* (10), 929-56.

47. Baldwin, J.; Michnoff, C. H.; Malmquist, N. A.; White, J.; Roth, M. G.; Rathod, P. K.; Phillips, M. A., High-throughput screening for potent and selective inhibitors of Plasmodium falciparum dihydroorotate dehydrogenase. *J Biol Chem* **2005,** *280* (23), 21847-53.

48. Gamo, F. J.; Sanz, L. M.; Vidal, J.; de Cozar, C.; Alvarez, E.; Lavandera, J. L.; Vanderwall, D. E.; Green, D. V.; Kumar, V.; Hasan, S.; Brown, J. R.; Peishoff, C. E.; Cardon, L. R.; Garcia-Bustos, J. F., Thousands of chemical starting points for antimalarial lead identification. *Nature* **2010,** *465* (7296), 305-10.

49. Patel, V.; Booker, M.; Kramer, M.; Ross, L.; Celatka, C. A.; Kennedy, L. M.; Dvorin, J. D.; Duraisingh, M. T.; Sliz, P.; Wirth, D. F.; Clardy, J., Identification and characterization of small molecule inhibitors of Plasmodium falciparum dihydroorotate dehydrogenase. *J Biol Chem* **2008,** *283* (50), 35078-85.

50. Coteron, J. M.; Marco, M.; Esquivias, J.; Deng, X.; White, K. L.; White, J.; Koltun, M.; El Mazouni, F.; Kokkonda, S.; Katneni, K.; Bhamidipati, R.; Shackleford, D. M.; Angulo-Barturen, I.; Ferrer, S. B.; Jimenez-Diaz, M. B.; Gamo, F. J.; Goldsmith, E. J.; Charman, W. N.; Bathurst, I.; Floyd, D.; Matthews, D.; Burrows, J. N.; Rathod, P. K.; Charman, S. A.; Phillips, M. A., Structure-guided lead optimization of triazolopyrimidine-ring substituents identifies potent Plasmodium falciparum dihydroorotate dehydrogenase inhibitors with clinical candidate potential. *J Med Chem* **2011,** *54* (15), 5540-61.

51. Guler, J. L.; Freeman, D. L.; Ahyong, V.; Patrapuvich, R.; White, J.; Gujjar, R.; Phillips, M. A.; Derisi, J.; Rathod, P. K., Asexual Populations of the Human Malaria Parasite, Plasmodium falciparum, Use a Two-Step Genomic Strategy to Acquire Accurate, Beneficial DNA Amplifications. *PLoS pathogens* **2013,** *9* (5), e1003375.

52. Schlitzer, M.; Ortmann, R., Feeding the antimalarial pipeline. *ChemMedChem* **2010,** *5* (11), 1837-40.

53. Goldberg, D. E.; Siliciano, R. F.; Jacobs, W. R., Jr., Outwitting evolution: fighting drug-resistant TB, malaria, and HIV. *Cell* **2012,** *148* (6), 1271-83.

54. Hegreness, M.; Shoresh, N.; Damian, D.; Hartl, D.; Kishony, R., Accelerated evolution of resistance in multidrug environments. *Proc Natl Acad Sci U S A* **2008,** *105* (37), 13977-81.

55. Brown, K. M.; Costanzo, M. S.; Xu, W.; Roy, S.; Lozovsky, E. R.; Hartl, D. L., Compensatory mutations restore fitness during the evolution of dihydrofolate reductase. *Molecular biology and evolution* **2010,** *27* (12), 2682-90.

56. Lambros, C.; Vanderberg, J. P., Synchronization of Plasmodium falciparum erythrocytic stages in culture. *The Journal of parasitology* **1979,** *65* (3), 418-20.

57. (a) Johnson, D. J.; Fidock, D. A.; Mungthin, M.; Lakshmanan, V.; Sidhu, A. B.; Bray, P. G.; Ward, S. A., Evidence for a central role for PfCRT in conferring Plasmodium falciparum resistance to diverse antimalarial agents. *Mol Cell* **2004,** *15* (6), 867-77; (b) Sidhu, A. B.; Uhlemann, A. C.; Valderramos, S. G.; Valderramos, J. C.; Krishna, S.; Fidock, D. A., Decreasing pfmdr1 copy number in plasmodium falciparum malaria heightens susceptibility to mefloquine, lumefantrine, halofantrine, quinine, and artemisinin. *J Infect Dis* **2006,** *194* (4), 528-35.

58. Aurrecoechea, C.; Brestelli, J.; Brunk, B. P.; Dommer, J.; Fischer, S.; Gajria, B.; Gao, X.; Gingle, A.; Grant, G.; Harb, O. S.; Heiges, M.; Innamorato, F.; Iodice, J.; Kissinger, J. C.; Kraemer, E.; Li, W.; Miller, J. A.; Nayak, V.; Pennington, C.; Pinney, D.

F.; Roos, D. S.; Ross, C.; Stoeckert, C. J., Jr.; Treatman, C.; Wang, H., PlasmoDB: a functional genomic database for malaria parasites. *Nucleic Acids Res* **2009,** *37* (Database issue), D539-43.

59. Li, H.; Durbin, R., Fast and accurate short read alignment with Burrows-Wheeler transform. *Bioinformatics* **2009,** *25* (14), 1754-60.

60. DePristo, M. A.; Banks, E.; Poplin, R.; Garimella, K. V.; Maguire, J. R.; Hartl, C.; Philippakis, A. A.; del Angel, G.; Rivas, M. A.; Hanna, M.; McKenna, A.; Fennell, T. J.; Kernytsky, A. M.; Sivachenko, A. Y.; Cibulskis, K.; Gabriel, S. B.; Altshuler, D.; Daly, M. J., A framework for variation discovery and genotyping using next-generation DNA sequencing data. *Nat Genet* **2011,** *43* (5), 491-8.

61. Li, H.; Handsaker, B.; Wysoker, A.; Fennell, T.; Ruan, J.; Homer, N.; Marth, G.; Abecasis, G.; Durbin, R., The Sequence Alignment/Map format and SAMtools. *Bioinformatics* **2009,** *25* (16), 2078-9.

62. Johnson, J. D.; Dennull, R. A.; Gerena, L.; Lopez-Sanchez, M.; Roncal, N. E.; Waters, N. C., Assessment and continued validation of the malaria SYBR green I-based fluorescence assay for use in malaria drug screening. *Antimicrobial agents and chemotherapy* **2007,** *51* (6), 1926-33.

63. Phillips, M. A.; Gujjar, R.; Malmquist, N. A.; White, J.; El Mazouni, F.; Baldwin, J.; Rathod, P. K., Triazolopyrimidine-based dihydroorotate dehydrogenase inhibitors with potent and selective activity against the malaria parasite Plasmodium falciparum. *J Med Chem* **2008,** *51* (12), 3649-53.

64. Deng, X.; Gujjar, R.; El Mazouni, F.; Kaminsky, W.; Malmquist, N. A.; Goldsmith, E. J.; Rathod, P. K.; Phillips, M. A., Structural plasticity of malaria dihydroorotate dehydrogenase allows selective binding of diverse chemical scaffolds. *J Biol Chem* **2009,** *284* (39), 26999-7009.

65. Ingolia, N. T., Genome-wide translational profiling by ribosome footprinting. *Methods in enzymology* **2010,** *470*, 119-42.

66. McNicholas, S.; Potterton, E.; Wilson, K. S.; Noble, M. E., Presenting your structures: the CCP4mg molecular-graphics software. *Acta crystallographica. Section D, Biological crystallography* **2011,** *67* (Pt 4), 386-94.

67. Bopp, S. E.; Manary, M. J.; Bright, A. T.; Johnston, G. L.; Dharia, N. V.; Luna, F. L.; McCormack, S.; Plouffe, D.; McNamara, C. W.; Walker, J. R.; Fidock, D. A.; Denchi, E. L.; Winzeler, E. A., Mitotic evolution of Plasmodium falciparum shows a stable core genome but recombination in antigen families. *PLoS genetics* **2013,** *9* (2), e1003293.

68. Hayton, K.; Su, X. Z., Drug resistance and genetic mapping in Plasmodium falciparum. *Current genetics* **2008,** *54* (5), 223-39.

69. White, R. M.; Cech, J.; Ratanasirintrawoot, S.; Lin, C. Y.; Rahl, P. B.; Burke, C. J.; Langdon, E.; Tomlinson, M. L.; Mosher, J.; Kaufman, C.; Chen, F.; Long, H. K.; Kramer, M.; Datta, S.; Neuberg, D.; Granter, S.; Young, R. A.; Morrison, S.; Wheeler, G.

N.; Zon, L. I., DHODH modulates transcriptional elongation in the neural crest and melanoma. *Nature* **2011,** *471* (7339), 518-22.

70. Chait, R.; Shrestha, S.; Shah, A. K.; Michel, J. B.; Kishony, R., A Differential Drug Screen for Compounds That Select Against Antibiotic Resistance. *PloS one* **2010,** *5* (12).

71. Robert, V.; Trape, J. F.; Rogier, C., Malaria parasites: elimination is not eradication. *Clinical microbiology and infection : the official publication of the European Society of Clinical Microbiology and Infectious Diseases* **2011,** *17* (11), 1597-9.

72. Kaneko, A., A community-directed strategy for sustainable malaria elimination on islands: short-term MDA integrated with ITNs and robust surveillance. *Acta tropica* **2010,** *114* (3), 177-83.

73. Karunamoorthi, K., Vector control: a cornerstone in the malaria elimination campaign. *Clinical microbiology and infection : the official publication of the European Society of Clinical Microbiology and Infectious Diseases* **2011,** *17* (11), 1608-16.

74. Chaccour, C. J.; Kobylinski, K. C.; Bassat, Q.; Bousema, T.; Drakeley, C.; Alonso, P.; Foy, B. D., Ivermectin to reduce malaria transmission: a research agenda for a promising new tool for elimination. *Malar J* **2013,** *12*, 153.

75. Ekland, E. H.; Fidock, D. A., Advances in understanding the genetic basis of antimalarial drug resistance. *Current opinion in microbiology* **2007,** *10* (4), 363-70.

76. Cohen, J. M.; Smith, D. L.; Cotter, C.; Ward, A.; Yamey, G.; Sabot, O. J.; Moonen, B., Malaria resurgence: a systematic review and assessment of its causes. *Malar J* **2012,** *11*, 122.

77. Laufer, M. K.; Thesing, P. C.; Eddington, N. D.; Masonga, R.; Dzinjalamala, F. K.; Takala, S. L.; Taylor, T. E.; Plowe, C. V., Return of chloroquine antimalarial efficacy in Malawi. *N Engl J Med* **2006,** *355* (19), 1959-66.

78. Kevin J. Bowers, E. C., Huafeng Xu, Ron O. Dror, Michael P. Eastwood, Brent A. Gregersen, John L. Klepeis, Istvan Kolossvary, Mark A. Moraes, Federico D. Sacerdoti, John K. Salmon, Yibing Shan, David E. Shaw, Scalable Algorithms for Molecular Dynamics Simulations on Commodity Clusters. *Proceedings of the ACM/IEEE Conference on Supercomputing* **2006**.

79. Livak, K. J.; Schmittgen, T. D., Analysis of relative gene expression data using real-time quantitative PCR and the 2(T)(-Delta Delta C) method. *Methods* **2001,** *25* (4), 402-408.

80. Fidock, D. A.; Wellems, T. E., Transformation with human dihydrofolate reductase renders malaria parasites insensitive to WR99210 but does not affect the intrinsic activity of proguanil. *Proc Natl Acad Sci U S A* **1997,** *94* (20), 10931-6.

81. Muller, S.; Kappes, B., Vitamin and cofactor biosynthesis pathways in Plasmodium and other apicomplexan parasites. *Trends in parasitology* **2007,** *23* (3), 112-21.

82. Chan, X. W.; Wrenger, C.; Stahl, K.; Bergmann, B.; Winterberg, M.; Muller, I. B.; Saliba, K. J., Chemical and genetic validation of thiamine utilization as an antimalarial drug target. *Nature communications* **2013,** *4*, 2060.

83. Meierjohann, S.; Walter, R. D.; Muller, S., Regulation of intracellular glutathione levels in erythrocytes infected with chloroquine-sensitive and chloroquine-resistant Plasmodium falciparum. *The Biochemical journal* **2002,** *368* (Pt 3), 761-8.

84. Anderson, T.; Nkhoma, S.; Ecker, A.; Fidock, D., How can we identify parasite genes that underlie antimalarial drug resistance? *Pharmacogenomics* **2011,** *12* (1), 59-85.

85. Straimer, J.; Lee, M. C.; Lee, A. H.; Zeitler, B.; Williams, A. E.; Pearl, J. R.; Zhang, L.; Rebar, E. J.; Gregory, P. D.; Llinas, M.; Urnov, F. D.; Fidock, D. A., Site-specific genome editing in Plasmodium falciparum using engineered zinc-finger nucleases. *Nature methods* **2012,** *9* (10), 993-8.

86. Beurdeley, M.; Bietz, F.; Li, J.; Thomas, S.; Stoddard, T.; Juillerat, A.; Zhang, F.; Voytas, D. F.; Duchateau, P.; Silva, G. H., Compact designer TALENs for efficient genome engineering. *Nature communications* **2013,** *4*, 1762.

87. Cong, L.; Ran, F. A.; Cox, D.; Lin, S.; Barretto, R.; Habib, N.; Hsu, P. D.; Wu, X.; Jiang, W.; Marraffini, L. A.; Zhang, F., Multiplex genome engineering using CRISPR/Cas systems. *Science (New York, N.Y.)* **2013,** *339* (6121), 819-23.

88. Mali, P.; Yang, L.; Esvelt, K. M.; Aach, J.; Guell, M.; DiCarlo, J. E.; Norville, J. E.; Church, G. M., RNA-guided human genome engineering via Cas9. *Science (New York, N.Y.)* **2013,** *339* (6121), 823-6.

89. Painter, H. J.; Morrisey, J. M.; Mather, M. W.; Vaidya, A. B., Specific role of mitochondrial electron transport in blood-stage Plasmodium falciparum. *Nature* **2007,** *446* (7131), 88-91.

90. Michel, J. B.; Yeh, P. J.; Chait, R.; Moellering, R. C., Jr.; Kishony, R., Drug interactions modulate the potential for evolution of resistance. *Proc Natl Acad Sci U S A* **2008,** *105* (39), 14918-23.

91. Prevention, C. f. D. C. a. Distribution of malaria in the United States, 1882-1935. http://www.cdc.gov/malaria/about/history/elimination_us.html (accessed 17 July 2013).

92. Fidock, D. A., Microbiology. Eliminating malaria. *Science (New York, N.Y.)* **2013,** *340* (6140), 1531-3.

APPENDIX

ORGANIC LETTERS

2010
Vol. 12, No. 20
4661−4663

Asterogynins: Secondary Metabolites from a Costa Rican Endophytic Fungus

Shugeng Cao,[†] Leila Ross,[†] Giselle Tamayo,[‡] and Jon Clardy*[,†]

Department of Biological Chemistry and Molecular Pharmacology, Harvard Medical School, 240 Longwood Avenue, Boston, Massachusetts 02115, and Unidad Estrategica de Bioprospeccion, Instituto Nacional de Biodiversidad (INBio), Santo Domingo de Heredia, Costa Rica

jon_clardy@hms.harvard.edu

Received August 19, 2010

ABSTRACT

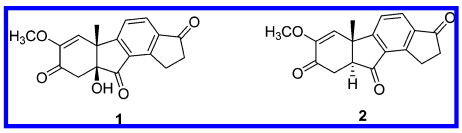

An endophytic fungus isolated from the small palm *Asterogyne martiana* produced two unusual steroid-like metabolites, asterogynin A (1) and asterogynin B (2), along with the known compounds viridiol (3) and viridin (4). Asterogynins A and B were characterized by NMR and MS spectroscopic analysis.

Fungi have made noteworthy contributions to our store of naturally occurring small molecules as they have contributed more than a quarter by most reckonings, and these contributions have come from only a tiny fraction of the world's estimated 1.5 million fungal species. Only ∼5% of the fungal species have been scientifically studied, and a minority of these have been studied chemically.[1−3] The endophytic fungi that live inside of vascular plants constitute one of the richest sources of poorly examined fungi. As part of a longstanding collaborative research project with INBio (National Biodiversity Institute), we have begun characterizing some of the chemical diversity of Costa Rican endophytes. Costa Rica's location on the slender land bridge between North and South American organisms makes it a natural mixing bowl for the organisms of both continents. As a result, the country's many different ecological niches contain over 9000 species of vascular plants.

In one recent project, extracts from Costa Rican endophytes were screened for their ability to bind *Pf*Hsp86, an essential protein-folding chaperone from *Plasmodium falciparum*, the parasite responsible for the most deadly form of human malaria. *Plasmodium falciparum* encodes three full-length Hsp90 genes for the proteins *Pf*Hsp86, *Pf*GRP94, and *Pf*TRAP1. *Pf*Hsp86 has 59% amino acid identity with human Hsp90α2, and its highly conserved ATP-binding Bergerat fold has 75% identity. *Pf*Hsp86 could be a drug target for malaria as the *Plasmodium* parasites transition between cold-blooded mosquito vectors and warm-blooded and often febrile human hosts, a transition that should create a substantial requirement for assisted protein folding.[4] Some known human Hsp90 inhibitors, like geldanamycin, inhibit parasite growth through *Pf*Hsp86 inhibition.[4]

The dichloromethane extract of CR1488E, which was isolated from the host plant *Asterogyne martiana* (Arecaceae) and whose closest relative based on DNA sequencing is *Chalara alabamensis*, was active with an EC_{50} value of ∼24 μg/mL. Here we report the isolation and structure elucidation of asterogynins A (**1**) and B (**2**) from CR1488E.

[†] Harvard Medical School.
[‡] Instituto Nacional de Biodiversidad (INBio).

(1) Hawksworth, D. L. *Mycol. Res.* **1991**, *95*, 641–655.
(2) Pimm, S. L.; Russell, G. J.; Gittleman, J. L.; Brooks, T. M. *Science* **1995**, *269*, 374–350.
(3) Henkel, T.; Brunne, R. M.; Muller, H.; Reichel, F. *Angew. Chem., Int. Ed.* **1999**, *38*, 643–647.
(4) (a) Acharya, P.; Kumar, R.; Tatu, U. *Mol. Biochem. Parasitol.* **2007**, *153*, 85–94. (b) Kumar, R.; Musiyenko, A.; Barik, S. *Malaria J.* **2003**, *2:30*, doi:10.1186/1475-2875-2-30.

10.1021/ol101972g
Published on Web 09/14/2010

The dichloromethane extract of CR1488E was separated by C-18 prep-HPLC to yield compounds **1**, **2**, **3**, and **4**. Compounds **3** and **4** were identified as the known natural products viridiol[5] and viridin,[6] respectively. The viridin class of steroidal furans contains potent antifungal agents and covalent inhibitors of phosphatidylinositol 3-kinase (PI3 kinase) and polo-like kinase.[7] As viridin-like compounds react with the ATP-binding site of kinases, it is likely that they could also bind the ATP pocket of chaperone and other proteins.

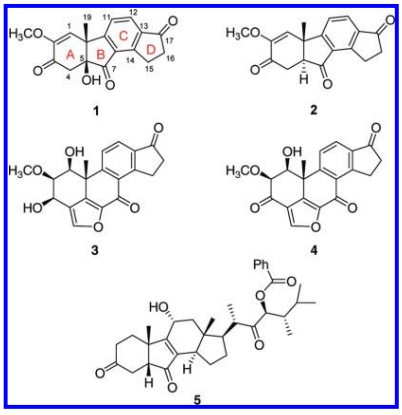

The ^{1}H NMR spectrum of **1**[8] in CD_3OD showed two aromatic protons and one olefinic proton, one methoxy, three methylenes, and one methyl group. The ^{13}C NMR spectrum exhibited 18 signals, including three carbonyls, six aromatic carbons, one double bond, two quaternary and three secondary carbons, one methoxy, and one methyl group. These assignments were further confirmed by the HSQC spectrum. The HRMS (positive-ion mode) had an ion peak at *m*/*z* 295.0969, consistent with a molecular composition of $C_{18}H_{15}O_4$ ([M − H_2O + H], calcd 295.0970), a molecular formula that required 11 double-bond equivalents. Besides three carbonyls, one double bond, and an aromatic ring, there must be three more rings in the molecule. In the COSY spectrum of **1**, two cross-peaks from two coupling systems [CH═CH (aromatic: δ_H 7.78, d, J = 8.0 Hz, H-11; 8.01, d, J = 8.0 Hz, H-12) and CH_2−CH_2 (δ_H 3.37, m, H-15; 2.74, m, H-16)] were observed. Rings C and D were readily established from the HMBC correlations between the carbonyl at ring D and one aromatic proton and the two coupling methylenes. The ^{13}C chemical shifts of the carbons in rings C and D (δ_c 130.6, C-8; 166.1, C-9; 131.6, C-11; 124.8, C-12; 139.0, C-13; 156.8, C-14; 25.3, C-15; 37.0, C-16; 207.9, C-17) matched those of demethoxyviridin and its analogues[9] very well, which further confirmed these two rings. The carbonyl in ring A (δ_c 192.5, C-3) had to be an α,β-unsaturated ketone (δ_c 120.7, C-1; 150.5, C-2) since its ^{13}C chemical shift was <195 ppm, and the olefinic proton (δ_H 6.05, s, H-1) showed a strong HMBC correlation to that carbonyl carbon. In the HMBC spectrum (Figure 1), the

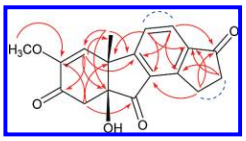

Figure 1. Key HMBC (arrows) and COSY (dashed curves) correlation of (**1**).

methyl group (δ_H 1.54, s, H_3-19) had correlations with the protonated olefinic carbon at δ_c 120.7 (C-1), which indicated that it must be at the β-position of the α,β-unsaturated ketone, one aromatic carbon (δ_c 166.1, C-9), and two quaternary carbons (δ_c 49.0, C-10; 82.5, C-5), one of which was oxygenated. Although no HMBC correlations in CD_3OD between the third methylene and any carbon was observed, rings A and B were deduced to be six- and five-membered rings, respectively, with the oxygenated quaternary carbon connected to the methylene (δ_c 44.5, C-4) at ring A and carbonyl (δ_c 204.2, C-7) at ring B. To check this, both HSQC and HMBC spectra of compound **1** were collected in C_6D_5N, and correlations between the methylene at ring A and C-2, C-3, C-5, C-7, and C-10 were observed. In the ROESY spectrum of **1** in C_6D_5N, H_3-19 showed correlation to 5-OH (Figure 2), indicating a *cis* relationship between these two functional groups. Hence, the structure of **1** was determined as shown.

Compound **2**[10] had a molecular formula of $C_{18}H_{16}O_4$. The only difference between **1** and **2** was the substituent at C-5. In the HMBC spectrum of **2**, the methyl group had correlations to the protonated olefinic carbon, one aromatic carbon and the quaternary carbon, and the tertiary carbon, indicating a methine at the 5 position. No ROESY cross-peak between H_3-19 and 5-H was observed. Hence, the structure of **2** was determined as shown.

(5) Wipf, P.; Kerekes, A. D. *J. Nat. Prod.* **2003**, *66*, 716–718.
(6) Jones, R. W.; Hancock, J. G. *Can. J. Microbiol.* **1987**, *33*, 963–966.
(7) Wipf, P.; Halter, R. J. *Org. Biomol. Chem.* **2005**, *3*, 2053–2061.
(8) **Asterogynin A (1)**: colorless powder; $[\alpha]^{26}_D$ −5.4 (*c*, 0.11 MeOH); UV (MeOH) λ_{max} (log *e*) 235, 312 nm; ^{1}H NMR (400 MHz, pyridine-d_5) d 1.84 s (H_3-19), 2.62 m (H_2-16), 3.26 m (H_2-15), 3.26 m (H-4a), 3.46, J = 16 Hz, d (H-4b), 3.57 s (−OMe), 6.12 s (H-1), 7.76 d, J = 8.0 Hz (H-11), 8.12 d, J = 8.0 Hz (H-12), 8.92 s (5-OH); ^{1}H NMR (600 MHz, CD_3OD) d 1.54 s (H_3-19), 2.74 m (H_2-16 and H-4a), 2.94 m (H-4b), 3.37 m (H_2-15), 3.56 s (−OMe), 6.05 s (H-1), 7.78 d, J = 8.0 Hz (H-11), 8.01 d, J = 8.0 Hz (H-12); ^{13}C NMR (150 MHz, CD_3OD) d 25.3 (C-15), 25.8 (C-19), 37.0 (C-16), 44.5 (C-4), 49.0 (C-10), 55.8 (OMe), 82.5 (C-5), 120.7 (C-1), 124.8 (C-12), 130.6 (C-8), 131.6 (C-11), 139.0 (C-13), 150.5 (C-2), 156.8 (C-14), 166.1 (C-9), 192.5 (C-3), 204.2 (C-7), 207.9 (C-17); HRMS *m*/*z* 295.0969 ([M − H_2O + H], calcd for $C_{18}H_{15}O_4$, 295.0970).
(9) Giner, J.-L.; Kehbein, K. A.; Cook, J. A.; Smith, M. C.; Vlahos, C. J.; Badwey, J. A. *Bioorg. Med. Chem.* **2006**, *16*, 2518–2521.
(10) **Asterogynin B (2)**: colorless powder; $[\alpha]^{26}_D$ +46 (*c*, 0.03 MeOH); UV (MeOH) λ_{max} (log *e*) 235, 312 nm; ^{1}H NMR (600 MHz, CD_3OD) d 1.84 s (H_3-19), 2.14 and 3.29 m (H_2-4), 3.31 and 3.40 m (H_2-15), 3.45 s (−OMe), 5.91 s (H-2), 7.80 d, J = 7.8 Hz (H-11), 8.03 d, J = 7.8 Hz (H-12); ^{13}C NMR (150 MHz, CD_3OD) d 24.5 (C-19), 25.4 (C-15), 36.4 (C-16), 38.9 (C-4), 45.6 (C-10), 55.2 (OMe), 53.3 (C-5), 123.3 (C-1), 124.0 (C-12), 130.8 (C-8), 132.6 (C-11), 138.6 (C-13), 149.8 (C-2), 156.0 (C-14), 168.1 (C-9), 192.4 (C-3), 207.8 (C-17); HRMS *m*/*z* 297.1123 (calcd for $C_{18}H_{17}O_4$, 297.1127).

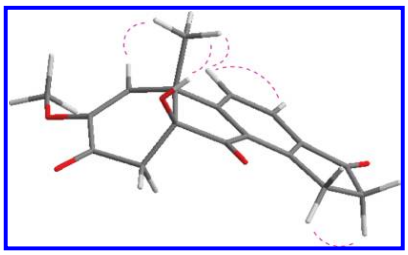

Figure 2. Key ROESY correlation of **1**.

Because of their overall structure and association with viridin (**4**) and viridiol (**3**), asterogynins A (**1**) and B (**2**) are likely sterol derivatives with a tetracyclic (6−5−6−5) carbocyclic ring system, which differs from the tetracyclic (6−6−6−5) of **3**, **4**, and other steroids. Only a few B-norsteroids (**5** is typical)[11] with more complex structures have been previously reported from other sources. The asterogynins A (**1**) and B (**2**) are quite different in having no remnants of the typical steroid side chain. They also lack the furan ring of **3** and **4**. Viridin (**4**) is a modified steroid,[12] and it is therefore likely that asterogynins A (**1**) and B (**2**) are also derived from the steroidal pathway. Whether they are further elaborations of viridin/viridiol through oxidative removal of the furan ring or arise from a separate pathway is not clear.

All four compounds were tested against *Pf*Hsp86, but only compound **3** was active with an EC_{50} value of 5.5 ± 1.2 μg/mL. Further biological evaluations of compounds **1** and **2** are now being conducted and will be reported in due course.

Acknowledgment. This work was generously supported by NIH U01 TW007404 (J.C. and G.T.). Medicines for Malaria Ventures supported the antimalarial assays.

Supporting Information Available: Experimental procedure, and selected NMR (1D, 2D) and HRMS spectra. This material is available free of charge via the Internet at http://pubs.acs.org.

OL101972G

(11) Anke, T.; Werle, A.; Kappe, R.; Sterner, O. *J. Antibiot.* **2004**, *57*, 496–501.

(12) Wei, X.; Rodriguez, A. D.; Wang, Y.; Franzblau, S. G. *Tetrahedron Lett.* **2007**, *48*, 8851–8854.